

**G-PROTEIN REGULATION OF VOLTAGE-GATED SODIUM
CHANNELS BY ALLOSTERIC MODULATORS OF THE
CALCIUM-SENSING RECEPTOR**

By

Glynis Brown Mattheisen

A DISSERTATION

Presented to the Neuroscience Graduate Program
and the Oregon Health & Science School of Medicine
in partial fulfillment of
the requirements for the degree of

Doctor of Philosophy

June 2018

School of Medicine

Oregon Health & Science University

CERTIFICATE OF APPROVAL

This is to certify that the Ph.D. dissertation of
Glynis Brown Mattheisen
has been approved on June 12, 2018

Advisor, Stephen M. Smith, M.D., Ph.D.

Member and Chair, Laurence Trussell, Ph.D.

Member, John Williams, Ph.D.

Member, Henrique von Gersdorff, Ph.D.

Member, Eric Schnell, M.D., Ph.D.

TABLE OF CONTENTS

LIST OF TABLES AND FIGURES.....	6
ACKNOWLEDGEMENTS.....	7
INTRODUCTION.....	8
<i>Voltage-Gated Sodium Channel Gating.....</i>	8
<i>Intrinsic VGSC Properties Influencing the Action Potential.....</i>	10
<i>Extrinsic Voltage-Gated Sodium Channel Modulation.....</i>	13
<i>The Convergence of G-Proteins and Ion Channels.....</i>	14
<i>G-Proteins and Voltage-Gated Sodium Channels.....</i>	17
<i>The Calcium-Sensing Receptor.....</i>	18
<i>Calcium-Sensing Receptor Modulators.....</i>	19
<i>Anandamide and the Calcium-Sensing Receptor.....</i>	22
<i>Significance of Anandamide in Physiology and Disease-States.....</i>	22
<i>Voltage-Gated Sodium Channel Regulation by Allosteric Modulators of the CaSR.....</i>	24
CHAPTER 1. STRONG G-PROTEIN MODULATION OF SODIUM CHANNELS	
SUMMARY.....	26
INTRODUCTION.....	27
RESULTS.....	28
<i>Allosteric CaSR Agonists Reduce VGSC Current.....</i>	28
<i>Allosteric CaSR Modulators Inhibit VGSCs by a CaSR-Independent Pathway.....</i>	30
<i>G-Protein-Mediated Changes to VGSC Current.....</i>	31
<i>Molecular Targets for G-Protein-Mediated VGSC Inhibition.....</i>	33
<i>Cinacalcet Promotes Inactivation of VGSC Current.....</i>	37
<i>Cinacalcet Inhibits VGSC Current in Acutely Isolated Neocortical Neurons.....</i>	40
DISCUSSION.....	41

METHODS.....	47
FIGURES AND TABLES.....	52
CHAPTER 2. CENTRAL ANANDAMIDE SIGNALING VIA THE CALCIUM-SENSING RECEPTOR AND VOLTAGE-GATED SODIUM CHANNELS	
SUMMARY.....	74
INTRODUCTION.....	75
RESULTS.....	78
<i>AEA Activates the CaSR.....</i>	78
AEA Inhibits VGSCs.....	81
<i>Anandamide Inhibits VGSCs by a CaSR-Independent Pathway.....</i>	81
<i>G-Protein-Mediated Changes to VGSC Current.....</i>	82
<i>AEA-Induced Inhibition Reversed Via Hyperpolarization.....</i>	83
DISCUSSION.....	84
METHODS.....	89
FIGURES.....	94
SUMMARY AND CONCLUSIONS.....	99
<i>G-Protein Modulation of Voltage-Gated Sodium Channels.....</i>	100
<i>CaSR Allosteric Modulators Shift Voltage-Gated Sodium Channels into a Deeply Inactivated State.....</i>	102
<i>Anandamide Inhibits VGSCs through Direct and Indirect Mechanisms.....</i>	106
<i>Anandamide's Roles in Synaptic Transmission.....</i>	108
<i>Clinical Significance of an Endocannabinoid Pathway for VGSC Inhibition...</i>	111
<i>Mechanisms for Voltage-Gated Sodium Channel Modulation.....</i>	111
<i>Voltage-Gated Sodium Channel Gating is Sensitive to Phosphorylation.....</i>	112
<i>Calcium and Calmodulin Regulate VGSCs.....</i>	114
<i>Further Post-translational Modifications of Voltage-Gated Sodium Channels.....</i>	116

<i>Gβγ can Directly Bind VGSCs</i>	117
<i>Potential GPCRs for CaSR Allosteric Modulator Binding</i>	118
<i>GPRC6A</i>	119
<i>Orphan Receptors GPR55, GPR18, and GPR1196A</i>	119
<i>Summary and Conclusions</i>	120
REFERENCES.....	123

LIST OF TABLES AND FIGURES

CHAPTER 1. STRONG G-PROTEIN MODULATION OF SODIUM CHANNELS	
FIGURE 1.1: Inhibition of VGSC current by CaSR allosteric agonist cinacalcet	52
FIGURE 1.2: CaSR allosteric agonists and antagonists inhibit VGSC current in wildtype (<i>Casr^{+/+}</i>) and CaSR null (<i>Casr^{-/-}</i>) mutants	55
FIGURE 1.3: Allosteric CaSR modulator block of VGSC current is GTP-dependent	57
FIGURE 1.4: Cinacalcet-induced inhibition of VGSC current is not mediated by mGluR1, mGluR5, or GABA _B receptors nor does it require PKA or PKC	60
FIGURE 1.5: Cinacalcet-induced inhibition does not show reliance on Gβγ or Rho family of small G-proteins	63
FIGURE 1.6: Cinacalcet negatively shifts steady-state inactivation of VGSCs in a G-protein dependent manner	65
FIGURE 1.7: Cinacalcet block is use-dependent and recovers following hyperpolarization	67
FIGURE 1.8: Cinacalcet inhibition is independent of extracellular calcium	69
FIGURE 1.9: Cinacalcet inhibits VGSC current in acutely isolated neurons and is reversed by strong hyperpolarization	71
TABLE 1.1: ANOVA results	73
CHAPTER 2. CENTRAL ANANDAMIDE SIGNALING VIA THE CALCIUM-SENSING RECEPTOR AND VOLTAGE-GATED SODIUM CHANNELS	
FIGURE 2.1: AEA activates the CaSR and inhibits VGSCs.	94
FIGURE 2.2: AEA inhibition of VGSCs is independent of CB ₁ receptors and CaSRs but requires G-protein signaling	96
FIGURE 2.3: AEA inhibition of VGSCs is reversed by strong hyperpolarization	98

Acknowledgments

I would like to thank my mentor, Dr. Stephen Smith, for training me in electrophysiology, frequently leaving chocolate on my desk, and encouraging me to think deeply about the project.

I would like to thank the members of the Smith Lab who have all helped me along the way. In particular, I thank Courtney Williams who first taught me electrophysiology and Briana Knight who has been my close friend and an unparalleled source of support.

I thank Dr. Gary Westbrook for inviting me to join the Neuroscience Graduate Program and encouraging in me in my career as well as Liz Lawson-Weber for assisting me with graduate school matters.

Lastly, I thank Drs. John Williams, Laurence Trussell, Henrique von Gersdorff, and Eric Schnell for serving on my dissertation committee and advising me.

Introduction

The action potential is an electrical signal that facilitates interneuronal communication. Action potentials occur in response to excitatory input which depolarizes the cellular membrane and activates voltage-gated sodium channels (VGSCs). These channels set the threshold for action potential generation, drive neuronal depolarization, and conduct the signal to sites of neurotransmitter release (Hodgkin and Huxley 1952). In doing so, VGSCs prove vital to neuronal excitability. This process takes place over milliseconds and is shaped by a multitude of factors including both the intrinsic properties of VGSCs and extrinsic interactions with additional signaling molecules. While intrinsic factors are coupled to neuronal identity, extrinsic factors provide more dynamic systems to modulate and refine the electrical signal (reviewed in Catterall 2012; Ahern et al. 2016).

Voltage-Gated Sodium Channel Gating

Excitable cells respond to and transmit electrical activity. In excitable neurons (Goldin 2001), vertebrate skeletal (Trimmer et al. 1989; Patlak and Ortiz 1986) and cardiac muscle (Balsler 1999; Patlak and Ortiz 1985), and endocrine cells (Morinville et al. 2007) VGSCs generate the rapid upstroke of the action potential and shape the electrical signal. At the negative resting membrane potential, channels are deactivated with conduction blocked by the activation gate. In response to depolarization, as with an excitatory neurotransmitter activating a ligand-gated ion channel to depolarize a region of neuronal membrane, VGSCs activate, conduct a large inward current within hundreds of microseconds, and drive the membrane potential toward the sodium reversal potential. This constitutes the upward stroke of the action potential (reviewed in Goldin

2003; Armstrong 2006). The transient, fast-inactivating component of VGSC current rapidly inactivates within 1-2 milliseconds (Hodgkin and Huxley 1952) with conduction blocked by the inactivation gate upon increasing depolarization. VGSC inactivation and a slower-activating, hyperpolarizing potassium channel conductance depolarize the membrane potential and the action potential concludes (reviewed in Goldin 2003; Armstrong 2006). Relief of VGSC inactivation occurs at negative potentials in a voltage- and time- dependent manner, setting the frequency at which action potentials can occur, and primes the channels for further activation (Hodgkin and Huxley 1952; Kuo and Bean 1994a). In some cases an inactivation-resistant persistent sodium current, a proportionately small residual current, may remain until channels deactivate (Hotson et al. 1979; Stafstrom et al. 1985; Llinás and Sugimori 2012). Certain cell types, such as cerebellar Purkinje neurons, also exhibit resurgent VGSC current that possesses its own voltage-dependence and kinetics, produced when inactivated VGSCs reopen in response to repolarization of the membrane (Raman and Bean 1997). The kinetics of voltage-dependent activation, voltage-dependent inactivation, persistent current, and resurgent current all distinctly influence the action potential waveform with repercussions to excitability.

The action potential threshold is the critical voltage to which the membrane must depolarize for an action potential to initiate (reviewed in Platkiewicz and Brette 2010). Once the threshold for action potential firing is reached an action potential will fire reliably (Noble and Stein 1966). While action potentials are a digital all-or-none signal in this regard, the VGSC conductance underlying this phenomenon is influenced by a

number of variables, giving rise to wide-ranging action potential shapes among neurons (Bean 2007). VGSC gating, kinetics, and conductance vary between channels based on inherent channel identity (Catterall 2012), as will be explored in the next section, as well as interactions of these channels with and modifications by other proteins.

Intrinsic VGSC Properties Influencing the Action Potential

VGSCs in the mammalian brain are heterotrimeric complexes of an α subunit a non-covalently bound β 1, splice variant β 1B, or β 3 subunit and a covalently bound β 2 or β 4 subunit (Messner and Catterall 1985; Hartshorne and Catterall 1981). The α subunit contains four (I-IV) homologous domains, each with six (S1-S6) transmembrane domains. The intracellular linker between S5 and S6 forms the P loop which comprises the channel pore and controls selectivity and permeation. Positively charged S4 acts as a voltage sensor with functions related to activation (reviewed in Catterall 2012; Ahern et al. 2016). While the α subunit can form a functional unit on its own with voltage sensor and pore-forming domains, adjacent β subunits fine-tune voltage-sensitivity and gating kinetics, while also directing membrane trafficking of the α subunit (Catterall 2000; Kazen-Gillespie et al. 2000; Qin et al. 2003; Yu et al. 2003).

Of the nine VGSC α subunits ($\text{Na}_v1.1-1.9$), the mammalian central nervous system is populated by $\text{Na}_v1.1$, $\text{Na}_v1.2$, $\text{Na}_v1.3$, and $\text{Na}_v1.6$ (Catterall 2012; Goldin 2001), with $\text{Na}_v1.6$ being the most abundant (Auld et al. 1988). $\text{Na}_v1.1$ and $\text{Na}_v1.3$ are expressed on neuronal soma (Westenbroek et al. 1989), $\text{Na}_v1.2$ almost exclusively in unmyelinated axons (Miyazaki et al. 2014), $\text{Na}_v1.6$ in myelinated axons of mature

neurons at the initial segment and nodes of Ranvier (Boiko et al. 2003; Caldwell et al. 2000), and $\text{Na}_V1.1$, $\text{Na}_V1.3$, and $\text{Na}_V1.6$ in dendrites (Westenbroek et al. 1989; Westenbroek et al. 1992; Caldwell et al. 2000). The differential subcellular distribution of these isoforms affects action potential waveform, initiation, propagation, frequency, and even back-propagation toward the postsynaptic terminal (Araya et al. 2007), changing how signals are integrated.

Each of the α subunits exhibit unique gating properties, voltage-dependence, and current profiles, with even more nuanced differences shown in use-dependent potentiation or use-dependent reduction of channel current, thereby contributing to specialized functional roles (Zhou and Goldin 2004). While these properties are altered by affiliated β subunits and post-translational modifications (Johnson et al. 2004; Calhoun and Isom 2014), relative characteristic differences between the neuronal isoforms have been identified in knockout studies and expression systems. All neuronal VGSC isoforms have faster inactivation kinetics than those isoforms expressed in the periphery for concise signaling (Savio-Galimberti et al. 2012). The most abundant isoform, $\text{Na}_V1.6$, (Auld et al. 1988) has depolarized activation and inactivation potentials compared to the other three neuronal isoforms (Rush et al. 2005; Chen et al. 2008), with use-dependent potentiation suggesting a resistance to inactivation during high frequency firing (Zhou and Goldin 2004). These features lend themselves to increased excitability at the nodes of Ranvier (Zhou and Goldin 2004). Recovery from inactivation is fastest with $\text{Na}_V1.1$ and $\text{Na}_V1.6$, facilitating action potential initiation and propagation at neuronal soma and axons (Qiao et al. 2014), while slower recovery with $\text{Na}_V1.2$ and

Na_v1.3 provides for use-dependent reductions in current and reduced excitability at sites where these isoforms are expressed (Qiao et al. 2014; Zhou and Goldin 2004). Within the four neuronal isoforms types, Na_v1.6 has the largest persistent current that increases at more positive membrane potentials, encouraging repetitive firing, while Na_v1.2 has the least persistent current, slowing high frequency activity (Goldin 2001).

The five mammalian β subunits (O'Malley and Isom 2015) can increase current density (Brackenbury and Isom 2011), shift the voltage range over which activation and inactivation occur (Yu et al. 2005), enhance inactivation rate, speed recovery from inactivation (Chen and Cannon 1995), and alter persistent and resurgent VGSC current (reviewed in Calhoun and Isom 2014). In addition, β subunits can receive post-translational modifications such as phosphorylation and glycosylation that alter channel gating (Johnson et al. 2004; Calhoun and Isom 2014). β subunits, therefore, influence many of the key conformational changes that VGSCs undergo during the action potential (Brackenbury and Isom 2011; Patino and Isom 2010), with specific combinations of α and β subunits contributing to the particular physiological characteristics of divergent cell types (Winters and Isom 2016).

The location and density of VGSCs control spatiotemporal features of the electrical signal and define the role of that input in neuronal processing (reviewed in Lai and Jan 2006). VGSC clustering at the axon initial segment and nodes of Ranvier to ensures saltatory conduction along the axon (reviewed in Freeman et al. 2016) while VGSCs in dendrites enhance back propagation of action potentials (Losonczy et al. 2008; Larkum

et al. 2007; Gasparini and Magee 2006; Gasparini et al. 2004). The kinetics of sodium currents differ immensely between divergent neuron types and even different regions of the same neuron (Engel and Jonas 2005). Patch-clamp experiments have demonstrated that axonal and somato-dendritic VGSCs differ in their voltage-dependent properties. While the explicit mechanisms producing variability in the VGSC signal are unknown, hypotheses include different VGSC α and β subunit compositions (Raman et al. 1997) at distinct cellular sites.

VGSC subunit identity and composition are intrinsic factors that are coupled to neuronal identity and known to influence firing properties of neurons. These, in addition to spatial distribution, influence the electrical behavior of neurons at a base level (reviewed in Lai and Jan 2006; Cusdin et al. 2008). We now find that these foundational properties can be further refined through protein signaling pathways and post-translational modifications (Catterall 2012), adding additional complexity to the electrical contributions of VGSCs.

Extrinsic Voltage-Gated Sodium Channel Modulation

It was once thought that the only point of regulation of the sodium channel signal was voltage-dependent gating on a millisecond time scale. Early voltage-clamp studies of VGSCs in neurons indicated that VGSCs are not subject to regulation via second messenger pathways (Hille 2001). An explanation for this finding is that the techniques used in these studies allowed for dialysis of the cytoplasm resulting in the loss or dilution of critical signaling components. Nevertheless, these studies led to the

widespread belief that VGSCs are functionally similar in divergent excitable cell types. This picture has since evolved with the identification of second messenger signaling cascades that modulate VGSC activity (Cantrell and Catterall 2001). A myriad of enzymes, including protein kinases A and C (Sigel and Baur 1988; Scheuer 2011; Murphy et al. 1993), calcium/calmodulin-dependent protein kinase (CAMK) II (Ashpole et al. 2012; Thompson et al. 2017), Fyn tyrosine kinases (Ahn et al. 2007; Scheuer 2011), and calcineurin (Murphy et al. 1993), modify VGSCs, culminating in short- and long-term changes to sodium currents (reviewed in Laedermann et al. 2015). Since the action potential is the penultimate pathway for neuronal output, VGSCs are strategically positioned to serve as an important point of regulation for neuronal signal transduction and post-translational modifications to these channels widely contribute to plasticity of the signal.

The Convergence of G-Proteins and Ion Channels

G-protein-coupled receptors (GPCRs) are a large protein family of integral membrane receptors (Vassilatis et al. 2003) that sense extracellular molecules such as peptides, lipids, or neurotransmitters and in turn activate intracellular signaling pathways by regulating the activity of bound heterotrimeric G-proteins (Lefkowitz 2013). Heterotrimeric G-proteins consist of a $G\alpha$ subunit that binds and hydrolyzes guanosine triphosphate (GTP) into guanosine diphosphate (GDP) and β and γ subunits that form an obligate dimer (Wettschureck and Offermanns 2005). In the absence of stimuli, GDP-bound $G\alpha$ and $G\beta\gamma$ associate with the receptor (Sondek et al. 1996). Binding of a ligand to the GPCR induces a conformational change that is transduced to

the G-protein and promotes the exchange of bound GDP for GTP (Ballesteros et al. 2001; Shapiro et al. 2002). GTP-bound $G\alpha$ dissociates and this exposes a new binding interface that provides for up to 100-fold higher affinity binding with effector proteins than $G\alpha$ in the GDP-bound state (Skiba et al. 1996). Upon activation, the $G\beta\gamma$ dimer also dissociates from the GPCR and diffuses in a membrane-delimited fashion to targets (Clapham and Neer 1997). Intrinsic hydrolysis of GTP by the $G\alpha$ subunit allows reassociation of GDP-bound $G\alpha$ subunit with $G\beta\gamma$, terminating G-protein signaling and thus reforming the heterotrimer (Kleuss et al. 1994). Importantly, both the $G\alpha$ subunit and the $G\beta\gamma$ dimer can mediate intracellular signaling (reviewed in Hamm 1998; Clapham and Neer 1997). In humans, there are at least 18 $G\alpha$ proteins, 5 types of $G\beta$, and 11 types of $G\gamma$ that can all combinatorially associate to preferentially activate different signaling pathways (Hermans 2003; Robillard et al. 2000).

The activity of GPCRs has been implicated in diverse processes including metabolism, development, hormonal homeostasis, and synaptic plasticity (reviewed in Rosenbaum et al. 2009; Hoffmann et al. 2008). In many of these processes, signaling cascades downstream of GPCRs control neuronal ion channel function. G-proteins dynamically modulate ion channels involved in synaptic transmission, exerting widespread effects on both voltage-gated calcium (VGCCs) and voltage-gated potassium channels (VGPCs). Over twenty neurotransmitters and their corresponding GPCRs have been found to modulate VACCs, including noradrenaline (Bean 1989; Lipscombe et al. 1989; McFadzean and Docherty 1989), γ -aminobutyric acid (GABA) (Deisz and Lux 1985; Grassi and Lux 1989; Dolphin and Scott 1987), dopamine (Drolet et al. 1997) and

acetylcholine (Beech et al. 1991; Bernheim et al. 1991; Shapiro et al. 1999). Fifteen GPCRs have also been shown to modulate VGPCs, including M2 muscarinic acetylcholine (mAChR) (Bünemann et al. 1995), A1 adenosine (Soejima and Noma 1984), D2 dopamine (Lacey et al. 1988; Saugstad et al. 1996), μ -, δ -, and κ -opioid (Grudt and Williams 1993; North et al. 1987), 5-HT_{1A} serotonin (Oh et al. 1995), metabotropic glutamate (mGluR) (Saugstad et al. 1996), and GABA_B receptors (Lacey et al. 1988) (reviewed in Hille 1992; Yamada et al. 1998). GPCR-induced modulation of VGCCs and VGPCs includes the indirect mechanisms of phosphorylation, membrane phospholipid interactions, and channel trafficking (reviewed in Zamponi and Currie 2013; Inanobe and Kurachi 2014). In addition, VGCCs and VGPCs are also directly modulated by the G $\beta\gamma$ dimer for reduced neuronal excitability. G $\beta\gamma$ inhibits VGCCs to provide negative feedback and terminate further neurotransmitter discharge (Herlitze et al. 1996; Ikeda 1996) while G $\beta\gamma$ activation of G-protein-coupled inwardly-rectifying potassium channels (GIRKs) (Lüscher et al. 1997) reduces action potential propagation from excitatory inputs and back propagation from soma to synapse (Ponce et al. 1996; Liao et al. 1996; Morishige et al. 1996).

Given the structural homology between VGSCs, VGPCs (Stühmer et al. 1989; Tikhonov and Zhorov 2005), and VGCCs (Ben-Johny et al. 2015; Yu and Catterall 2003) and the positioning of VGSCs as critical targets for the modulation of neuronal excitability, there is an auspicious opportunity for G-protein interaction. It is certain that further research will reveal additional functional relationships between these two key players in neuronal excitability.

G-Proteins and Voltage-Gated Sodium Channels

The first studies of the G-protein modulation of VGSCs were undertaken following the identification of several putative phosphorylation sites on the α subunit (Costa et al. 1982; Costa and Catterall 1984). These studies suggested that the channel can be regulated by second messenger pathways that activate phosphorylating kinases. Sigel and Bauer, presented the first electrophysiological evidence for G-protein modulation of VGSCs by demonstrating that protein kinase C (PKC) activation reduces the amplitude of chick brain VGSC currents in a heterologous expression system (Sigel and Baur 1988). Since these initial observations, complete pathways between GPCRs and changes in VGSC output have been described throughout the cortex. VGSCs are inhibited by activation of dopamine D1-like receptors (Cantrell et al. 1999), mGluR1 (Carlier et al. 2006), mAChR M1 (Cantrell et al. 1996), and serotonin 5-HT_{2A/C} receptors (Carr et al. 2002). While some studies report a decrease in channel conductance without a change to VGSC gating (Cantrell et al. 1999; Cantrell et al. 1996), others indicate G-protein interactions substantially shift channel voltage-dependent inactivation (Carlier et al. 2006; Carr et al. 2002) to reduce current amplitude. The primary biophysical mechanism of G-protein VGSC modulation is phosphorylation downstream of protein kinase A (PKA) or PKC, which has been observed in preparations from the hippocampus (Cantrell et al. 1999; Cantrell et al. 1996), neocortex (Carlier et al. 2006), and prefrontal cortex (Maurice et al. 2001; Carr et al. 2002). These pathways may function as negative feedback loops during periods of intense synaptic transmission to halt further neurotransmitter release. One study also gives evidence that VGSCs, like

VGCCs and VGPCs, are directly modulated by $G\beta\gamma$ and this interaction increases persistent VGSC current of $Na_v1.1$ and $Na_v1.2$ (Mantegazza et al. 2005), though additional research is necessary to fully understand the extent and physiological role of VGSC $G\beta\gamma$ modulation. Overall, data is amassing for the G-protein modulation of VGSCs and the varied roles this plays in intraneuronal signaling.

The Calcium-Sensing Receptor

The calcium-sensing receptor (CaSR) is a GPCR activated by extracellular calcium expressed in many tissues including the nervous system (Leach et al. 2015; Butters et al. 1997; Rogers et al. 1997). The CaSR has been studied extensively for its roles in maintaining calcium homeostasis in the kidney and parathyroid gland. CaSRs expressed on the parathyroid gland sense serum calcium levels and modulate parathyroid hormone synthesis and secretion to maintain serum calcium within a physiological range (reviewed in Tfelt-Hansen and Brown 2005). In the cerebellum and cerebral cortex, the CaSR is expressed at nerve terminals (Chen et al. 2010; Ruat et al. 1995) where it modulates evoked and spontaneous synaptic transmission (Smith et al. 2012; Smith et al. 2004).

Previous research in our lab has shown that presynaptic CaSRs decrease release probability at excitatory synapses in the neocortex through the regulation of a nonselective cation channel (NSCC) (Smith et al. 2004). This function forms a feedback loop wherein the CaSR represses a NSCC current as extracellular calcium increases and relieves inhibition on the channel when calcium falls (Smith et al. 2004). When

calcium falls at the cleft during periods of high synaptic activity, synaptic transmission is depressed due to the sensitivity of neurotransmitter release to calcium entry via VGCCs (Heidelberger et al. 1994; Schneggenburger and Neher 2000). CaSR activity is also reduced in low extracellular calcium, leading to the relief of suppression of the NSCC conductance. The addition of the NSCC current depolarizes the terminal to allow for continued neurotransmitter release. In our current theoretical model, increased NSCC activity may increase action potential duration, prolong calcium entry at the terminal, and thus increase release probability. Consequently, the CaSR may operate as part of a homeostatic pathway to prevent synaptic failure when extracellular calcium falls (reviewed in Jones and Smith 2016).

Calcium-Sensing Receptor Modulators

The drugs cinacalcet and calindol serve as positive allosteric modulators of the CaSR, enhancing its sensitivity to calcium, while negative allosteric modulators NPS 2143 and calhex decrease the sensitivity of the CaSR to extracellular calcium (reviewed in Ward and Riccardi 2012; Conigrave and Ward 2013). All four drugs exhibit high selectivity for the CaSR and are known to possess overlapping though not identical binding sites to the seventh transmembrane domain (TMD) of the receptor (Petrel et al. 2004; Magno et al. 2011).

Interestingly, cinacalcet, marketed under the name Sensipar, was the first drug of its class to be used clinically due to its high sensitivity for the CaSR (Brown 2010). Due to the CaSR's function in the parathyroid, allosteric modulators of the CaSR provide

therapeutic promise for disorders of calcium homeostasis (Bräuner-Osborne et al. 2007). Sensipar treats severe secondary hyperparathyroidism in patients receiving hemodialysis treatment for chronic kidney disease (Block and Chertow 2017). In this role, cinacalcet acts on parathyroid CaSR targets, thereby decreasing circulating parathyroid hormone levels and producing a concurrent decrease in serum calcium (Nemeth et al. 2004). Cardiovascular disease, a leading cause of death in patients with chronic kidney disease and a risk factor for secondary hyperparathyroidism, results from premature cardiovascular aging characterized by vascular calcification on a background of hypercalcemia secondary to high levels of parathyroid hormone (Davies and Hruska 2001). Cinacalcet prevents vascular calcification by reducing parathyroid hormone and should consequently reduce the risk of cardiovascular events in patients with chronic kidney disease (Marcocci et al. 2009; Valle et al. 2008; Rothe et al. 2011).

A trial called EVOLVE was designed to evaluate if cinacalcet reduced the risk of death and nonfatal cardiovascular events among patients with secondary hyperparathyroidism who were undergoing dialysis. The trial, published in *The New England Journal of Medicine* in 2012, concluded that while cinacalcet reduced the levels of parathyroid hormone effectively, treatment with cinacalcet did not lead to a statistically significant reduction in risk of death or cardiovascular events (EVOLVE Trial Investigators et al. 2012). The results indicated that adverse effects of cinacalcet may undermine its effectiveness in the treatment of hyperparathyroidism. A criticism of the EVOLVE trial was the high nonadherence rate for cinacalcet-medicated patients due to intolerable side effects (Pasch et al. 2017; Moe and Thadhani 2013; Parfrey et al. 2016).

Cinacalcet is lipid-soluble, meaning that it readily crosses the blood brain barrier. Neurological side effects of cinacalcet include paresthesia, vertigo, severe hearing loss, and altered mental status (Borchhardt et al. 2008). Despite its ability to readily diffuse into the nervous system and the results of the EVOLVE trial indicating adverse effects of cinacalcet in the central nervous system, the effects of cinacalcet in the brain have yet to be studied.

In investigating the role of the CaSR in synaptic transmission, we found direct CaSR agonists inhibit synaptic transmission (Phillips et al. 2008) and hypothesized that CaSR allosteric modulators may have the same effect. We found that allosteric CaSR modulators reduced GABAergic transmission between neocortical neurons. The nature of this inhibition indicated CaSR-mediated conduction block of the presynaptic action potential and this hypothesis was supported by the discovery that CaSR allosteric modulators strongly inhibit VGSCs. This finding was immediately relevant to the clinical usage of cinacalcet as well as our understanding of the role of the CaSR in the cortex. Further examination showed that both allosteric agonists and antagonists of the CaSR completely inhibited VGSC current. This inhibition was dependent on a G-protein pathway. In Chapter 1, we look at the mechanism underlying CaSR modulator-regulation of VGSCs, investigating the kinetics of this effect as well as potential effector proteins within the pathway.

Anandamide and the Calcium-Sensing Receptor

Endocannabinoids (eCBs) are a family of lipid molecules that target GPCRs and serve as key players in synaptic plasticity. The two major cannabinoid-signaling molecules in the central nervous system are anandamide (AEA) and 2-Arachidonoylglycerol (2-AG). Cannabinoid type 1 (CB₁) receptors have been shown to possess the highest sensitivity to AEA, however, data support the existence of additional receptors that respond to eCBs (reviewed in Castillo et al. 2012; Kano et al. 2009; Katona and Freund 2012; Alger 2012). We identified AEA as a positive allosteric modulator of the CaSR, acting to increase the sensitivity of the receptor to extracellular calcium in the same fashion as has been observed for calindol and cinacalcet. Given our finding that CaSR allosteric modulators inhibit VGSCs, we hypothesized that AEA may have the same effect on VGSCs and neuronal excitability. In Chapter 2, we look at AEA-induced inhibition of VGSCs, investigating the effect of AEA on VGSC gating and identifying potential G-protein pathways that may mediate the response.

Significance of Anandamide in Physiology and Disease-States

In the canonical pathway for cannabinoid function, eCBs are produced on-demand in postsynaptic neurons in response to stimulation then travel in a retrograde fashion to targets receptors on the presynaptic component. eCBs function primarily through presynaptically expressed CB₁ receptors throughout the cortex (Herkenham et al. 1990). Activation of presynaptic cannabinoid receptors can initiate both short- and long-term synaptic depression of excitatory and inhibitory nerve terminals (reviewed in Castillo et al. 2012; Kano et al. 2009; Katona and Freund 2012; Alger 2012). Recent

work shows that cannabinoid function is more diverse than previously believed. In addition to their role as instigators of synaptic depression, cannabinoids have also been shown to participate in non-retrograde signaling (Grueter et al. 2010; Chávez et al. 2010) and signaling via astrocytes (Stella 2010; Navarrete and Araque 2008). Furthermore, studies show that eCBs act on as-yet unidentified receptors to contribute to these processes of synaptic plasticity (reviewed in Begg et al. 2005). Our work addresses one of these off-target AEA effects in the cortex. In Chapter 2, we find that AEA produces VGSC inhibition to modulate neuronal excitability in a pathway that may contribute to eCB-mediated synaptic depression. This pathway represents a new target for eCBs in the cortex as well as a novel physiological mechanism for eCB control of intraneuronal signal integration and synaptic transmission.

Importantly, eCBs contribute to a range of physiological processes, including synaptic plasticity and learning (Heifets and Castillo 2009), pain (Guindon and Hohmann 2009), metabolism and energy homeostasis (Viveros et al. 2008), and neural development (Fride 2008). Dysregulation of the eCB system has been implicated in neuropsychiatric conditions such as depression (Huang et al. 2016), autism (Zamberletti et al. 2017), schizophrenia (Desfossés et al. 2012), addiction (Parsons and Hurd 2015; Volkow et al. 2017), and anxiety (Ruehle et al. 2012; Hillard 2014; Mechoulam and Parker 2013). eCBs have also shown therapeutic promise for Tourette's syndrome (Müller-Vahl 2013), Huntington's disease (Pazos et al. 2008), epilepsy (Alger 2004), Alzheimer's disease (Maroof et al. 2013), depression (Huang et al. 2016), and stroke (Hillard 2008). Advancing our understanding of the many roles of eCBs in the

nervous system will enhance our knowledge of disease states and synaptic transmission.

Voltage-Gated Sodium Channel Regulation by Allosteric Modulators of the CaSR

In this introduction I have outlined the characteristics of VGSCs that affect action potential waveform with consequences to intraneuronal signal processing. VGSCs introduce diversity to action potential shapes across neuronal types via subunit composition, direct protein interactions, and post-translational modifications. Next, in Chapter 1 of this dissertation, we show that allosteric modulators of the CaSR substantially reduce VGSC current. In a detailed look at the kinetic properties of VGSCs, it is shown that CaSR modulators produce a hyperpolarizing shift in steady-state inactivation of the channels, pushing them into a deeply inactivated state relieved only by strong, prolonged hyperpolarization. We establish that this pathway is independent of the CaSR but dependent on G-protein signaling. Cumulatively, these data indicate an important new pathway for modulating neuronal excitability in the cortex.

Following this study, we sought to identify the VGSC modulatory properties of the endogenous signaling ligand AEA. In Chapter 2, we show that AEA completely inhibited VGSC current also via a change in the inactivation properties of VGSCs. This block of VGSC current is also independent of the CaSR but requires G-protein activation. The VGSC inhibition also appeared independent of CB₁ receptors, indicating a novel site of

action of AEA as well as a new G-protein-dependent pathway for VGSCs regulation in the cortex.

The findings presented here are exciting in a number of ways. First, they lend further support to the idea that VGSCs are subject to dynamic modulation by second messenger pathways. Second, they show AEA has actions via the CaSR and independent of CB₁ receptors in the cortex. And third, they point to the existence of an as-yet unexplored eCB-activated pathway for synaptic plasticity in the cortex.

Chapter 1.

Strong G-Protein-Mediated Inhibition of Sodium Channels

Glynis Mattheisen^{1,2}, Timur Tsintsadze^{1,2}, and Stephen M. Smith^{1,2},

¹Department of Medicine, Division of Pulmonary & Critical Care Medicine, Oregon Health & Science University, Portland, Oregon 97239, USA.

²Section of Pulmonary & Critical Care Medicine, VA Portland Health Care System, Portland, Oregon 97239, USA.

Summary

Voltage-gated sodium channels (VGSCs) are strategically positioned to mediate neuronal plasticity due to their influence on action potential waveform. VGSC function may be strongly inhibited by local anesthetic and antiepileptic drugs and modestly modulated via second messenger pathways. Here, we report that allosteric modulators of the calcium-sensing receptor (CaSR), cinacalcet, calindol, calhex, and NPS 2143, completely inhibit VGSC current in the vast majority of cultured mouse neocortical neurons. This form of VGSC current block persisted in CaSR deficient neurons, indicating a CaSR-independent mechanism. Cinacalcet-mediated blockade of VGSCs was prevented by the guanosine diphosphate (GDP) analog GDP β S, indicating G-proteins mediated this effect. Cinacalcet inhibited VGSCs by increasing channel inactivation and block was reversed by prolonged hyperpolarization. Strong cinacalcet inhibition of VGSC currents was also present in acutely isolated mouse cortical neurons.

These data identify a dynamic signaling pathway by which G-proteins regulate VGSC current to indirectly modulate central neuronal excitability.

Introduction

Voltage-gated sodium channels (VGSCs) drive the action potential and are integral to neuronal function. However, the picture of the action potential as a digital all-or-none signal has evolved with the identification of persistent and regenerative types of VGSCs that produce variation in the action potential shape between neuronal types (Huang and Trussell 2008; Raman and Bean 1997). Additional variation in action potential waveform arises from several types of endogenous VGSC regulation including altered inactivation by β subunit interactions (Aman et al. 2009), regional variation in sodium channel density (Leão et al. 2005), and increased persistent VGSC current arising from the inherited β -subunit mutations that influence excitability (Kaplan et al. 2016). These indirect mechanisms regulate VGSC signaling and thereby account for action potential variation between neurons. However, such effects are stable over short periods of time. In contrast, local anesthetics and antiepileptic drugs target VGSCs and rapidly modulate action potentials by stabilizing channel inactivation (Kuo and Bean 1994b; Zeng et al. 2016). In addition, dynamic modulation of VGSCs via calmodulin (Pitt and Lee 2016) and G-protein coupled receptors (GPCRs) (Carr et al. 2003) has also been shown to contribute to neuronal plasticity.

The calcium-sensing receptor (CaSR) is a GPCR expressed in many tissues, including those of the nervous system (Leach et al. 2015). In the cerebral cortex, CaSRs are

expressed at nerve terminals (Chen et al. 2010) where they modulate evoked and spontaneous synaptic transmission (Phillips et al. 2008; Smith et al. 2012). Here, we report that allosteric CaSR modulators (ACMs) reduced GABAergic transmission between neocortical neurons and this was attributable to block of VGSCs. Further examination showed that both allosteric agonists and allosteric antagonists of the CaSR completely inhibited VGSC current. This block of VGSC current was independent of the CaSR but required G-protein activation. The CaSR allosteric agonist, cinacalcet, inhibited VGSC current by negatively shifting steady-state inactivation of the channels. This cinacalcet-induced inhibition was reversed by prolonged hyperpolarization. The VGSC inhibition appeared independent of class C GPCRs and occurred through a protein kinase A (PKA) and protein kinase C (PKC)-independent pathway. These data describe an important new mechanism for modulating neuronal excitability in the cortex.

Results

Allosteric CaSR Agonists Reduce VGSC Current

Direct CaSR agonists produced a graded inhibition of synaptic transmission in neocortical neurons (Phillips et al. 2008), leading us to hypothesize that cinacalcet, an allosteric agonist of the CaSR, would have the same effect. We evoked inhibitory postsynaptic currents (IPSCs) by stimulating presynaptic neurons with a theta electrode (Figure 1.1A). Application of cinacalcet (10 μ M) almost completely eliminated IPSCs within 100-200 s (Figure 1.1B; $96 \pm 1\%$ (mean \pm SEM) block in 8 recordings). In this neuron, voltage-clamped at -70 mV, IPSC amplitude ranged from 70-200 pA and quantal size was 30-40 pA. The initial effect of cinacalcet, appeared all-or-none and we

hypothesized this was due to block of the presynaptic action potential leading to the coordinated block of multiple presynaptic GABA release sites. Consistent with this finding, somatic action potentials were blocked by cinacalcet (Figure 1.1C). We next tested if cinacalcet modulated VGSC currents elicited in voltage-clamped neurons (30 ms step from -70 to -10 mV every 5 s; Figures 1D-1F). Tetrodotoxin (TTX; 1 μ M) reversibly reduced the rapidly activating and inactivating inward current (peak < 1 ms) by $98 \pm 1\%$ ($n = 6$, data not shown), confirming these conditions isolated the VGSC current. Application of cinacalcet (10 μ M) strongly inhibited the peak VGSC current by $98 \pm 1\%$ ($n = 11$) and the kinetics of block were described by a single exponential ($T = 61 \pm 8$ s) after a delay of 73 ± 9 s (Figure 1.1E). VGSC current inhibition by cinacalcet was concentration-dependent (Figures 1.1E and 1.1H) but reversed slowly and incompletely with the -70 mV holding potential (Figure 1.1F but see Figure 1.7B). In contrast, cinacalcet had no effect on voltage-gated potassium channel current (Figure 1.1G), showing cinacalcet action is specific to VGSCs.

The concentration-effect relationship for cinacalcet was determined by measuring the VGSC current immediately following whole-cell formation after incubation (50-70 min) in the drug. This approach was employed because cinacalcet was effective in all neocortical neurons (>300 recordings) and because at lower concentrations the slower rate of block and current rundown, could have confounded measurement of the IC_{50} . VGSC current density (pA/pF) was inversely related to cinacalcet concentration in neocortical neurons after 7 to 9 days in culture ($IC_{50} = 2.2 \pm 0.6$ μ M; Figure 1.1H, open circles). This was in agreement with the degree of block measured when we examined

the time course of inhibition with 1-10 μM cinacalcet (Figures 1.1E and 1.1H, solid squares). Taken together these data indicate that allosteric CaSR agonists strongly inhibit VGSCs in a concentration-dependent manner in neocortical neurons.

Allosteric CaSR Modulators Inhibit VGSCs by a CaSR-Independent Pathway

We hypothesized that cinacalcet inhibited VGSCs via the target CaSR and tested this idea first by examining if other CaSR modulators inhibited VGSC current. Calindol (5 μM), another CaSR allosteric agonist, strongly inhibited peak VGSC current (Figures 1.2A and 1.2D; $97 \pm 1\%$ steady-state inhibition, $n = 5$) elicited as above (see Figure 1.1E). Next, we tested if the CaSR was the target of these drugs by examining if VGSC current was insensitive to cinacalcet in neurons from CaSR null-mutants (*Casr*^{-/-}) (Chang et al. 2008) using the same protocol. Surprisingly, VGSC currents from *Casr*^{-/-} and wild-type neurons were equally sensitive to cinacalcet (Figures 1.2B and 1.2D; $100 \pm 1\%$, $n = 12$, $P = 0.2$). The time constant of the inhibition and latency of the effect of cinacalcet were also unchanged. Furthermore, direct stimulation of the CaSR by increasing the external calcium concentration to 10 mM, did not change the kinetics of VGSC block by cinacalcet (Figure 1.8A and 1.8B). These data indicated that cinacalcet-induced VGSC current inhibition is independent of the CaSR.

Upregulation of other similar compensatory proteins could explain why *Casr*^{-/-} neurons responded to CaSR agonists. Thus, we tested the effect of allosteric CaSR antagonists, NPS 2143 and calhex, on VGSC currents (elicited as in Figure 1.1E). NPS 2143 (5 μM) and calhex (5 μM) strongly blocked VGSC currents (Figures 1.2C and 1.2D; $99 \pm 1\%$, n

= 4 and $95 \pm 1\%$, $n = 7$, respectively). Both agents also inhibited VGSC currents in *Casr^{-/-}* neurons (data not shown). These data show that ACMs inhibit VGSC currents in wild-type and *Casr^{-/-}*, strongly indicating that these effects are not mediated by the CaSR.

G-Protein-Mediated Changes to VGSC Current

To determine if the cinacalcet-induced block of VGSC current relied on G-protein signaling within neocortical neurons, we tested the effect of the guanosine diphosphate (GDP) analog adenosine 5'-O-2-thiodiphosphate (GDP β S) on the cinacalcet-induced response. GDP β S inhibits G-protein cycling by competitively inhibiting the binding of guanosine triphosphate (GTP) to G-proteins (Eckstein et al. 1979; Suh et al. 2004). Cinacalcet (10 μ M) inhibited VGSC current by $90 \pm 3\%$ ($n = 10$), measured 250 s after onset of application, with 0.3 mM GTP in the recording pipette solution. In contrast, cinacalcet reduced VGSC current by only $8 \pm 3\%$ ($n = 12$, $P = 7 \times 10^{-15}$) at the same time point with 2 mM GDP β S in the pipette solution (Figures 1.3A and 1.3B). GDP β S also reduced calindol-induced inhibition of the VGSC currents to $29 \pm 8\%$ ($n = 6$) at 250 s compared to $66 \pm 11\%$ ($n = 5$, $P = 0.02$) in the control conditions (Figure 1.3B). The block of VGSCs by CaSR allosteric antagonists NPS 2143 and calhex was also G-protein-mediated. NPS 2143-induced inhibition was reduced from $96 \pm 1\%$ ($n = 4$) 250 s following NPS 2143 exposure to $5 \pm 13\%$ at the same time point in the presence of GDP β S (2 mM) ($n = 7$, $P = 0.0005$; Figures 1.3C and 1.3D). Calhex-induced inhibition of VGSC current was reduced from $82 \pm 4\%$ ($n = 7$) at 250 s to $33 \pm 10\%$ at the same time point in the presence of GDP β S ($n = 7$, $P = 0.0008$, Figure 1.3D).

We asked three questions to address the possibility that the four ACMs inhibited VGSCs via GDP β S-sensitive pathways that did not involve G-proteins. First, was GDP β S chemically inactivating the ACMs after they reached the intracellular compartment? The subsequent action of cinacalcet on VGSC currents was unaffected following preincubation with GDP β S (2 mM for 30 min at room temperature) indicating that GDP β S was not simply inactivating the ACMs (data not shown). Second, was GDP β S interfering with ACM inhibition of VGSC currents because of an action of the non-hydrolyzable part of the molecule? Adenosine diphosphate (ADP) is a nucleoside diphosphate structurally very similar to GDP involved in cellular energy metabolism and extracellular signaling (reviewed in Schwiebert and Zsembery 2003; Maruyama 1991). Like GDP β S, adenosine 5'-O-2-thiodiphosphate (ADP β S) is nonhydrolyzable due to an oxygen to sulfur switch at the terminal phosphate (Cusack and Hourani 1981; Oldham and Hamm 2008) but extremely unlikely to bind to the tight nucleotide pocket of G α (Oldham and Hamm 2008; Lambright et al. 1994). Unlike with GDP β S, ADP β S (2 mM) in the pipette did not slow or reduce the inhibition of VGSC current by cinacalcet (n = 8) compared to our control condition in recordings with 0.3 mM GTP (n = 12, Figures 1.3E and 1.3F). Third, did GDP β S alter VGSC resistance to direct blockers and thus reduce the effectiveness of ACMs? To address this question we tested if GDP β S affected the actions of other VGSC blockers (Rogawski et al., 2016). VGSC currents were reduced by $37 \pm 5\%$ and $46 \pm 5\%$ by the application of carbamazepine (Figure 1.3G, 100 μ M, n = 7) and phenytoin (100 μ M, n = 9) respectively. This effect was unchanged by GDP β S (Figure 3G; $32 \pm 5\%$ for carbamazepine, n =9; $39 \pm 6\%$ for phenytoin, n = 9) indicating

GDP β S was not simply increasing VGSC resistance to direct inhibitors. These experiments are consistent with GDP β S inhibiting ACM-mediated inhibition of VGSC currents via a GTP-dependent mechanism.

Basal activity of G-proteins has been reported in many systems arising from constitutive activity or low basal activation of the GPCR (Seifert and Wenzel-Seifert 2002). We hypothesized that non-hydrolyzable GTP analog and G-protein signaling activator guanosine 5'-O-[gamma-thio]triphosphate (GTP γ S) may accelerate rundown of VGSC current in the absence of ACMs if there was basal activity of this signaling pathway. VGSC currents were activated with 30 ms steps from -70 mV to -10 mV at 0.2 Hz and recordings were made with either GTP (0.3 mM), GDP β S (2 mM), or GTP γ S (500 μ M) in the pipette solution (Figure 1.3H). GTP γ S accelerated VGSC rundown compared with GTP and GDP β S (Figure 3H, two-way ANOVA with repeated measures, Interaction F (68,1768) = 2.13, $P < 0.0001$). With GTP and GDP β S in the pipette, VGSC currents decreased by $36 \pm 4\%$ ($n = 20$) and $34 \pm 6\%$ ($n = 24$) during the first 5 minutes of recording whereas the same decrease occurred in 95 s in the presence of GTP γ S ($n = 12$). These data indicate that the ACM-induced inhibition of VGSC current is independent of the CaSR but dependent on G-proteins.

Molecular Targets for G-Protein-Mediated VGSC Inhibition

To identify potential targets for cinacalcet, we tested if its action was affected by antagonists to GPCRs structurally similar to CaSR (Urwyler 2011). VGSC current was elicited with 30 ms voltage steps to -10 mV and neurons were perfused with a

metabotropic glutamate receptor (mGluR) mGluR1 or mGluR5 blocker (competitive antagonist or negative allosteric modulator) for a minimum of 120 s before the application of cinacalcet (6 μ M) (Figure 1.4A). Perfusion of the blockers continued during the application of cinacalcet. None of the mGluR1 and mGluR5- antagonists or negative allosteric modulators tested (30 μ M 2-Methyl-6-(phenylethynyl)-pyridine (MPEP), 50 μ M 3-Methoxybenzaldehyde [(3-methoxyphenyl)methylene]hydrazone (DMeOB), 150 μ M LY 367385, or 500 nM JNJ 16259685 slowed or reduced the cinacalcet-induced inhibition (Figure 1.4B). In addition, mGluR1 and mGluR5 agonists, (*RS*)-2-chloro-5-hydroxyphenylglycine (CHPG) (100 μ M) and (*S*)-3,5-dihydroxyphenylglycine (DHPG, 100 μ M), did not inhibit VGSC currents, indicating cinacalcet was not activating these receptors (data not shown). Similarly, application of glutamate (10 μ M; applied in the presence of ionotropic glutamate receptors antagonists 6-cyano-7-nitroquinoxaline-2,3-dione (CNQX) (10 μ M) and DL-2-amino-5-phosphonopentanoic acid (APV) (50 μ M) and GABA_A receptor antagonist bicuculline (10 μ M) did not affect VGSC current (Figure 1.4C; n = 9). Next, we tested if cinacalcet acted through class C GPCRs GABA_B receptors by applying cinacalcet in the presence of GABA_B receptor antagonist saclofen. Reducing GABA_B receptor activity with saclofen (500 μ M) did not alter the cinacalcet-induced response (Figure 1.4D; n = 6). Furthermore, stimulation of GABA_B receptors with baclofen (10 μ M) did not significantly reduce VGSC current in a manner similar to that observed with the application of cinacalcet (data not shown). These data indicate that cinacalcet does not inhibit VGSCs through the activation of metabotropic glutamate receptors or GABA_B receptors.

GPCRs can be coupled to a range of different G-protein complexes; the primary families being $G_{i/o}$, G_q , G_s , and G_{12} (Neves et al. 2002). Pertussis toxin (PTx) is a specific inhibitor of $G_{i/o}$ signaling (Ui et al. 1986). Pre-incubation with PTX (200 ng/mL) for either 16-24 (n = 8) or 48-72 hours (n = 6) did not alter the cinacalcet-induced inhibition of VGSC currents, indicating that the pathway was mediated by G-proteins other than $G_{i/o}$ (Figure 1.4E and 1.4F).

G-protein-activated phosphorylation of VGSCs by PKA and PKC reduces VGSC current by 20 -40% (Cantrell et al. 1999; Carlier et al. 2006; Carr et al. 2002). To test if these kinases mediate the cinacalcet-induced reduction in VGSC current, we performed whole-cell recordings with PKA- or PKC-specific blockers in the pipette solution (Figures 1.4G and 1.4H). The cinacalcet effect on steady-state inhibition, latency of action, and rate of inhibition of VGSC currents were unaffected by the PKA inhibitor PKI₆₋₂₂ (20 μ M; Figure 4F; n = 8). Additionally, PKC inhibitors PKI₁₉₋₃₆ (20 μ M, n = 4) and chelerythrine chloride (10 μ M, n = 7) did not affect the action of cinacalcet on VGSC currents (Figure 1.4H). Furthermore, the broad-spectrum kinase inhibitor staurosporine (100 nM, n = 8) was also ineffective in the pipette solution (Figure 1.4H). While the data do not rule out the involvement of staurosporine-resistant kinases, they indicate that cinacalcet-induced inhibition occurs in a PKA- and PKC-independent manner.

G-protein-dependent modulation can occur directly via $G\beta\gamma$ binding to VGSCs and a resultant change in gating properties or via small G-proteins. To test the first hypothesis, we blocked $G\beta\gamma$ with the small molecule inhibitor gallein which binds to $G\beta\gamma$ and

prevents its interaction with effector proteins (Lehmann et al. 2008; Seneviratne et al. 2011). Pre-incubation with gallein (50 μ M) for 24 hours (n = 11) did not alter the cinacalcet-induced inhibition of VGSC currents compared the vehicle control (n= 7; Figure 1.5IA and 1.5B). These data, however, do not completely rule out a G β γ -dependent mechanism as gallein has been shown to exhibit G β γ isoform-specific inhibition and does not block the G β γ -dependent effects on N-type voltage-gated calcium channels (VGCCs), G-protein-coupled inwardly-rectifying potassium channels (GIRKs), extracellular signal-regulated kinase ERK1/2 (Bonacci et al. 2006), or adenylyl cyclases ACII, IV, and VI (reviewed in Lin and Smrcka 2011).

To test the second hypothesis that a small G-protein may inhibit VGSCs, we blocked the Rho family of small G-proteins with glucosylation via *Clostridium difficile* (Just et al. 1995). Rho proteins are GTP-binding proteins that regulate the actin cytoskeleton, myosin filaments, and cell cycle progression (Chen et al. 2015). Pre-incubation with *C. difficile* (500 pg/mL) for 24 hours (n = 8) did not alter the cinacalcet-induced inhibition of VGSC currents compared the control (n= 11; Figure 1.5C and 1.5D). These data therefore indicate that cinacalcet does not stimulate Rho family small G-proteins to inhibit VGSCs. This does not discount the action of other classes of small G-proteins in this process but removes the possibility of this expansive family of easily pharmacologically-targeted proteins.

Cinacalcet Promotes Inactivation of VGSC Current

To determine how cinacalcet inhibited VGSC current, we evaluated the effect of cinacalcet on VGSC gating properties. VGSC gating properties were tested in neocortical neurons with shorter processes (24 to 48 hours in culture to reduce space clamp errors). Activation was studied by eliciting VGSC currents with a series of 10 ms voltage steps from -70 mV to between -65 and +40 mV in 5 mV increments at 0.2 Hz (Figure 1.6A). Steady-state inactivation was then studied by activating VGSC currents with a 20 ms test pulse to -10 mV preceded by a 500 ms conditioning step to between -140 and -20 mV in 10 mV increments (Figure 1.6C). Cinacalcet (1 μ M) was then applied until the VGSC current had decreased by ~50% and VGSC current activation and inactivation reexamined. In the exemplar, cinacalcet reduced the peak VGSC currents by ~50% at voltages above -40 mV (Figure 1.6B). However, strong hyperpolarization reversed the inhibition of the VGSC current to only 10% (Figure 1.6D), consistent with cinacalcet promoting VGSC inactivation. Average conductance-voltage plots, derived from the current-voltage curves, were normalized to facilitate comparison of half-activation voltages ($V_{0.5}$). The change in $V_{0.5}$ ($\Delta V_{0.5}$) for the steady-state inactivation was strongly shifted (-11 ± 3 mV) by the application of cinacalcet; the average $V_{0.5}$ for control and cinacalcet were -69 ± 3 mV and -81 ± 5 mV, respectively (Figure 1.6E; $n = 11$; $P = 0.002$). A smaller $\Delta V_{0.5}$ was seen for activation (Figure 1.6E; -33 ± 1 mV and -36 ± 1 mV in control and cinacalcet, respectively, $n = 15$; $P = 3 \times 10^{-5}$). The shift in gating confirms that cinacalcet promotes the inactivated state, thereby reducing the amplitude of the VGSC current. GDP β S also blocked the hyperpolarizing shift in steady-state inactivation of VGSCs (Figure 1.6F; $\Delta V_{0.5} = -3 \pm 1$ mV, $n = 9$; $P > 0.05$) consistent

with the proposal that cinacalcet inhibits VGSCs by a G-protein-mediated mechanism that stabilizes the inactivated state.

Since strong hyperpolarization (-140 mV for 500 ms) only partially reversed the inactivation by cinacalcet, we tested if a greater fraction of inhibition was reversible with longer hyperpolarizing pulses (Jo and Bean 2011; Karoly et al. 2010). A double-pulse protocol (S1 and S2, each -10 mV for 10 ms) was used to elicit VGSC currents (I_{S1} and I_{S2}) in control or after complete block by cinacalcet (10 μ M; Figures 1.7A). I_{S2} was fully recovered within <10 ms in control experiments. After full block by cinacalcet, I_{S2} recovered to $81 \pm 1\%$ of I_{S1} (pre- cinacalcet application) after a 3 s step to -120 mV (Figures 1.7A and 1.7B). The time course of recovery of I_{S2} was described by a single exponential ($T = 841 \pm 73$ ms; $n = 10$).

VGSC inactivation could arise from cinacalcet-mediated signals binding preferentially to specific channel states (Karoly et al. 2010) and thus be use-dependent. We tested this hypothesis by examining the rate of VGSC current inhibition on duration of voltage step and the duty cycle of activation. VGSC currents were activated with depolarizing steps (5 or 30 ms) at rates of 0.2 - 5 Hz (Figure 1.7C). G-protein mediated modulation of an ion channel is a multi-step process that has previously been shown to have complex kinetics (see Yakubovich et al. 2005) that can be approximated by the function $f(t) = Ae^{-(t/T)^2} + B$ (equation 1). The kinetics of VGSC inhibition by cinacalcet were well-described by this function, where t represents time, T the time constant of the inhibition, and A and B represent constants (Figure 1.7C). The modest change in time constant at

different stimulation frequencies indicated little use-dependent inhibition at rates of 0.2 Hz – 5 Hz stimulation (Figure 1.7D). In contrast, inhibition was slowed when we examined the action of cinacalcet at substantially lower rates of VGSC opening and closing (Figure 1.7E). VGSC currents were elicited by 30 ms depolarizing steps (-70 to -10 mV) at a frequency of 0.2 Hz but then paused immediately prior to cinacalcet (10 μ M) application. After the first 200 s of cinacalcet application the voltage protocol was resumed revealing that cinacalcet-mediated inhibition of VGSC currents was substantially smaller in the absence of the depolarizing steps (60 ± 7 %, $n = 7$) than in control experiments (84 ± 4 %, $n = 11$; $P = 0.006$; Figures 1.7E). These data indicate that cinacalcet-induced inhibition of VGSC is impaired at very low rates of channel activity and hence inhibition is use-dependent.

Ca^{2+} -bound calmodulin (CaM) has been shown to bind to VGSCs and to shift VGSC inactivation (Tan et al. 2002; Yan et al. 2017). We hypothesized that increases in intracellular [Ca^{2+}]_i ([Ca^{2+}]_i), might accelerate cinacalcet-mediated inhibition of VGSCs by facilitating inactivation. Using our standard protocol (Figure 1.1E) we found elevation of [Ca^{2+}]_i by increasing Ca^{2+} entry via voltage-gated Ca^{2+} channels (VGCCs) (Figured 1.8A and 1.8B) did not affect the action of cinacalcet on VGSC currents. Attenuating intracellular buffering with Ca^{2+} buffer ethylenediaminetetraacetic acid (EDTA) in pipette (Figures 1.8C and 1.8D) also did not change cinacalcet-induced VGSC inhibition. Interestingly block of VGCCs with the non-selective VGCC blocker, Cd^{2+} , tended to slow the rate of VGSC current block by cinacalcet (Figures 1.8A and 1.8B, $P = 0.13$). The data do not support the hypothesis that Ca^{2+} -bound CaM is accelerates cinacalcet-

mediated inhibition of VGSCs but we cannot exclude the possibility that binding interactions such as these may contribute to use-dependence.

Cinacalcet Inhibits VGSC Current in Acutely Isolated Neocortical Neurons

To rule out distortion of the kinetics of action of cinacalcet by voltage-clamp errors or long diffusion path lengths arising from neuronal processes, we examined VGSC currents in acutely isolated central neurons with short processes (Figure 1.9). VGSC currents were elicited with a 5 ms step from -70 mV to 0 mV. Just as in cultured neocortical neurons, VGSC currents in neurons isolated from acute neocortical and hippocampal slices were strongly and uniformly sensitive to cinacalcet (10 μ M); inhibited by $91 \pm 2\%$ and $95 \pm 1\%$ in neocortical ($n = 8$) and hippocampal ($n = 10$) neurons, respectively (Figures 1.9A and 1.9C). The kinetics of cinacalcet inhibition of VGSC currents in these acutely isolated neurons were well described by equation 1 (Figure 1.9A). The rate of inhibition by cinacalcet was faster in the acutely isolated cells in comparison to cultured neocortical neurons (Figure 1.9D). Cinacalcet mediated VGSC current inhibition was also reversed by strong hyperpolarization in the acutely isolated neurons, with complete recovery achieved by a 1 s step to -120 mV (Figure 1.9B). These data indicate that strong cinacalcet-mediated inhibition of VGSC currents occurred in both acutely isolated and cultured cortical neurons.

G-protein-mediated inhibition of VGSC currents was described in a subgroup of neocortical and hippocampal neurons via activation of muscarinic acetylcholine M1 receptors (mAChR) and D1-like dopamine receptors (Cantrell et al. 1996; Cantrell et al.

1997). While cinacalcet substantially inhibited VGSC currents in these recordings, the dopamine agonist SKF 81297 (1 μ M) and mAChR M1 agonist carbachol (20 μ M) had no effects on VGSC currents in acutely isolated neurons from the neocortex (Figures 1.9A and 1.9C) and hippocampus (Figure 1.9C) or in cultured neocortical neurons (Figure 1.9E), confirming that cinacalcet and these neurotransmitters act via distinct pathways.

Discussion

VGSCs generate the upstroke of the action potential that has classically been described as a digital, all-or-none signal. We have described a new pathway that is apparently ubiquitous in neocortical and hippocampal neurons and inhibits VGSCs in a graded manner by a G-protein-dependent mechanism. A number of features about this pathway are interesting. First, allosteric CaSR agonists stimulate this pathway. Second, this pathway appears independent of the CaSR because it is insensitive to external $[Ca^{2+}]$, occurs in *Casr*^{-/-} mutants, and is also stimulated by allosteric CaSR antagonists. Third, this GTP-dependent inhibition of VGSCs is not mediated by mGluR1, mGluR5, or GABA_B receptors, which have strong structural homology with the CaSR. Fourth, this form of VGSC modulation is independent of PKA and PKC. Finally, the G-protein-mediated inhibition of VGSCs shifts steady-state inactivation of VGSCs and this can be reversed by prolonged hyperpolarization.

G-protein-mediated regulation of voltage-gated calcium and potassium channels has been a major area of scientific interest (Hille et al. 2014; Holz et al. 1986; Pfaffinger et al. 1985; Weiss and Zamponi 2015). In contrast, G-protein regulation of VGSCs has

received substantially less attention. Earlier studies showed that VGSC currents in the neocortex and hippocampus were reduced by ~20-40% through mAChR M1, D1-like dopamine receptor, mGluR1, and serotonin 5-HT_{2A/C} receptor activation (Cantrell et al. 1996; Cantrell et al. 1997; Carlier et al. 2006; Carr et al. 2002). In contrast, our findings show near complete inhibition of VGSCs is possible in a large majority of cortical neurons and this points to the existence of a signaling pathway that could substantially regulate neuronal activity in the cortex. The effectiveness of GDPβS to block the action of all four tested ACMs on VGSC currents and GTPγS to accelerate the rate of decrease of basal VGSC currents strongly indicate the involvement of G-proteins in the pathway (Figure 1.3). These established tools competitively inhibit endogenous ligands interacting with the G-protein nucleotide-binding pocket (Lambright et al. 1996; Lu and Ikeda 2016; Oldham and Hamm 2007; Suh et al. 2004). Non-hydrolyzable GDPβS reduces G-protein activation by GTP despite GPCR activation whereas GTPγS will enhance G-protein signaling because it attenuates endogenous nucleotide hydrolysis that terminates G-protein activity (Oldham and Hamm 2007). The likelihood of GDPβS acting via unidentified G-protein independent pathways seemed low because we excluded direct chemical modification of cinacalcet, off-target effects of the terminal sulfur atom, and reduced sensitivity of VGSC to direct blockers as causes for GDPβS block of cinacalcet-mediated VGSC inhibition (Figure 1.3). Another possibility is that cinacalcet blocks VGSCs by directly binding to and stabilizing a slow inactivated state of the channel and that GDPβS modulates the high-affinity state to prevent cinacalcet binding. The inability of GDPβS to impact VGSC block by phenytoin or carbamazepine

makes this mechanism less likely but does not rule it out. On balance, data point to VGSC inhibition by cinacalcet being mediated by G-proteins.

A number of questions remain about the mechanism of inhibition of VGSCs by ACMs. What is the identity of the GPCR that mediates the effects of ACMs on VGSCs? We found cinacalcet-mediated inhibition was independent of the CaSR and other class C GPRs: mGluR1, mGluR5, and the GABA_B receptor (Figures 1.4B and 1.4D). Cinacalcet-mediated inhibition of VGSCs was also distinguished from other GPCR-mediated pathways (mAChR M1, D1-like dopamine receptors, 5-HT_{2A/C} receptor, and mGluR1) (Cantrell et al. 1997; Cantrell et al. 1996; Carlier et al. 2006; Carr et al. 2002) by its resistance to PKA and PKC inhibition (Figure 1.4H). Furthermore, stimulation of mAChR receptors and D1-like dopamine receptors did not reduce VGSC currents in cinacalcet-sensitive neurons indicating further separation between the mechanisms underlying cinacalcet-mediated and other forms of G-protein-mediated inhibition of VGSCs (Figures 1.9C and 1.9E).

VGSCs and VGCCs share a number of properties (Ben-Johny et al. 2015) and by analogy with VGCCs, where G-protein interactions appear complex, there may be several sites at which VGSCs are targeted by G-proteins (Proft and Weiss 2015). For one, VGSCs include six serine residues on the α subunit of the channel that serve as candidate molecular targets for GPCR-activated kinase inhibition of VGSCs (Rossie and Catterall 1989; Rossie et al. 1987; Smith and Goldin 1996; West et al. 1991). Another possible mechanism for cinacalcet-induced inhibition is the direct action of the G $\beta\gamma$

dimer of the G-protein complex on these channels. This type of G-protein-to-ion-channel interaction has been observed with both potassium and calcium channels (Clapham 1996; Ikeda 1996; Krapivinsky et al. 1995; Navarro et al. 1996). Interestingly, $G\beta_2\gamma_3$ has been shown to interact with $Na_v1.2$ at the C terminus and this interaction increases persistent sodium channel current in proportion to transient VGSC current in tsA-201 cells (Mantegazza et al. 2005). Future experiments will address the identity of the major players responsible for inhibition of VGSCs by ACMs.

Acting indirectly, cinacalcet promoted VGSC inactivation and so decreased VGSC availability at -70 mV. This provides the mechanism of VGSC inhibition by cinacalcet (Figure 1.6) and is similar to how other G-protein mediated forms of VGSC inhibition occur (Cantrell et al. 1999; Carr et al. 2002). Prolonged hyperpolarization reversed cinacalcet-mediated VGSC modulation (Figure 1.7B and 1.9B), indicating the reduced reversibility observed in earlier experiments (Figure 1.11) did not simply result from VGSC loss or rundown. Instead the slow recovery from inactivation following strong hyperpolarization may be due to the promotion of slow VGSC inactivation or due to slow dissociation of blocking molecules from the fast inactivation state (Karoly et al. 2010). Certainly the near-complete relief of ACM-induced inhibition of VGSCs by the G-protein signaling blocker $GDP\beta S$ suggests that this effect is due to an indirect action of cinacalcet on VGSCs, in contrast to the use-dependent pore-blockers (Karoly et al. 2010; Kuo and Bean 1994b). Cinacalcet-mediated inhibition of VGSCs was significantly reduced at very low frequencies of VGSC activation (Figures 1.7C and 1.7E) implying that low rates of VGSC cycling will attenuate the effectiveness of the G-protein

dependent pathway or conversely that the pathway will become more influential when neuronal excitability is increased. As we showed, changes in intracellular calcium did not impact cinacalcet-mediated inhibition of VGSC currents. Neither elevating $[Ca^{2+}]_i$ by increasing Ca^{2+} entry via VGCCs, attenuating intracellular Ca^{2+} buffering with EDTA, nor decreasing $[Ca^{2+}]_i$ by reducing Ca^{2+} entry via VGCCs with Cd^{2+} affected cinacalcet-mediated inhibition of VGSC currents, indicating no substantial CaM-VGSC interaction underlying this pathway (Figure 1.8).

What are the other functional implications for this pathway? Multiple lines of evidence indicate that VGSC density and gating characteristics are important in shaping action potentials within a specific neuron (Bean 2007; Lewis and Raman 2014). VGSC current inhibition that relies on slow inactivation has been shown to reduce a neuron's ability to sustain trains of spikes (Carr et al. 2003). We predict that the strong, slow inhibition of VGSC by CaSR modulators should have similar effects. In addition to modulating general cellular excitability, the pathway may have other important actions. Inhibition of VGSCs in a branching axon provides a mechanism by which failures in synaptic transmission could be explained (Figure 1.1B). Regulation of action potential propagation throughout the axonal arbor has been proposed as an important form of synaptic plasticity (Debanne 2004). One such example is in the nucleus of the solitary tract where a significant fraction of synapses respond to arginine vasopressin (AVP) by switching from a release probability of 0.9 at ~20 release sites in the same axon to a complete failure of transmission (Bailey et al. 2006). The simplest explanation for this is that AVP acts to cause failure of action potential propagation at a proximal axonal

branch point. Identification of the receptor by which cinacalcet inhibits VGSC current may allow us to determine if such a mechanism contributes to synaptic plasticity.

Cinacalcet has been used to treat forms of hyperparathyroidism in an attempt to reduce the complications of elevated serum calcium levels (Nemeth and Goodman 2016). Despite reducing parathyroid hormone (PTH) levels, cinacalcet did not reduce mortality (EVOLVE Trial Investigators et al. 2012). Could harmful off-target effects in neurons explain cinacalcet's apparent lack of efficacy? It may seem unlikely, given that at clinical doses cinacalcet serum levels are ~50 nM (Padhi and Harris 2009) so that only ~2% of the VGSCs would be blocked (Figure 1.1E). However, similarly small fractions of VGSCs are blocked by clinically effective doses of phenytoin (Brodie et al. 1985; Kane et al. 2013). Moreover cinacalcet's high volume of distribution and partition coefficient indicate higher brain concentrations due to accumulate are likely. Consequently, we cannot dismiss the possibility that clinically important off-target effects of cinacalcet may arise from VGSC block. CaSR modulators that are not lipophilic and less likely to cross the blood brain barrier are being synthesized and tested clinically (Martin et al. 2014), indicating cinacalcet actions in the brain may be important.

In conclusion, we have shown that a broad range of GPCR modulators block VGSC currents in a GTP-dependent fashion. The strength of block and reversal by hyperpolarization confirm that this mechanism is positioned to regulate neuronal excitability under a range of physiological and pathological conditions.

Methods

Neuronal Cell Culture

Neocortical neurons were isolated from postnatal day 1–2 mouse pups of either sex as described previously (Phillips et al. 2008). All animal procedures were approved by V.A. Portland Health Care Health Care System Institutional Animal Care and Use Committee in accordance with the U.S. Public Health Service Policy on Humane Care and Use of Laboratory Animals and the National Institutes of Health Guide for the Care and Use of Laboratory Animals. Animals were decapitated following general anesthetic with isoflurane and then the cerebral cortices were removed. Cortices were incubated in trypsin and DNase and then dissociated with a heat polished pipette. Dissociated cells were cultured in MEM plus 5% FBS on glass coverslips. Cytosine arabinoside (4 μ M) was added 48 hours after plating to limit glial division. Cells were used between 1 and 12 days in culture. Homozygous lox *Casr*, nestin-cre negative females and positive males were mated to produce conditional cre *Casr*^{-/-} mutants (Chang et al. 2008). DNA extraction was performed using the Hot Shot Technique (Truett et al. 2000) with a 1-2hr boil. Primers used for cre PCR were: Nes-Cre 1: GCAAACAGGCTCTAGCGTTTCG, Nes-Cre 2: CTGTTTCACTATCCAGGTTACGG; run on a 1% agarose gel. Primers for lox PCR are: P3U: TGTGACGGAAAACATACTGC, Lox R: GCGTTTTTAGAGGGAAGCAG. Samples were run on a 1.5% agarose gel for identification as *Casr*^{-/-} or *Casr*^{+/+}.

Acute Isolated Neurons

Mice postnatal day 11 to 19 were decapitated under anesthesia then brain was rapidly dissected and placed in chilled, oxygenated (4 °C, 95% O₂, 5% CO₂) choline chloride-based artificial cerebrospinal fluid (ACSF) and horizontal or coronal slices (400 μm thick) were cut with vibratome Leica VT 1200S. Slices were incubated in standard ACSF for 1 hour and then treated for 30-40 min with 0.5 mg/ml protease type XIV (Sigma Aldrich) in Tyrode's solution (below) containing only 100 μM of CaCl₂. After enzyme treatment, slices were rinsed with standard ACSF and mechanically dissociated using glass pipettes of decreasing size. Cells were used <1 hour after dissociation.

Electrophysiological Recordings

Cells were visualized with a Nikon Diaphot, Leica DM IRB inverted microscope, or Scientifica SliceScope. Whole-cell voltage-and current-clamp recordings were made from cultured neocortical neurons using a HEKA EPC10 USB amplifier or Axoclamp 200B. Except where stated in the text, extracellular Tyrode's solution contained (mM) 150 NaCl, 4 KCl, 10 HEPES, 10 glucose, 1.1 MgCl₂, 1.1 CaCl₂, pH 7.35 with NaOH. Extracellular choline chloride based ACSF (ChACSF) contained (mM) 122 choline chloride, 2.5 KCl, 1.25 NaH₂PO₄, 25 NaHCO₃, 8 Glucose, 0.8 CaCl₂, 4 MgCl₂. Extracellular standard ACSF contained (mM) 129 NaCl, 3.3 KCl, 25 NaHCO₃, 5 Glucose, 0.4 Na₂HPO₄, 0.4 KH₂PO₄, 1 MgCl₂, 1.5 CaCl₂. VGSC current recordings were made using a cesium methane-sulfonate intracellular solution containing (mM) 113 CsMeSO₃, 1.8 EGTA, 10 HEPES, 4 MgCl₂, 0.2 CaCl₂, 4 NaATP, 0.3 NaGTP, 14 creatine phosphate, pH 7.2 with TEA hydroxide. In some experiments GTP was

replaced with 2 mM GDP β S (Figures 1.3A-D), 2 mM ADP β S (Figures 1.3E and 1.3F), or 0.5 mM GTP γ S (Figure 1.3H). IPSCs (Figure 1.1B) were recorded using a potassium chloride-rich intracellular solution containing (mM) 118 KCl, 1 EGTA, 10 HEPES, 4 MgCl₂, 1 CaCl₂, 4 NaATP, 0.3 NaGTP, 14 creatine phosphate, 1 QX-314, pH 7.2 with KOH. To pharmacologically isolate IPSCs 10 μ M CNQX was added to the bath. IPSCs were completely blocked by 40 μ M gabazine or 10 μ M bicuculline indicating that they were mediated by GABA. Recordings of action potentials (Figure 1.1C) and potassium channel current (Figure 1.1G) were made using a potassium gluconate-rich intracellular solution containing (mM) 135 K-Gluconate, 10 HEPES, 4 MgCl₂, 4 NaATP, 0.3 NaGTP, 10 creatine phosphate, pH 7.2 with KOH. To record isolate action potentials 40 μ M CNQX, 80 μ M APV, and 40 μ M gabazine were added to the bath. Electrodes used for recording had resistances ranging from 2 to 4 M Ω . Voltages indicated have been corrected for liquid junction potentials. All experiments were performed at room temperature (20-24 °C).

Data Acquisition and Analysis

Whole-cell voltage-and current-clamp recordings were filtered at 3-5 kHz using a Bessel filter, and sampled at 100 kHz. Leak current was subtracted online using a -p/n protocol. R_s was compensated by 60-90%. Analysis was performed using Igor Pro (Wavemetrics, Lake Oswego, OR). Unless otherwise stated, recordings were only included if the rate of baseline rundown was < 10% over 100 seconds. Data values are reported as mean \pm SEM. Statistical significance was determined using *Student's t-test, two-tailed* (Microsoft Excel) unless otherwise noted. The action of nucleotide on the rate

of VGSC rundown was evaluated using a two-way ANOVA (Graphpad, Prism, version 6). ANOVA is reported in Table 1.1.

Solution Application

Solutions were gravity fed through a glass capillary (1.2 mm outer diameter) placed ~1 mm from the patch pipette tip. Most reagents were obtained from Sigma-Aldrich (Darmstadt, Germany). NPS 2143, PKI₁₉₋₃₆, staurosporine, saclofen, SKF 81297, carbachol, and CHPG were supplied by Tocris (Bristol, United Kingdom). PKI₆₋₂₂, JNJ 16259685, and baclofen were supplied by Santa Cruz Biotechnology (Dallas, United States). PTx was supplied by Millipore Sigma (Burlington, Massachusetts). Cinacalcet was supplied by Toronto Research Chemicals (Toronto, Canada) and TTX by Alomone (Jerusalem, Israel). Phenytoin, carbamazepine, and CHPG were dissolved in DMSO (final concentration 0.125%). Gallein was dissolved in DMSO (final concentration 0.05%). NPS 2143, Calhex, MPEP, DMeOB, staurosporine, and chelerythrine chloride were dissolved in DMSO to a final concentration of $\leq 0.03\%$ DMSO. JNJ 16259685 was dissolved in ethanol (final concentration 0.05%). Appropriate vehicle controls were performed for all experiments.

Acknowledgements

This work was supported by grants NIGMS (R01 GM097433) and U.S. Department of Veterans Affairs (BX002547) awarded to SMS. In addition, GBM was supported by ARCS, NHLBI (T32HL083808) and NINDS (1F31NS095463). The *Casr*^{-/-} mice were kindly provided by Dr. Wenhan Chang, UCSF and San Francisco VAMC. We are

grateful to Dr Courtney Williams for performing the experiments examining synaptic transmission (Figure 1.1B) and to Briana Knight for help with cell culture. We thank the Smith lab members and Drs Henrique von Gersdorff, Laurence Trussell, and John Williams for productive discussion. The authors declare no competing financial interests.

Author Contributions

G.M. and S.S. designed the study and wrote the manuscript. G.M. and T.T. (Figures 1.9A-D) conducted experiments. G.M., S.S. ,and T.T. analyzed the data.

Figures

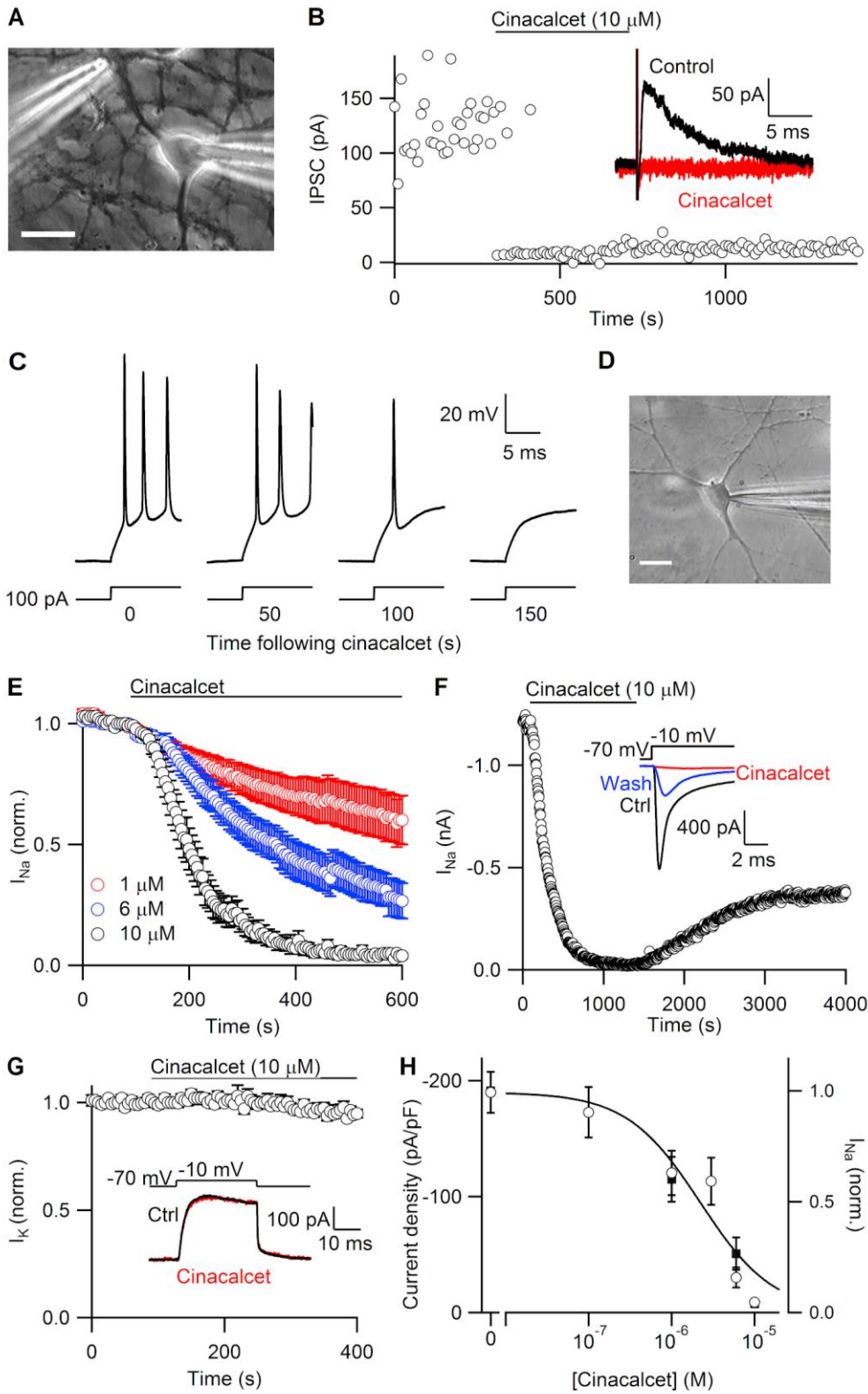


Figure 1.1. Inhibition of VGSC current by CaSR allosteric agonist cinacalcet. (A) Image of whole-cell voltage clamp recording from a cultured neocortical neuron with theta electrode used to evoke IPSCs. Scale bar indicates 10 μm . (B) Diary plot showing GABA-evoked IPSC amplitude was reduced by application of 10 μM cinacalcet (application indicated by horizontal bar). *Inset*, Representative IPSCs in vehicle control (black) and after steady-state effect of cinacalcet (red). (C) Current clamp recordings showing action of cinacalcet on response to 100 pA current injections. (D) Image of whole-cell voltage clamp recording from a cultured neocortical neuron. Scale bar indicates 10 μm . (E) Diary plot of average normalized VGSC current elicited by a 30 ms test pulse to -10 mV from a holding potential of -70 mV every 5 s during perfusion of 10 μM (n = 11), 6 μM (n = 9), or 1 μM cinacalcet (n = 9). (F) Exemplar plot of peak VGSC current elicited as in E following application of 10 μM cinacalcet with recovery. *Inset*, Representative VGSC current in control conditions (ctrl, black), at maximal cinacalcet-induced block (red), and at the point of greatest recovery (blue). (G) Diary Plot of average normalized voltage-gated potassium channel current elicited by a 30 ms, 60 mV depolarizing step every 5 s during bath perfusion of 10 μM cinacalcet (n = 5). *Inset*, Representative potassium current in control conditions (ctrl, black) and at maximal cinacalcet-induced block (red). (H) Concentration-effect relationship for cinacalcet on VGSC currents. *Left axis*, indicates current density following incubation in cinacalcet for 50-70 minutes at the indicated concentration (open circles). VGSC amplitude was measured immediately following whole cell formation with a 30 ms test pulse to -10 mV from a holding potential of -70 mV and normalized to measured cell capacitance (n \geq 10

for each group). Data fit with Hill equation with $IC_{50} = 3.5 \pm 1 \mu\text{M}$ cinacalcet and Hill Coefficient = 0.98. *Right axis*, Normalized VGSC current from E 510 s following the application of 10 μM (n = 11), 6 μM (n = 9), or 1 μM cinacalcet (n = 9) (solid squares). Error bars show mean value \pm SEM.

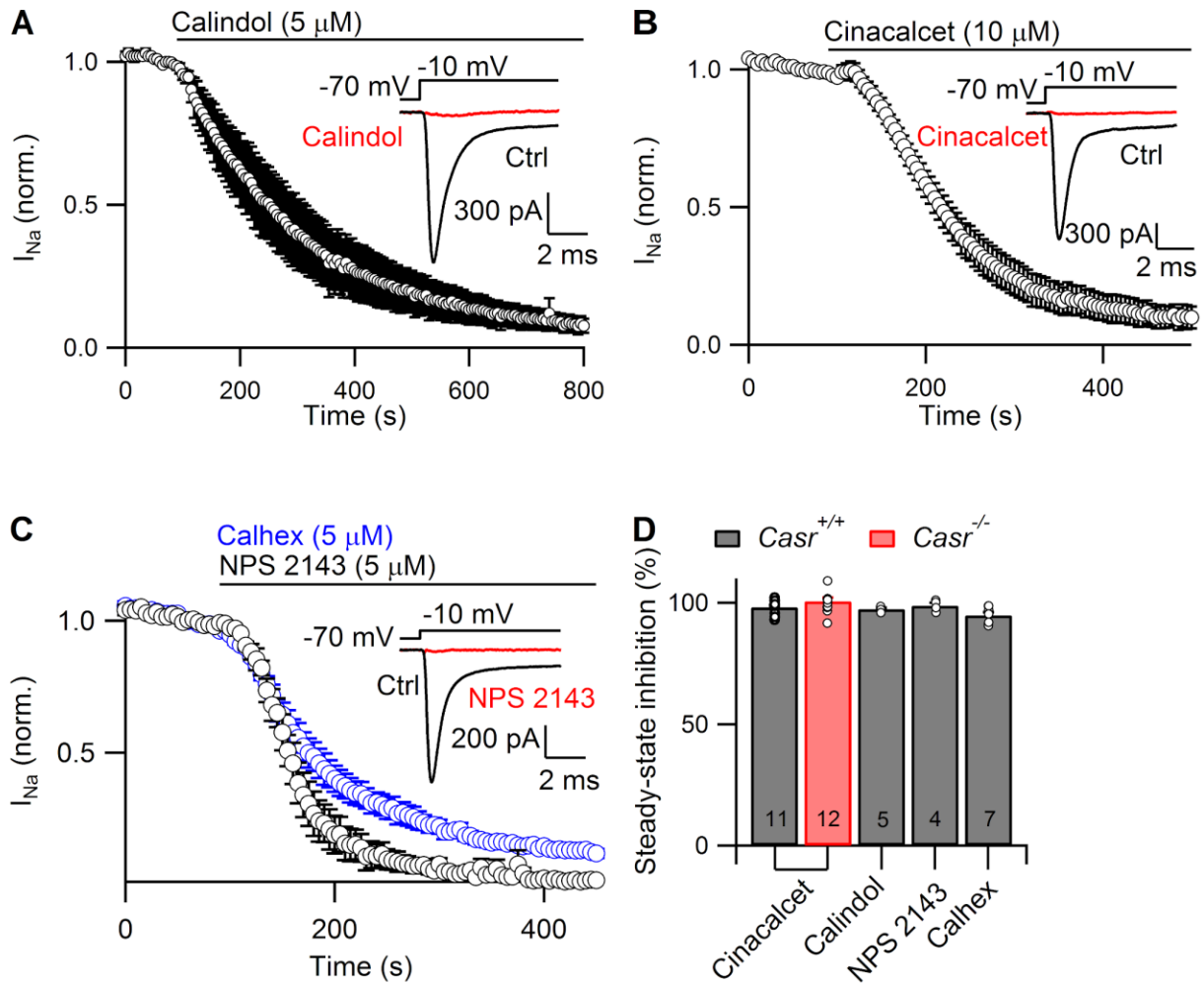


Figure 1.2. CaSR allosteric agonists and antagonists inhibit VGSC current in wildtype ($Casr^{+/+}$) and CaSR null ($Casr^{-/-}$) mutants. (A) Diary plot of average normalized VGSC current (elicited as in Figure 1E) during perfusion of 5 μM calindol ($n = 5$). *Inset*, Representative traces show VGSC current in control (ctrl, black) conditions and after steady-state block by calindol (red). (B) Plot of average normalized VGSC current (elicited as in Figure 1.1E) during perfusion of 10 μM cinacalcet recorded in $Casr^{-/-}$ neocortical neurons ($n = 12$). *Inset*, Representative traces show VGSC current in control conditions (ctrl, black) and after steady-state inhibition by cinacalcet (red). (C) Diary plot

of average normalized VGSC current elicited (as in Figure 1.1E) during bath perfusion of 5 μ M calhex (blue, $n = 7$) or 5 μ M NPS 2143 (black, $n = 4$) recorded in *Casr^{+/+}* neocortical neurons. *Inset*, Representative traces show VGSC current in control conditions (ctrl, black) and after steady-state inhibition by NPS 2143 (red). (D) Bar graph summarizing the effects of 10 μ M cinacalcet, 5 μ M calindol, 5 μ M calhex, or 5 μ M NPS 2143 on VGSC current in *Casr^{+/+}* (black) and *Casr^{-/-}* (red) neocortical neurons. Number in middle of bar indicates n for the given data set. Error bars show mean value \pm SEM.

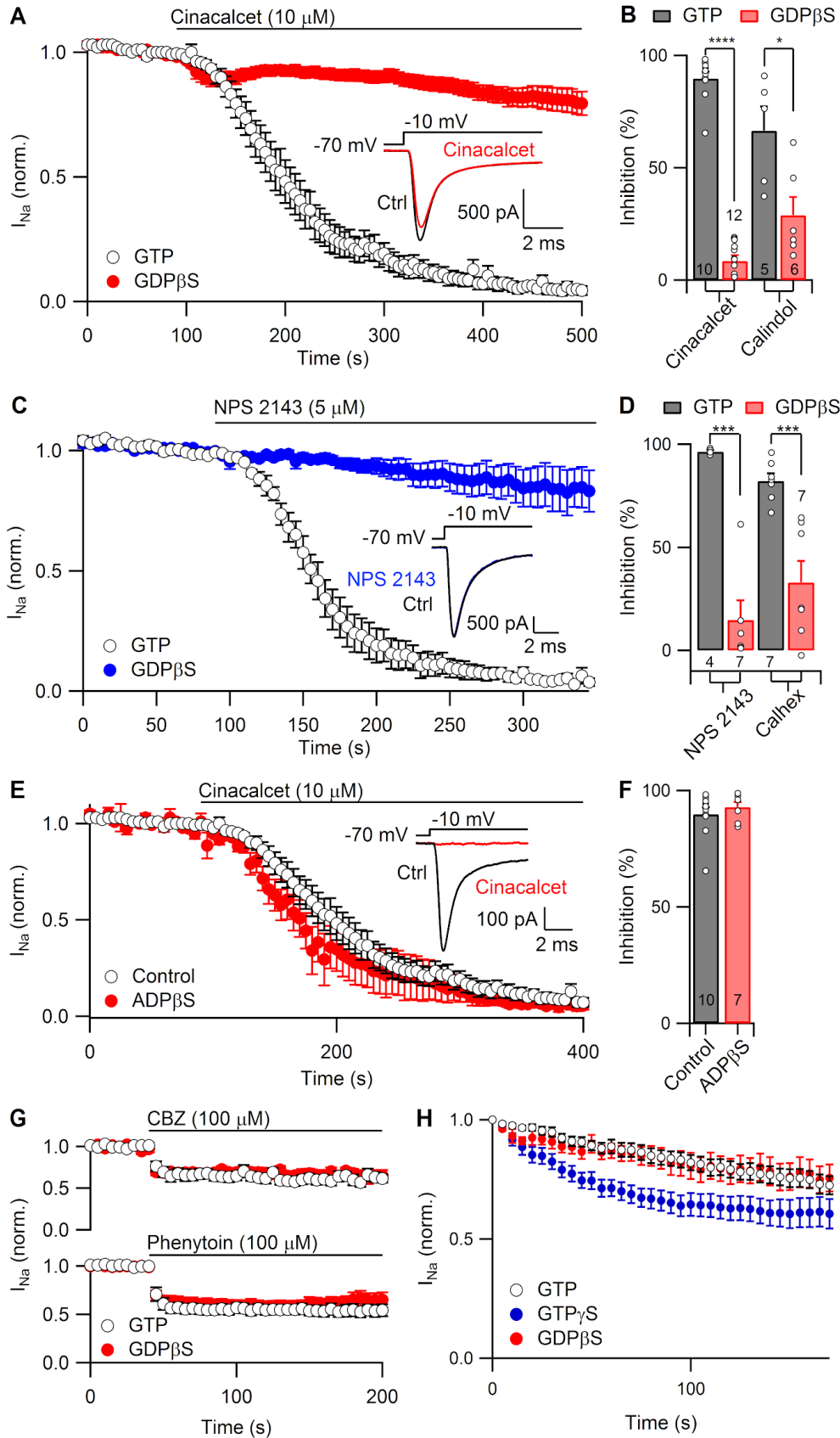


Figure 1.3. Allosteric CaSR modulator block of VGSC current is GTP-dependent. (A) Plot of average normalized VGSC current (elicited as for Figure 1.1E) during perfusion of 10 μ M cinacalcet in control conditions (black, n = 10) or with 2 mM GDP β S in pipette solution (red, n = 12). *Inset*, Representative traces show VGSC current baseline in the presence of 2 mM GDP β S prior to (ctrl, black) and 250 s after the application of cinacalcet (red). (B) Bar graph summarizing the effects of 10 μ M cinacalcet and 5 μ M calindol on VGSC current in control conditions (black) and in recordings with 2 mM GDP β S (red) 250 s following drug exposure. (C) Plot of average normalized VGSC current (elicited as in Figure 1.1E) during perfusion of 5 μ M NPS 2143 recorded in control conditions (black, n = 4) and with 2 mM GDP β S (blue, n = 7) in recording solution. *Inset*, Representative traces show VGSC current baseline in the presence of 2 mM GDP β S prior to (ctrl, black) and 250 s after the application of NPS 2143 (blue). (D) Bar graph summarizing the effects of 5 μ M NPS 2143 and 5 μ M calhex on VGSC current in control conditions (black) and with 2 mM GDP β S (red) after 250 s of drug application. (E) Plot of average normalized VGSC current (elicited as in Figure 1.1E) during perfusion of 10 μ M cinacalcet recorded in control conditions (black, n = 10) and with 2 mM ADP β S (red, n = 7) in the recording solution. *Inset*, Representative traces show VGSC current baseline in the presence of 2 mM ADP β S prior to (ctrl, black) and 250 s after the application of cinacalcet (red). (F) Bar graph summarizing the effects of 10 μ M cinacalcet on VGSC current in control conditions (black) and in recordings with 2 mM ADP β S (red) 250 s following drug exposure. (G) Diary plot of average normalized VGSC current (elicited as in Figure 1.1E) during perfusion of 100 μ M carbamazepine (top) or 100 μ M phenytoin (bottom) recorded in control conditions (black, phenytoin n =

9, carbamazepine n =7) and with 2 mM GDP β S (red, phenytoin n = 9, carbamazepine n =9) in pipette solution. (H) Plot of average normalized VGSC current (elicited as for Figure 1.1E) with 0.3 mM GTP (black), 2 mM GDP β S (red), or 500 μ M GTP γ S (blue) in the pipette solution. Error bars show mean value \pm SEM. Asterisk indicate probability with $P^{****} < 0.0001$, $P^{***} < 0.001$, and $P^* < 0.05$, *student's t-test, two-tailed*.

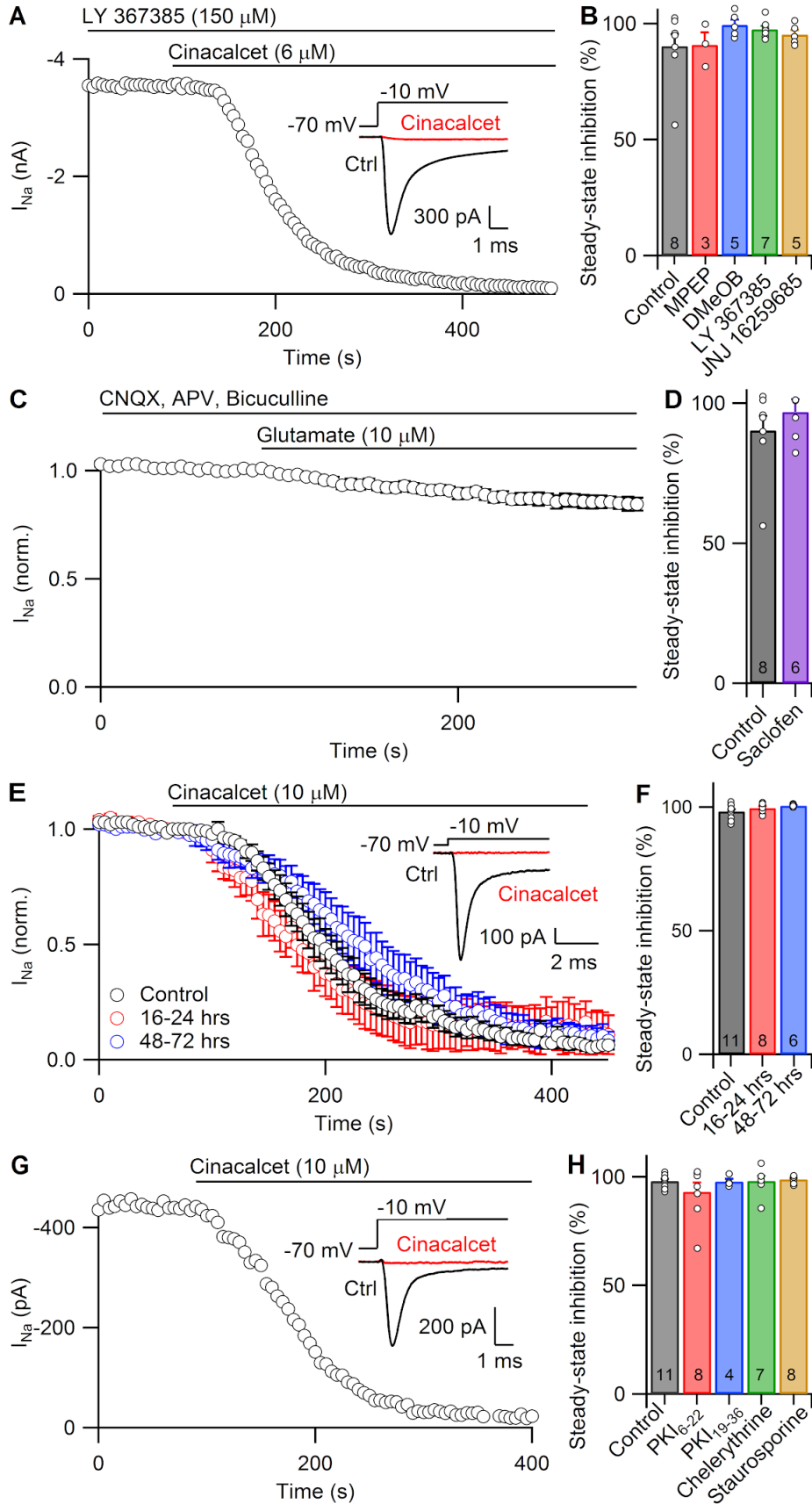


Figure 1.4. Cinacalcet-induced inhibition of VGSC current is not mediated by mGluR1, mGluR5, or GABA_B receptors nor does it require activation of PKA or PKC. (A) Exemplar plot of peak VGSC current (elicited as in Figure 1.1E) during perfusion of 6 μ M cinacalcet. mGluR1 antagonist LY 367385 (150 μ M) was applied for a minimum of 120 s prior to and during the perfusion of cinacalcet. *Inset*, Representative traces show VGSC current in control (ctrl, black) conditions and after steady-state block by cinacalcet (red). (B) Bar graph summarizing the effects of 6 μ M cinacalcet on VGSC current in the presence of mGluR1 or mGluR5 antagonists and negative allosteric modulators (30 μ M MPEP, 50 μ M DMeOB, 150 μ M LY, 500 nM JNJ) perfused a minimum of two minutes prior to and during cinacalcet perfusion. (C) Diary plot of average normalized VGSC current (elicited as in Figure 1.1E) during perfusion of 10 μ M glutamate (n = 9) in the presence of ionotropic glutamate receptor antagonists CNQX (10 μ M), APV (50 μ M), and bicuculline (10 μ M). (D) Bar graph summarizing the effects of 6 μ M cinacalcet on VGSC current in the presence of GABA_B receptor antagonist saclofen (500 μ M) perfused a minimum of two minutes prior to and during cinacalcet application. (E) Plot of average normalized VGSC current (elicited as in Figure 1.1E) during perfusion of 10 μ M cinacalcet after 16-24 hours (n = 8) or 48-72 hours (n = 6) incubation in 200 ng/mL PTx versus control condition (n = 11). *Inset*, Representative traces show VGSC current in control (ctrl, black) conditions and after steady-state block by cinacalcet (red) with 48-72 hours incubation in PTx. (F) Bar graph summarizing the effects of 10 μ M cinacalcet on VGSC current after 16-24 or 48-72 hour incubation with 200 ng/mL PTx. (G) Exemplar plot of peak VGSC current (elicited as in Figure 1.1E) during perfusion of 10 μ M cinacalcet in a recording with 5 μ M PKC inhibitor PKI₁₉₋₃₆ in

the recording pipette. *Inset*, Representative traces show VGSC current in control (ctrl, black) conditions and after steady-state block by cinacalcet (red) in recording with PKI₁₉₋₃₆ (H) Bar graph summarizing the effects of 10 μ M cinacalcet on VGSC current with 20 μ M PKI₆₋₂₂, 5 μ M PKI₁₉₋₃₆, 10 μ M chelerythrine chloride, or 100 nM staurosporine in the recording pipette. Error bars show mean value \pm SEM.

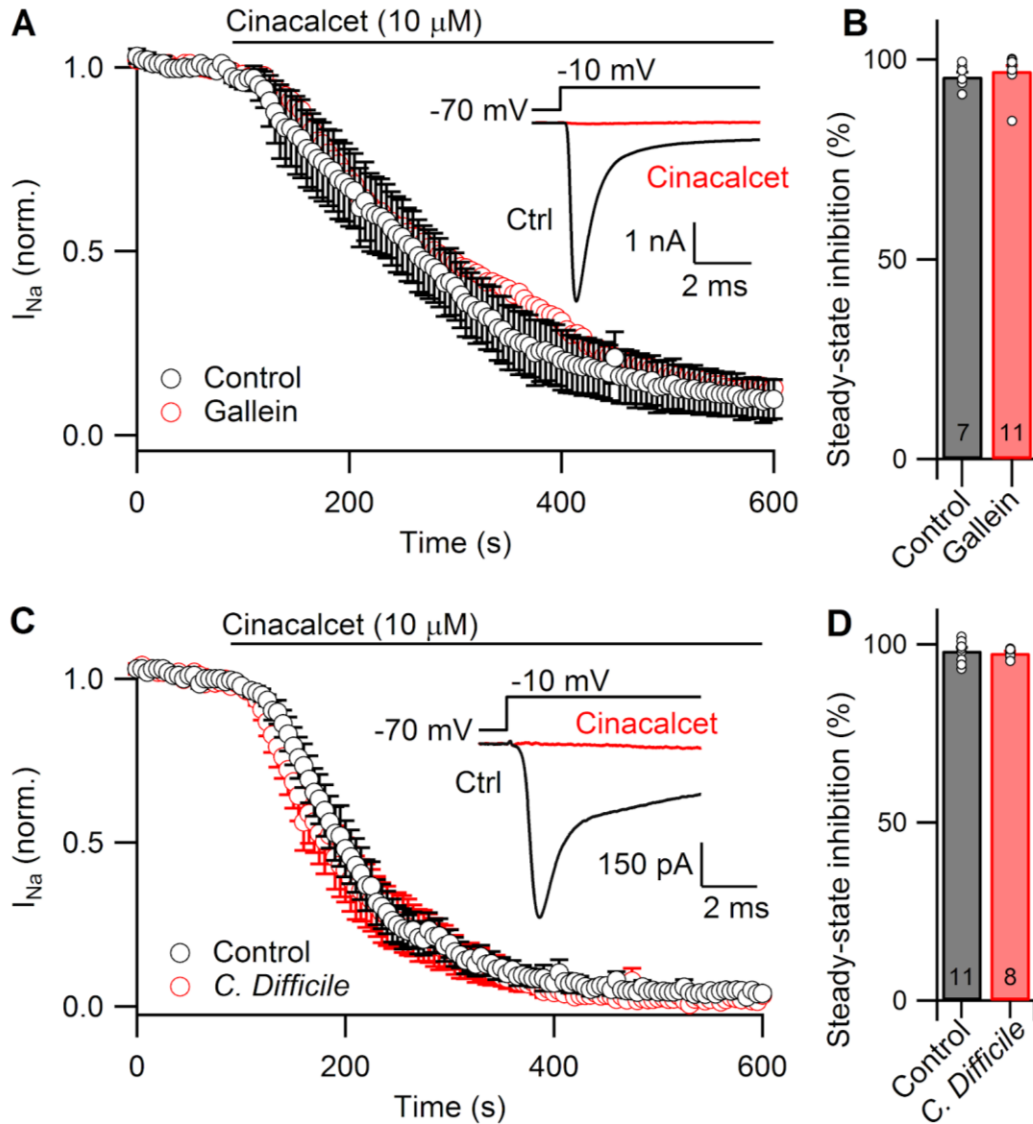


Figure 1.5. Cinacalcet-induced inhibition does not show reliance on G $\beta\gamma$ or Rho family of small G-proteins. (A) Diary plot of average normalized VGSC current (elicited as in Figure 1.1E) during perfusion of 10 μM cinacalcet in 0.05% DMSO vehicle control (black, n = 7) and after 24 hr incubation in 50 μM gallein in 0.05% DMSO (red, n =11). *Inset*, Representative traces show VGSC current in control (ctrl, black) conditions and after steady-state block by cinacalcet (red) with 24 hr incubation in gallein. (B) Bar graph summarizing the effects of 10 μM cinacalcet on VGSC current after 24 hr

incubation in gallein (50 μ M). (C) Diary plot of average normalized VGSC current (elicited as in Figure 1.1E) during perfusion of 10 μ M cinacalcet in control (black, n = 11) and after 24 hr incubation in 500 pg/mL *C. Difficile* (red, n = 8). *Inset*, Representative traces show VGSC current in control (ctrl, black) conditions and after steady-state block by cinacalcet (red) with 24 hr incubation in *C. Difficile*. (D) Bar graph summarizing the effects of 10 μ M cinacalcet on VGSC current after 24 hr incubation in 500 pg/mL *C. Difficile*. Error bars show mean value \pm SEM.

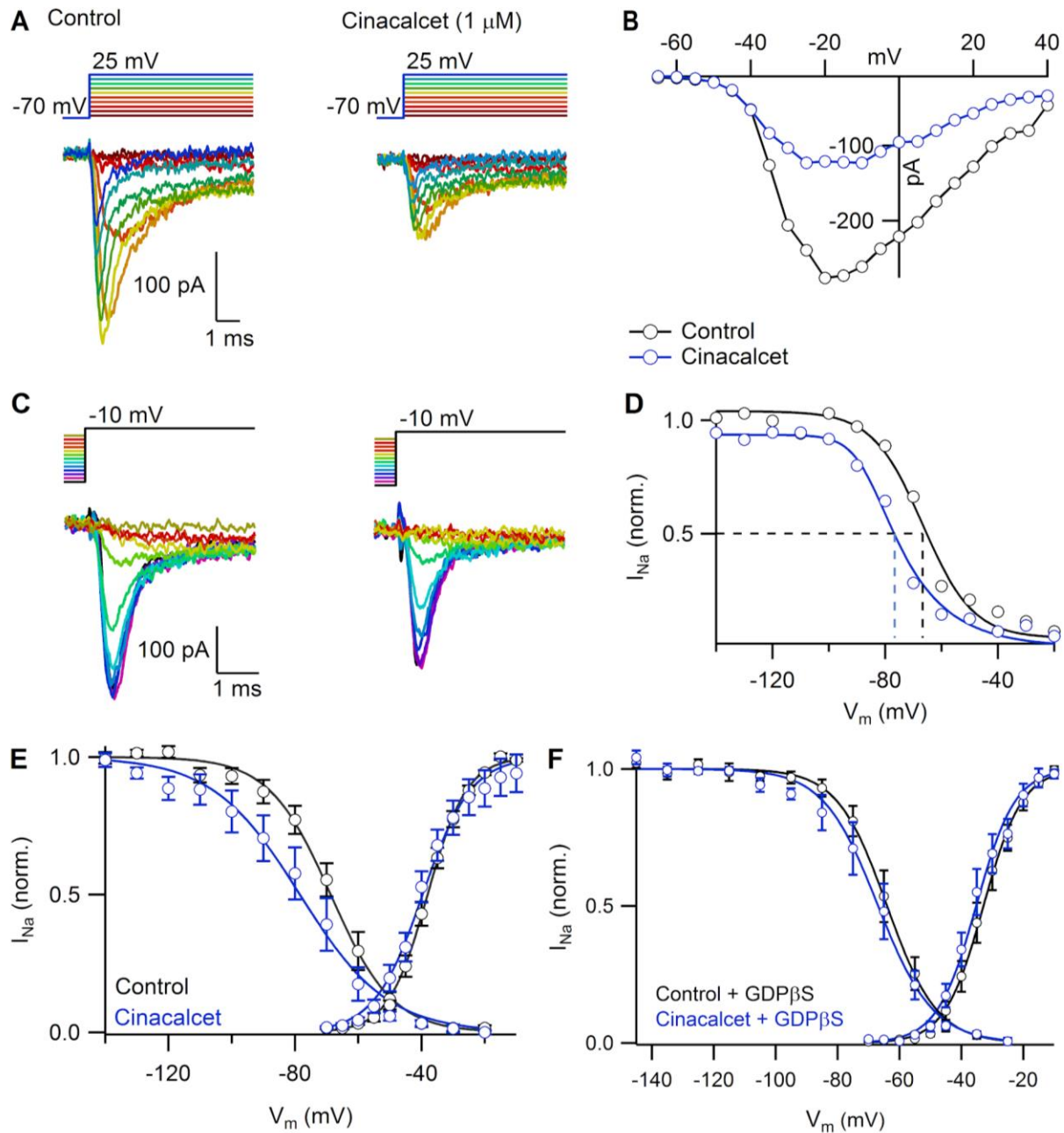


Figure 1.6. Cinacalcet negatively shifts steady-state inactivation of VGSCs in a G-protein dependent manner. (A) Representative traces from a protocol used to study the voltage-dependence of activation wherein depolarizing steps are made from a -70 mV holding potential up to +40 mV at 5 mV intervals in control conditions (left) and at ~50%

inhibition by 1 μ M cinacalcet in the same cell (right). (B) Single cell current-voltage relationship in control conditions (black) and at ~50% inhibition by cinacalcet (blue) fit to the Boltzmann equation. (C) Representative traces from a protocol used to study the voltage-dependence of channel inactivation wherein test pulse to -10 mV are made following a 500 ms prepulse between -120 mV and -20 mV at 10 mV intervals in control conditions (left) and at ~50% inhibition by 1 μ M cinacalcet in the same cell (right). (D) Single cell inactivation curves in control conditions (black) and at ~50% inhibition by cinacalcet (blue) fit to the Boltzmann equation and normalized to control data. (E) Average activation and inactivation curves in control conditions (black) and at ~50% inhibition by cinacalcet (blue). The lines are best fit to the Boltzmann equation (activation: $V_{0.5}$ control = -33 ± 1 mV, $V_{0.5}$ cinacalcet = -36 ± 1 mV, $n = 11$, $P = 3 \times 10^{-05}$, *paired t-test*; inactivation: $V_{0.5}$ control = -69 ± 3 mV, $V_{0.5}$ cinacalcet = -81 ± 5 mV, $n = 15$, $P = 0.002$, *paired t-test*). (F) Average activation and inactivation curves in control conditions (black) and at a timepoint at which ~50% inhibition by cinacalcet would be expected (blue) in recordings with 2 mM GDP β S. The lines are best fit to the Boltzmann equation (activation: $V_{0.5}$ control = -28 ± 2 mV, $V_{0.5}$ cinacalcet = -30 ± 2 mV, $n = 12$, $P = 0.08$, *paired t-test*; inactivation: $V_{0.5}$ control = -59 ± 2 mV, $V_{0.5}$ cinacalcet = -63 ± 3 mV, $n = 9$, $P = 0.054$, *paired t-test*). Error bars show mean value \pm SEM.

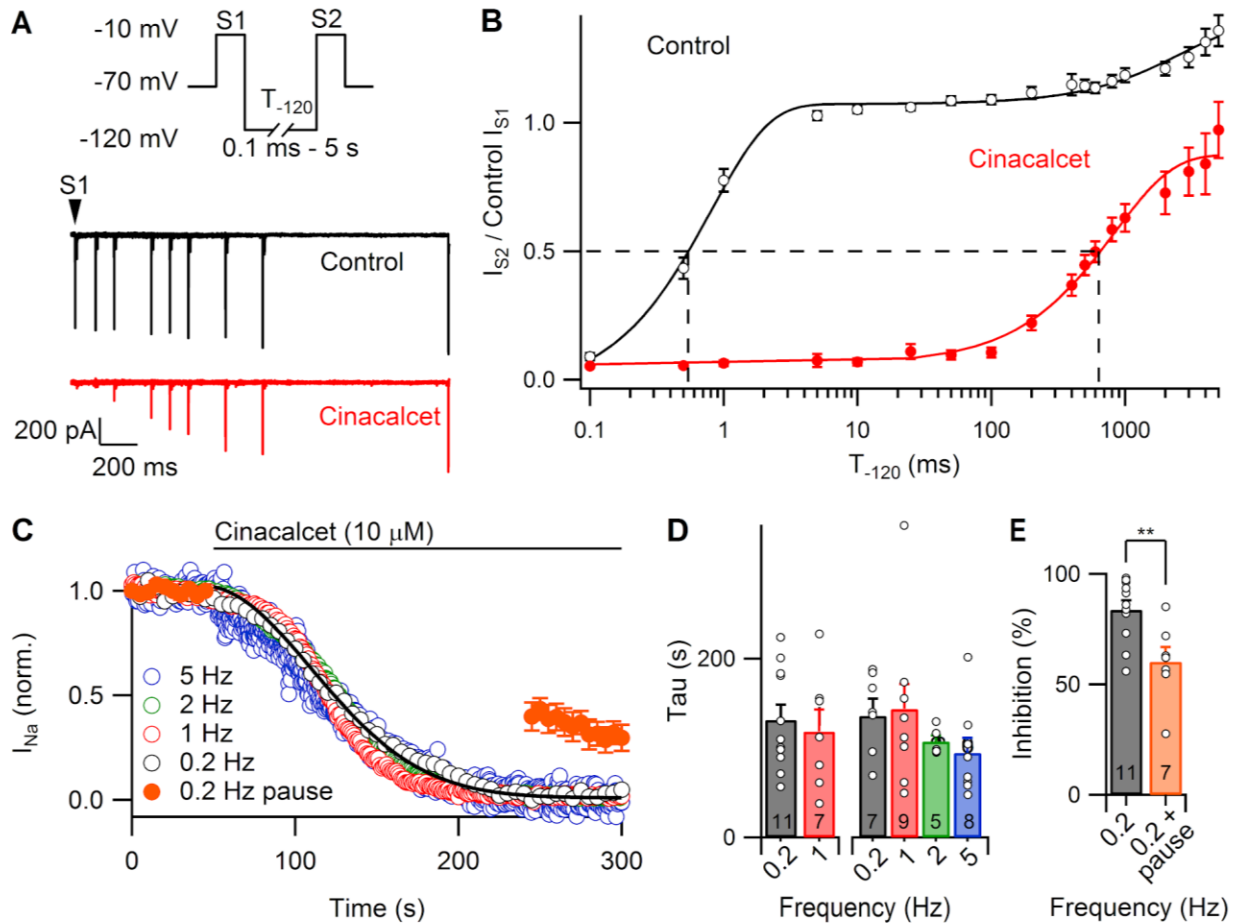


Figure 1.7. Cinacalcet block is use-dependent and recovers following hyperpolarization. (A) Representative traces from a double pulse protocol (S1 and S2) used to elicit VGSC currents in control (top, black) or after complete block by 10 μ M cinacalcet (bottom, red). Test pulses S1 and S2 are 10 ms in length and separated by a variable-length recovery period at -120 mV. (B) Graph showing double-exponential increase in VGSC current amplitude with increased time at -120 mV in control conditions (black) ($T_1 = 0.807 \pm 0.055$ ms; $T_2 = 2583 \pm 983$ ms, $n = 13$) and single-exponential recovery of VGSC current after full inhibition with 10 μ M cinacalcet (red) with increased period at -120 mV ($T = 841 \pm 72$ ms; $n = 10$). (C) Diary plot of VGSC current elicited by a 5 ms test pulse from -70 mV to -10 mV at either 0.2 Hz (black, open), 1 Hz (red, open), 2 Hz (green, open), or 5 Hz (blue, open). (D) Bar graph showing the time constant τ (s) for different frequencies: 0.2 Hz (black), 1 Hz (red), 2 Hz (green), and 5 Hz (blue). Sample sizes (n) are indicated below each bar. (E) Bar graph showing the percentage of inhibition for 0.2 Hz (black) and 0.2 Hz pause (orange) conditions. The pause condition shows significantly less inhibition (**).

open), 5 Hz (blue, open), or 0.2 Hz with pause (average of 7; orange, solid) during perfusion of 10 μ M cinacalcet. Black line shows fit on 2 Hz data using Equation 1. (D) Bar graph summarizing the effect of stimulation frequency on the time constant of cinacalcet inhibition of VGSC current by 10 μ M cinacalcet. Currents elicited with 30 ms (left) or 5 ms (right) steps to -10 mV (E) Bar graph summarizing the effect of 10 μ M cinacalcet inhibition of VGSC current in recordings with 0.2 Hz stimulation ($n = 11$) and recordings where the activation of VGSCs with a 30 ms, +60 mV step was not made until 200 s after drug application (frequency = 0.2 Hz with pause, $n = 7$). Error bars show mean value \pm SEM. Asterisk indicates probability with $P^{**} < 0.01$, *student's t-test, two-tailed*.

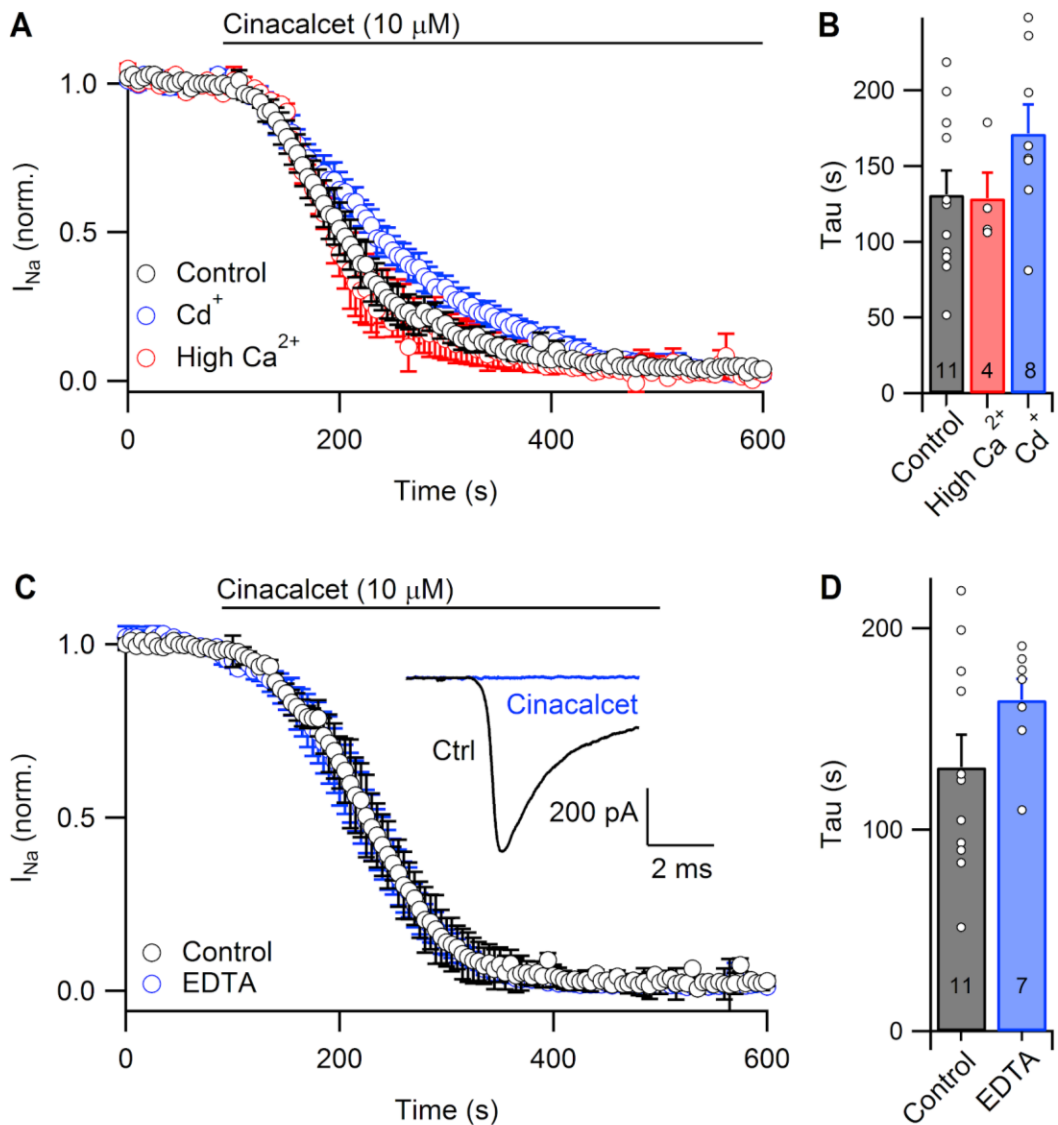


Figure 1.8. Cinacalcet inhibition is independent of calcium. (A) Diary plot of average normalized VGSC current in cultured neocortical neurons during bath application of 10 μM cinacalcet in control condition (black; $n = 11$), in the presence of 50 μM cadmium (Cd^+ ; $n = 8$; blue) to block VACCs, and in the presence of 10 mM extracellular calcium (High Ca^{2+} ; $n = 4$; red). VGSC current was measured with 5 ms steps from -70 mV to 0 mV at 0.2 Hz. (B) Bar graph showing the time constant of the inhibition (Tau) by cinacalcet (10 μM) in control conditions (black), in the presence of 50 μM cadmium

(Cd⁺; blue), and in the presence of 10 mM extracellular calcium (High Ca²⁺; red). (C) Diary plot of average normalized VGSC current in cultured neocortical neurons during bath application of 10 μM cinacalcet in control condition (1.8 mM EGTA, black; n = 11) and with 1.8 mM EDTA in the recording pipette (n = 7; blue). VGSC current was measured with 5 ms steps from -70 mV to 0 mV at 0.2 Hz. *Inset*, Representative traces show VGSC current in control (ctrl, black) conditions and after steady-state block by cinacalcet (blue) with 1.8 mM EDTA in the recording pipette. (D) Bar graph showing the time constant of the inhibition (Tau) by cinacalcet (10 μM) in control conditions (n = 11; black) and with 1.8 mM EDTA in the recording pipette (n = 7; blue). Error bars show mean value ± SEM.

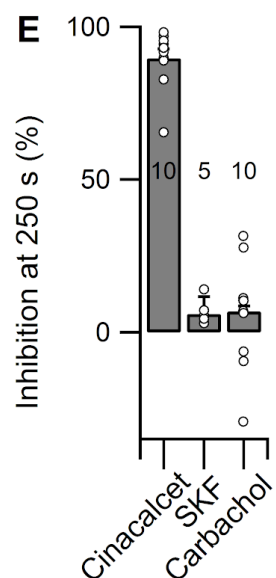
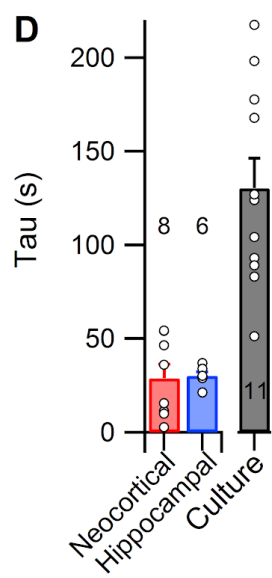
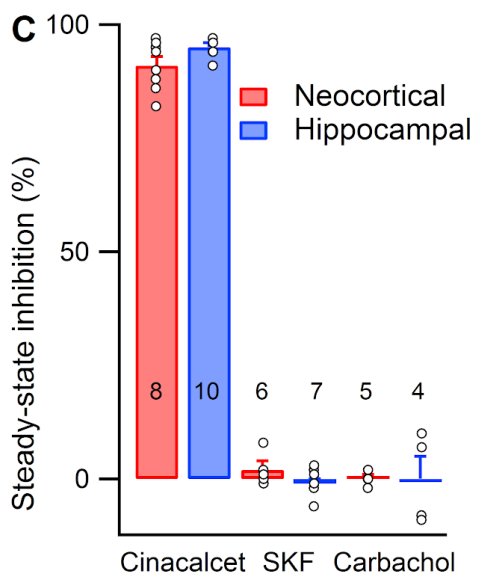
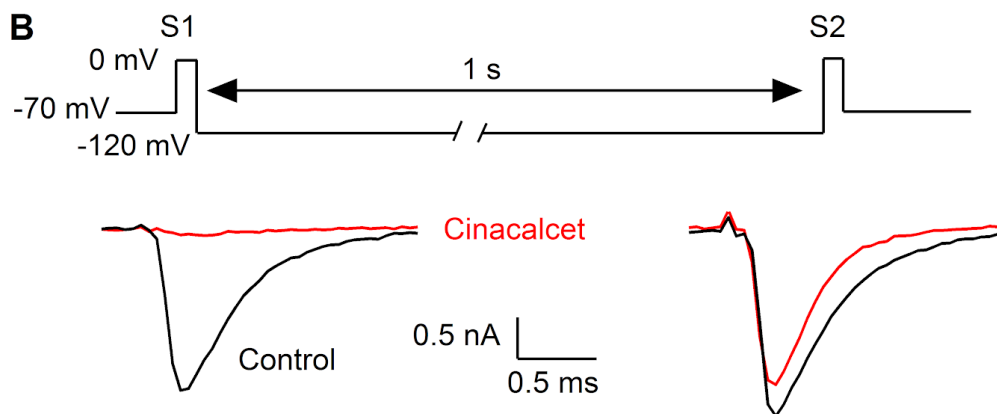
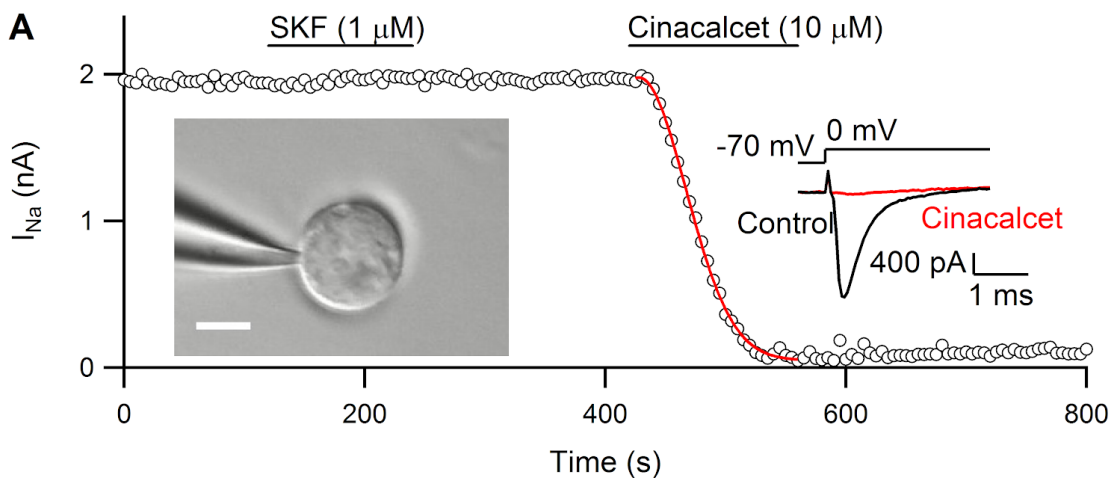


Figure 1.9. Cinacalcet inhibits VGSC current in acutely isolated neurons and is reversed by strong hyperpolarization. (A) Diary plot of VGSC current in acutely isolated neocortical neuron during bath application of 10 μ M cinacalcet and 1 μ M D1-like dopamine receptor agonist SKF 81927. VGSC current was measured with 5 ms steps from -70 mV to 0 mV at a frequency of 0.2 Hz. Red line shows Equation 1 fit used on all data sets to calculate the time constant of the inhibition. *Inset left*, Image of acutely isolated neocortical neuron during whole-cell patch clamp recording. Scale bar indicates 15 μ m. *Inset right*, Representative traces show VGSC current in control conditions (ctrl, black) and at steady-state inhibition by cinacalcet (red). (B) Representative traces from a double pulse protocol (S1, S2; 10 ms at 0 mV) used to elicit VGSC currents in control (black) or after complete block by 10 μ M cinacalcet (red) (S1 and S2 separated by a 1 s recovery period at -120 mV). (C) Bar graph showing steady-state inhibition of VGSC current produced by cinacalcet (10 μ M), SKF 81927 (1 μ M), or carbachol (20 μ M) in acutely isolated neurons from the hippocampus (blue) or neocortex (red). (D) Bar graph showing the time constant of the inhibition by cinacalcet (10 μ M) from recordings of cells in the neocortex (red, n = 8) and hippocampus (blue, n = 6) in acutely dissociated slice (right) and in cultured cortical neurons (left; black, n = 11). (E) Bar graph showing inhibition of VGSC current 250 s following drug exposure induced by cinacalcet (10 μ M), SKF 81927 (1 μ M), or carbachol (20 μ M) in cultured neocortical neurons. Error bars show mean value \pm SEM.

Table 1.1. GTPyS accelerated VGSC rundown compared with GTP and GDPβS. Related to Figure 3H.

ANOVA table	SS	DF	MS	F (DFn, DFd)	P value
Interaction	1.162	68	0.01710	F (68, 1768) = 2.127	P < 0.0001
Time	13.25	34	0.3898	F (34, 1768) = 48.50	P < 0.0001
nucleotide	5.993	2	2.997	F (2, 52) = 3.708	P = 0.0312
Subjects (matching)	42.03	52	0.8082	F (52, 1768) = 100.6	P < 0.0001
Residual	14.21	1768	0.008038		

Chapter 2.

Central AEA-signaling via the CaSR and VGSCs

Glynis Mattheisen^{1,2}, Xiaohua Wang³, and Stephen M. Smith^{1,2}

¹Department of Medicine, Division of Pulmonary & Critical Care Medicine, Oregon Health & Science University, Portland, Oregon, 97239, USA.

²Section of Pulmonary & Critical Care Medicine, VA Portland Health Care System, Portland, Oregon, USA.

³School of Medicine, Department of Pathology, Oregon Health & Science University, Portland, Oregon, 97239, USA.

Summary

Voltage-gated sodium channels (VGSCs) are strategically positioned to mediate cellular plasticity due to their influence on action potential waveform. Modulation of VGSCs by second messenger pathways presents an avenue for dynamic regulation of cellular excitability. Here we report that the endocannabinoid anandamide (AEA) completely inhibits VGSC current in neocortical neurons. Endocannabinoids (eCBs) and their receptors are prolific throughout the cerebral cortex where they have been shown to contribute to activity-based synaptic depression. Data show that AEA serves as a strong allosteric modulator of the calcium-sensing receptor (CaSR), introducing an intriguing new pathway for eCB signaling in the cortex. However, AEA-mediated inhibition of VGSCs persisted in CaSR-deficient neurons and when target cannabinoid receptor type

1 (CB₁) receptors were antagonized, suggesting an off-target CaSR- and CB₁-independent mechanism. Inhibition of VGSCs was prevented by the guanosine diphosphate (GDP) analog guanosine 5'-[β-thio]diphosphate (GDPβs), establishing that G-proteins mediated this effect. AEA-induced inhibition of VGSCs was reversed by prolonged hyperpolarization, indicating AEA shifts the voltage-dependence of inactivation of the channels to reduce current amplitude. These data identify a dynamic signaling pathway by which AEA regulates VGSC current to indirectly modulate neuronal excitability and synaptic transmission.

Introduction

Endocannabinoids (eCBs) are a family of lipid molecules that serve as key players in synaptic plasticity. Anandamide (AEA) is a major cannabinoid-signaling molecule produced endogenously in the mammalian central nervous system mediating effects primarily via the cannabinoid type 1 (CB₁) receptor (Devane et al. 1992). However, pharmacological and knockout studies point to other central AEA receptors with high sensitivity to AEA (reviewed in Castillo et al. 2012; Kano et al. 2009; Katona and Freund 2012; Alger 2012). We have identified AEA as a positive allosteric modulator of the calcium-sensing receptor (CaSR), a G-protein-coupled receptor (GPCR) expressed throughout the cortex (Chen et al. 2010; Ruat et al. 1995). This high affinity interaction indicates additional signaling roles for AEA. Interestingly, allosteric modulators of the CaSR have been shown to reduce VGSC current via a G-protein dependent pathway and induced hyperpolarizing shift in steady-state inactivation of the channels

(Mattheisen et al. 2018). In this study, we sought to characterize the relationship between AEA and the CaSR and to identify VGSC modulatory properties of AEA.

In the canonical pathway for cannabinoid function, eCBs are acutely produced in postsynaptic neurons in response to stimulation then travel in a retrograde fashion to targets receptors on the presynaptic component (reviewed in Castillo et al. 2012; Kano et al. 2009; Katona and Freund 2012). The dominant hypothesis is that eCBs function primarily through presynaptically expressed CB₁ receptors on both GABAergic and glutamatergic terminals (Zygmunt et al. 1999). Activation of these receptors initiates both short- and long- term synaptic depression of excitatory (Lévénés et al. 1998; Maejima et al. 2001; Kreitzer and Regehr 2001b) and inhibitory (Kreitzer and Regehr 2001a; Yoshida et al. 2002; Diana et al. 2002) synapses. While retrograde synaptic depression is the best-characterized eCB system, recent work shows that cannabinoid function is more diverse than previously believed. eCBs have also been shown to participate in non-retrograde signaling via vanilloid receptor type 1 (TRPV1) channels (reviewed in Castillo et al. 2012), signaling via astrocytes (reviewed in Metna-Laurent and Marsicano 2015; Navarrete et al. 2014), and long-term potentiation (Carlson et al. 2002; Chevaleyre and Castillo 2004; Chevaleyre and Castillo 2003).

Our data shows that AEA acts as an allosteric modulator of the CaSR, a GPCR widely expressed GPCR at nerve terminals throughout the cortex. The CaSR has been shown to decrease release probability at excitatory synapses in the neocortex through the regulation of a nonselective cation channel (NSCC) (Smith et al. 2004). This function

forms a feedback loop wherein low extracellular calcium reduces CASR activation and relieves NSCC inhibition. The addition of the depolarizing force of the NSCC current may increase action potential duration, prolong calcium entry at the terminal, and thus increase release probability. Consequently, the CaSR may operate as part of a homeostatic pathway to prevent synaptic failure when extracellular calcium falls (reviewed in Jones and Smith 2016). The activation of the CaSR by AEA and the contribution of this pathway to neuronal signaling have yet to be explored.

Importantly, dysregulation of the eCB system has been implicated in neuropsychiatric conditions, such as depression (Huang et al. 2016), autism (Zamberletti et al. 2017), schizophrenia (Desfossés et al. 2012), addiction (Parsons and Hurd 2015; Volkow et al. 2017), and anxiety (Ruehle et al. 2012; Hillard 2014; Mechoulam and Parker 2013). eCBs have also been suggested to have therapeutic promise for Tourette's syndrome (Müller-Vahl 2013), Huntington's disease (Pazos et al. 2008), epilepsy (Alger 2004), Alzheimer's disease (Maroof et al. 2013), depression (Huang et al. 2016), and stroke (Hillard 2008). Understanding the mechanisms of action of cannabinoids in the central nervous system will enhance our understanding of disease states and synaptic physiology while introducing avenues for new pharmacological therapies.

Data shown here present additional CaSR-independent roles for AEA in the cortex through the inhibition of voltage-gated sodium channels (VGSCs). VGSCs drive the action potential and are integral to neuronal function (Hodgkin and Huxley 1952).

Second-messenger pathways downstream of GPCRs have been identified that act on

VGSCs and these indirect mechanisms introduce dynamic points of action potential regulation (Mattheisen et al. 2018) (reviewed in Cantrell and Catterall 2001). These pathways heavily influence neuronal excitability and thereby influence signal processing in neuronal networks. Using whole-cell patch-clamp recording, we found that AEA completely inhibited VGSC current in neocortical neurons. This block of VGSC current was independent of the CaSR but required G-protein activation. Additionally, the VGSC inhibition appeared independent of CB₁ receptors, indicating off-target effects in the cortex. AEA-induced inhibition was shown to be due to a shift in VGSC inactivation as it was reversed by prolonged hyperpolarizing voltage steps. Our data, therefore, indicate that neuronal VGSCs are strongly regulated by the eCB AEA in a G-protein-dependent mechanism. These data indicate an important new pathway for modulating neuronal excitability.

Since VGSCs are strategically positioned to serve roles in mediating both long- and short-term synaptic plasticity (reviewed in Castillo et al. 2012), determining the extent to which these pathways influence signal processing as well as the proliferation of these pathways throughout the cortex is pivotal in understanding neuronal networks.

Results

AEA Activates the CaSR

While the CaSR and CB₁ receptors share little structural homology, alignment has shown sequence similarities within the transmembrane domains known to bind allosteric modulators. During a targeted screen for CaSR modulators, we determined that the

CaSR is sensitive to AEA. Human embryonic kidney (HEK) cells were transiently transfected with the CaSR and function studied 24 hours later. Intracellular calcium ($[Ca^{2+}]_i$) was measured in single cells using the Ca^{2+} -sensitive fluorophore X-Rhod1 after 30 minutes of loading. X-Rhod1's relatively low affinity means that the fluorescence signal is not saturated in these experiments and its red-shift permits clear separation of the Ca^{2+} fluorescence from CaSR-EGFP (enhanced green fluorescent protein) signals. When expressed in HEK cells, CaSR activation resulted in a concentration-dependent increase in $[Ca^{2+}]_i$. The perfusion of CaSR-expressing HEK cells with AEA (10 μ M) resulted in a transient increase in fluorescence (F/F_0) of 0.36 ± 0.02 on average ($n = 22$), indicating a rise in $[Ca^{2+}]_i$ (Figure 2.1A). In the same cells that responded to AEA, an increase in extracellular calcium ($[Ca^{2+}]_o$) from 1 mM to 5 mM produced an even larger increase in $[Ca^{2+}]_i$. Untransfected cells did not respond ($n = 6$), suggesting that the action of AEA was due to an effect on the CaSR. Furthermore, GABA, nicotine, glutamate, and the solvent (DMSO, 0.05%) did not increase $[Ca^{2+}]_i$ in CaSR-transfected cells (data not shown). Taken together, these data support that the CaSR is activated by AEA.

AEA shifted the CaSR concentration-effect relationship for $[Ca^{2+}]_o$ in CaSR-transfected HEK cells similar to the effect of CaSR positive allosteric modulators calindol and cinacalcet. F/F_0 was measured as described above except basal $[Ca^{2+}]_o$ was 0.2 mM to attenuate CaSR desensitization (Tfelt-Hansen and Brown 2005). Basal F/F_0 was measured for 30 seconds in each cell then control Tyrode's or AEA (5 μ M) applied for further 90 seconds, eliciting no response at 0.2 mM. Thereafter, $[Ca^{2+}]_o$, alone or

together with AEA, was stepped to a test dose between 0.5-50 mM. Cells were washed for 5 minutes between applications. Peak $F-F_0/F_0$ versus $[Ca^{2+}]_o$ was fitted with the Hill equation and revealed that the concentration-effect curve was left-shifted by AEA from 2.4 ± 0.1 mM to 1.7 ± 0.04 mM with no change in the maximal effect or Hill coefficient (1.0 and 2.50 respectively; Figure 2.1B). These data strongly suggest that AEA has an allosteric effect on HEK cells transfected with CaSR. In comparison, calindol (5 μ M), a known allosteric CaSR agonist, shifted the dose-response curve from 2.4 ± 0.1 mM to 1.8 ± 0.1 mM (Figure 2.1B).

Allosteric modulators of the CaSR have been shown to inhibit VGSC current through an as-yet unidentified G-protein or GPCR (Mattheisen et al. 2018). The allosteric modulators known to produce this effect, cinacalcet, calhex, calindol, and NPS 2143, all share overlapping binding sites centered around an ionic interactions between glutamate residue (Glu-837), located on transmembrane domain 7 of the CaSR, and negatively charged amino groups of the drugs (Magno et al. 2011; Petrel et al. 2004). AEA shifts the dose-response curve for the CaSR to $[Ca^{2+}]_o$ similarly to cinacalcet and calindol and possesses a positively charged amino group, suggesting a similar affinity for the allosteric modulator binding pocket. We tested if AEA also interacts with Glu-837 by mutating the glutamate to an isoleucine (CaSR-E837I). The average response to increasing $[Ca^{2+}]_o$ from 1 to 5 mM was retained by CaSR-E837I whereas the response to AEA was substantially reduced (Figure 2.1C). These observations support the idea that AEA and allosteric CaSR modulators bind to an overlapping site on the CaSR. These findings lead us to hypothesize that AEA would also inhibit VGSC current.

AEA Inhibits VGSCs

We tested if AEA modulated VGSC currents by stepping voltage-clamped neurons from -70 to -10 mV for 30 ms at 0.2 Hz. Tetrodotoxin (TTX; 1 μ M) reversibly reduced the rapidly activating and inactivating inward current (peak < 1 ms) by $98 \pm 1\%$ (n = 6, data not shown), confirming these conditions isolated the VGSC current. Application of AEA (10 μ M) strongly inhibited the peak VGSC current with steady-state block developing over 400 to 500 sec (Figure 2.1D). On average, 10 μ M AEA reduced peak VGSC by $98 \pm 1\%$ (n = 8). The kinetics of block were well described by $f(t) = Ae^{-(t/\tau)^2}$ where t represents time, T the time constant of the inhibition, and A and B represent constants, with the time constant of inhibition (T) 198 ± 34 s on average (n = 8). Reversal of the AEA-mediated block of the VGSC current was slower and usually incomplete. Taken together these data indicate that AEA, much like other allosteric modulators of the CaSR, strongly inhibits VGSCs in neocortical neurons.

Anandamide Inhibits VGSCs by a CaSR-Independent Pathway

Due to its high affinity interaction with the CaSR, we hypothesized that AEA inhibited VGSCs by a CaSR-mediated pathway and tested this idea by examining if VGSC current was insensitive AEA in neurons from CaSR null (*Casr*^{-/-}) mutants. Surprisingly, VGSC currents from *Casr*^{-/-} ($95 \pm 4\%$ steady-state inhibition, n = 4) and wild-type (*Casr*^{+/+}; $98 \pm 1\%$, n = 8) neurons were equally sensitive to AEA (10 μ M; Figures 2.2A and 2.2B). This finding is unsurprising as other CaSR allosteric modulators were also

shown to exert their effects on VGSCs independently of the CaSR (Mattheisen et al. 2018).

Next, we tested if AEA was blocking VGSCs via CB₁ receptors. We applied CB₁ antagonist AM 251 for two minutes prior to and then during AEA (10 μM) application. Reducing the activity of CB₁ receptors with AM 251 (10 μM) did not alter the steady-state inhibition of VGSC current induced by AEA (93 ± 2%, n = 5) (Figures 2.2C and 2.2D) nor did it slow the time constant of the inhibition. These data indicate that the inhibition of VGSCs by AEA is independent of CB₁ receptors and indicates off-target effects of low micromolar AEA concentrations in the cortex with substantial reductions in neuronal excitability.

G-Protein-Mediated Changes to VGSC Current

To determine if the AEA-induced block of VGSC current relied on G-protein signaling within neocortical neurons, we tested the effect of guanosine diphosphate (GDP) analog guanosine 5'-[β-thio]diphosphate (GDPβS) on the cinacalcet-induced response. GDPβS inhibits G-protein cycling by competitively inhibiting the binding of GDP to G-proteins (Eckstein, 1979). AEA (10 μM) inhibited VGSC current by 71 ± 7% (n = 8), measured 250 s after onset of application. In contrast, AEA reduced VGSC current by only 3 ± 3% (n = 6) at the same time point with the inclusion of GDPβS (2 mM) in the recording pipette (Figures 2.2E and 2.2F; $P = 5 \times 10^{-6}$). These data indicate that AEA action on VGSCs occurs via a G-protein intermediate but independently of either the CaSR or CB₁ receptors. This finding is interesting for two reasons. First, it identifies a previously

unknown pathway for the G-protein modulation of VGSCs, indicating a dynamic regulation pathway for the control of neuronal excitability. Second, it shows that AEA can off off-target effects in the cortex to depress synaptic transmission outside of its known CB₁-mediated action.

AEA-Induced Inhibition Reversed Via Hyperpolarization

Given the strong response of VGSCs, we tested if hyperpolarizing pulses could reverse guanosine triphosphate (GTP)-dependent block. A double pulse protocol was used to elicit VGSC currents in control or after complete block by AEA (10 μM). Within the protocol, VGSC current was elicited by two 10 ms steps (S1, S2) to -10 mV separated by a variable length recovery period at -120 mV. The time course of recovery following full block was described by two exponentials ($T_1 = 1.58 \pm 0.10$ ms, $T_2 = 4228 \pm 163$ ms, $n = 4$). Before AEA application, S2 was fully recovered by 100 ms, after which it increased linearly with time stepped to -120 mV. In contrast, after full block by AEA (S1 = 0), S2 recovered to $107 \pm 21\%$ of S1 recorded in control conditions before AEA application with a 2 s period at -120 mV ($T_1 = 5.0 \pm 0.1.4$ ms, $T_2 = 542 \pm 42$ ms; $n = 3$; Figure 2.3). The recovery of VGSC current with strong hyperpolarization following AEA exposure suggests that AEA pushes the voltage-dependence of inactivation toward more negative potentials than under normal physiological conditions. This mechanism could have notable repercussions to a neuron's ability to respond to produce burst of action potentials and repetitive firing.

Discussion

AEA is a major nervous system signaling molecule with established roles in synaptic plasticity (Zygmunt et al. 1999; Chávez et al. 2010; Lerner and Kreitzer 2012; Puente et al. 2011). We have described two important new roles for AEA: AEA as a positive allosteric modulator of the CaSR and AEA as a potent inhibitor of VGSCs. While the local synaptic cleft concentrations of eCBs during periods of high synaptic activity are unknown, basal AEA levels are quite high and reach up to 0.8 $\mu\text{moles/kg}$ brain tissue (Cravatt et al. 2001). This indicates that AEA activation of CaSRs and inhibition of VGSCs at the low micromolar level can contribute to eCB-induced signaling via two separate mechanisms, proposing exciting new roles for AEA in central neurons.

Here, we identify AEA as a positive allosteric modulator of the CaSR and VGSC inhibitor via a G-protein-dependent pathway. AEA was shown to enhance CaSR sensitivity to $[\text{Ca}^{2+}]_o$, extending the activation range of the receptor (Figures 2.1A and 2.1B). This interaction required a single glutamate residue (Glu837) (Figure 2.1C) shown to be critical for CaSR-allosteric modulator binding (Magno et al. 2011; Petrel et al. 2004). Additionally, AEA produced near-complete inhibition of VGSCs (Figure 2.1D) which was reversed by long hyperpolarizing steps (Figure 2.3). This data suggests that AEA shifts VGSCs into a deeply inactivated state such that fewer channels are available to open from resting membrane potential, severely dulling neuronal excitability. Interestingly, this inhibition was independent of AEA's target receptor CB_1 (Figure 2.2B) and independent of the CaSR (Figure 2.2A). These data show that AEA has strong action in the cortex on CaSRs as well as an unidentified cannabinoid receptor for the

inhibition of VGSCs. These interactions may play an important role in eCB-mediated synaptic plasticity to further depress neuronal excitability to impede synaptic signaling.

Endocannabinoids, including AEA, are manufactured by a series of enzymes activated in response to neuronal firing. They are released from the postsynaptic cells after a depolarization and diffuse to adjacent nerve terminals where they activate presynaptic receptors and decrease release of neurotransmitter (depolarization-induced suppression of excitation; DSE or depolarization-induced suppression of inhibition; DSI). While the explicit details of DSI and DSE have yet to be fully elucidated, there are two preeminent hypotheses: DSI and DSE can occur via inhibition of N- and P/Q-type calcium channels (Mackie et al. 1995; Twitchell et al. 1997; Nogueron et al. 2001; Kreitzer and Regehr 2001b; Mackie and Hille 1992) or via increased potassium conductance (Deadwyler et al. 1993; Schweitzer 2000) and the activation of g-protein-coupled inwardly-rectifying potassium channels (GIRKs) (Mackie et al. 1995; Henry and Chavkin 1995). Given the data presented here, the activation of the CaSR by AEA as well as inhibition of VGSCs by AEA provide other mechanisms by which release of neurotransmitter could be reduced by eCBs.

First, AEA may contribute to synaptic depression via stimulation of presynaptic CaSRs and consequent inhibition of a CaSR-suppressed NSCC conductance. Previous research in our lab has shown that activation of presynaptic CaSRs by extracellular calcium decreases release probability at excitatory synapses in the neocortex through the regulation of a NSCC (Smith et al. 2004). When extracellular calcium falls during

periods of high synaptic activity, CaSR suppression of a depolarizing NSCC current is reduced and the addition of the depolarizing NSCC current to the terminal will prolong the action potential, enhance calcium entry into the terminal via voltage-dependent calcium channels and continued neurotransmitter release. This may function as a homeostatic pathway to prevent synaptic failure when extracellular calcium falls (reviewed in Jones and Smith 2016). AEA stimulation of the CaSR may similarly reduce terminal depolarization and lead to reduced neurotransmitter release as has been observed in eCB-mediated DSI and DSE.

Second, AEA may inhibit VGSCs to further contribute to synaptic depression. DSI has been observed in the presence of TTX, indicating that it does not rely on VGSCs and subsequent axonal conduction block for expression (Wilson and Nicoll 2001). However, TTX-insensitive DSI of miniature inhibitory postsynaptic currents (mIPSCs) has also been shown to be more variable than DSI of evoked inhibitory postsynaptic currents (eIPSCs) or of spontaneous inhibitory postsynaptic current (sIPSCs) in the absence of TTX (Wilson and Nicoll 2001). Moreover, DSI of mIPSCs has not been shown to be mechanistically equivalent to the DSI of eIPSCs. Hence, the data do not exclude a role for VGSCs in mechanisms of DSI.

AEA-induced VGSC inhibition was independent of the CaSR and CB₁ receptors. While mechanisms of DSI and DSE are shown to primarily require CB₁ receptor activation (Ohno-Shosaku et al. 2001; Wilson and Nicoll 2001; Maejima et al. 2001; Kreitzer and Regehr 2001b), some studies have indicated a role of other cannabinoid targets in the

suppression of neurotransmitter release (Hájos and Freund 2002; Rouach and Nicoll 2003; Breivogel et al. 2001) and several lines of data support the existence of additional receptors that respond to cannabinoids (Pertwee 2015; Okada et al. 2005; Hájos et al. 2001). Orphan GPCRs, GPR18 (Rajaraman et al. 2016), GPR55 (Pertwee 2015) and GPR119 (Overton et al. 2006), are activated by AEA in nanomolar to micromolar concentrations and all three are expressed in the cortex with unexplored roles in synaptic transmission. These receptors represent potential targets for AEA in this G-protein dependent pathway to VGSC inhibition.

AEA has previously been suggested to act as an inhibitor of VGSC current. Similar to the data collected here, AEA inhibited VGSCs in both mice synaptosomes (Nicholson et al., 2003), preparations of the rat ventricular myocytes (Al Kury et al., 2014b), rat dorsal root ganglion (Kim et al. 2005), *Xenopus* oocytes (Okura et al. 2014), and the frog parathyroid gland (Okada et al. 2005), where AEA produced a significant hyperpolarizing shift in steady-state inactivation of the channels (Al Kury, Voitychuk, Yang, et al. 2014; Kim et al. 2005; Okura et al. 2014; Okada et al. 2005). AEA inhibition of VGSC current was similarly insensitive to CB₁ antagonist AM 251 (Al Kury, Voitychuk, Ali, et al. 2014; Nicholson et al. 2003; Kim et al. 2005) as well as CB₂ antagonists AM 630 (Kim et al. 2005) and SR 144528 (Al Kury, Voitychuk, Ali, et al. 2014). Due to the absence of known cannabinoid receptor involvement, the inhibition was suggested to be due to direct interaction of AEA and VGSCs (Al Kury, Voitychuk, Ali, et al. 2014; Nicholson et al. 2003). Radioligand binding studies using [³H] batrachotoxinin A 20-alpha benzoate ([³H]BTX-B) displacement at neurotoxin binding site 2 of the VGSC

suggested that AEA can directly interact with VGSCs (Al Kury, Voitychuk, Ali, et al. 2014; Nicholson et al. 2003). This data, however, does not exclude AEA acting via a second messenger pathway. In fact, Okada *et al.* showed that G-protein activator Guanosine 5'-O-(3-thiotriphosphate) (GTP γ S) enhances AEA-induced inactivation of VGSCs, suggesting a G-protein-dependent mechanism in a preparation lacking CB₁ and CB₂ receptors (Okada et al. 2005). These data support the conclusions of our study that a novel endocannabinoid pathway exists for indirect VGSC modulation independent with alterations in VGSC gating.

In our current understanding of AEA action in the cortex through the activation of CB₁ receptors, the inhibition of VGSCs and stimulation of the CaSR to inhibit NSCCs would prove synergistic. Consequently, AEA-mediated VGSC inhibition and CaSR activation may serve roles in synaptic plasticity with repercussions to the processes of learning (Heifets and Castillo 2009), pain (Sagar et al. 2008; Karbarz et al. 2009; Guindon and Hohmann 2009; Calignano et al. 1998; Richardson et al. 1998; Guindon et al. 2006), metabolism and energy homeostasis (Viveros et al. 2008), and neural development (Fride 2008) over which eCBs express influence. The response of VGSCs to AEA that we see here could constitute a lower affinity dampening mechanism within the hierarchy of excitation suppression controls that AEA exerts in the brain. These results suggest that VGSCs may function as components within the eCB signaling pathways for retrograde and/or local suppression of neuronal excitability.

Methods

Neuronal Cell Culture

Neocortical neurons were isolated from postnatal day 1–2 mouse pups of either sex as described previously (Phillips et al., 2008). All animal procedures were approved by V.A. Portland Health Care Health Care System Institutional Animal Care and Use Committee in accordance with the U.S. Public Health Service Policy on Humane Care and Use of Laboratory Animals and the National Institutes of Health Guide for the Care and Use of Laboratory Animals. Animals were decapitated following general anesthetic with isoflurane and then the cerebral cortices were removed. Cortices were incubated in trypsin and DNase and then dissociated with a heat polished pipette. Dissociated cells were cultured in MEM plus 5% FBS on glass coverslips. Cytosine arabinoside (4 μ M) was added 48 hours after plating to limit glial division. Cells were used between 1 and 9 days in culture.

Homozygous lox *Casr*, nestin-cre negative females and positive males were mated to produce conditional cre *Casr^{f/-}* mutants (Chang et al., 2008). DNA extraction was performed using the Hot Shot Technique (Truett et al., 2000) with a 1-2hr boil. Primers used for cre PCR were: Nes-Cre 1: GCA AAA CAG GCT CTAG CGT TCG, Nes-Cre 2: CTG TTT CAC TAT CCA GGT TAC GG; run on a 1% agarose gel. Primers for lox PCR are: P3U: TGT GAC GGA AAA CAT ACT GC, Lox R: GCG TTT TTA GAG GGA AGCA G. Samples were run on a 1.5% agarose gel for identification as *Casr^{f/-}* or *Casr^{+/+}*.

HEK Cell Culture and Transient Transfection

HEK 293 cells were maintained in Dulbecco's modified Eagle's medium supplemented with 5% fetal bovine serum (FBS). For $[Ca^{2+}]_i$ imaging and CaSR expression localization experiments, 10^5 cells were seeded onto 1.2 cm diameter coverglass coated with 0.1 mg/ml poly-D-lysine in 0.5 mL medium. After one day in culture, cells were transfected with plasmid DNA following mixing with 50 μ l Opti-MEM[®] I Reduced Serum Medium and 2 μ l Lipofectamine[™] 2000 (Invitrogen). For Western blotting and co-immunoprecipitation experiments, 10^6 cells were cultured in in each well of 6-well plate. After one day in culture, cells were transfected with a mix of plasmid DNA using 250 μ l Opti-MEM[®] I Reduced Serum Medium and 10 μ l Lipofectamine[™] 2000 (Invitrogen) per well. In both conditions, the cells were incubated with the mixture for 20 min. The transfection medium was replaced with DMEM containing 5% FBS 6 hrs later. Cells were grown for another 24 hours.

Plasmid Construction

The vector containing the whole length WT rat DRG CaSR, pEGFP/CaSR, was a kind gift from Dr. Emmanuel K. Awumey of North Carolina Central University. CaSR-E837I was engineered using whole length rat DRG CaSR and the QuickChange II XL Site-Directed Mutagenesis Kit (Stratagene, La Jolla, CA). *Casr*-EGFP and *Casr*-E837I-EGFP plasmids were obtained by Hind III and BamH I digestion of the EGFP vector and respective DNA sequences inserted at the Hind III and BamH I sites of pEGFP-N3 multiple cloning site to allow formation of EGFP-tagged proteins. Insertion was confirmed by sequencing.

Measurement of $[Ca^{2+}]_i$ response

$[Ca^{2+}]_i$ was measured in HEK cells transiently transfected with *Casr*-EGFP plasmids or empty vector using the fluorescent indicator, X-Rhod-1. Cells were loaded for 30 min at 37 °C with 2 μ M X-Rhod-1 in Tyrode's solution, and placed on the stage of an Olympus IX70 inverted microscope equipped with an Olympus PlanApo N 60x/1.42 oil-immersion objective. Using Semrock BrightLine[®] TXRED-4040B-OMF-ZERO filter set, X-Rhod-1 loaded cells were excited at 580 nm with an Osram HLX Xenophot 64625 (12V, 100W) light source, and emission at 600 nm was captured by a Hamamatsu ORCA-ER digital camera every 2 seconds. Images were processed using Wasabi image software and IgorPro. $[Ca^{2+}]_i$ was reported as emission fluorescence ratios (F/F_0) where F_0 is the baseline fluorescence. About 20 cells with similar cell surface GFP fluorescence were analyzed from a single field. Each experiment was performed on three coverslips.

Electrophysiological Recordings

Cells were visualized with a Leica DM IRB inverted microscope. Whole-cell voltage-and current-clamp recordings were made from cultured neocortical neurons using a HEKA EPC10 USB amplifier. Except where stated in the text, extracellular Tyrode's solution contained (mM) 150 NaCl, 4 KCl, 10 HEPES, 10 glucose, 1.1 $MgCl_2$, 1.1 $CaCl_2$, pH 7.35 with NaOH. VGSC current recordings were made using a cesium methane-sulfonate intracellular solution containing (mM) 113 $CsMeSO_3$, 1.8 EGTA, 10 HEPES, 4 $MgCl_2$, 0.2 $CaCl_2$, 4 NaATP, 0.3 NaGTP, 14 creatine phosphate, pH 7.2 with TEA hydroxide or a cesium methane-sulfonate intracellular solution containing (mM) 113 $CsMeSO_3$, 1.8 EGTA, 10 HEPES, 4 $MgCl_2$, 0.2 $CaCl_2$, 4 NaATP, 2 $GDP\beta S$, 14 creatine phosphate, pH

7.2 with TEA hydroxide (Figures 2.2E and 2.2F). Electrodes used for recording had resistances ranging from 2 to 4 M Ω . Voltages indicated have been corrected for liquid junction potentials. All experiments were performed at room temperature (20-24 °C).

Data Acquisition and Analysis

Whole-cell voltage-and current-clamp recordings were made using a HEKA EPC10 USB amplifier, filtered at 3-5 kHz using a Bessel filter, and sampled at 100 kHz. Leak current subtracted using a $-p/4$ or $-p/5$ protocol. R_s was compensated by 60-90%. Recordings were only included if the rate of baseline rundown was $< 10\%$ over 100 seconds. Analysis was performed using Igor Pro (Wavemetrics, Lake Oswego, OR). Data values are reported as mean \pm SEM. Statistical significance was determined using Student's t-test, two-tailed (Microsoft Excel) unless otherwise noted. P values of less than 0.05 were considered significant.

Solution Application

Solutions were gravity fed through a glass capillary (1.2 mm outer diameter) placed ~ 1 mm from the patch pipette tip. Most reagents were obtained from Sigma-Aldrich (Darmstadt, Germany). TTX was supplied by Alomone (Jerusalem, Israel). X-Rhod-1 was supplied by Thermofisher Scientific (Waltham, MA, USA). AEA and AM 251 were obtained from Sigma-Aldrich (Darmstadt, Germany). AEA was dissolved in 0.0125% EtOH and AM 251 in 0.02% DMSO. Appropriate vehicle controls were performed for all experiments.

Acknowledgements

This work was supported by grants NIGMS (R01 GM097433) and U.S. Department of Veterans Affairs (BX002547) awarded to SMS. In addition, GBM was supported by ARCS, NHLBI (T32HL083808) and NINDS (F31NS095463). The *Casr*^{-/-} mice were kindly provided by Dr. Wenhan Chang, UCSF and San Francisco VAMC. The vector containing the whole length WT rat DRG CaSR, *Casr-EGFP*, was a kind gift from Dr. Emmanuel K. Awumey of North Carolina Central University. We thank the Smith lab members and Drs Henrique von Gersdorff, Laurence Trussell, and John Williams for productive discussion. The authors declare no competing financial interests.

Author Contributions

G.M. and S.S. designed the study. G.M. wrote the manuscript. G.M. and X.W. (Figures 2.1A-C) conducted experiments and analyzed the data.

Figures

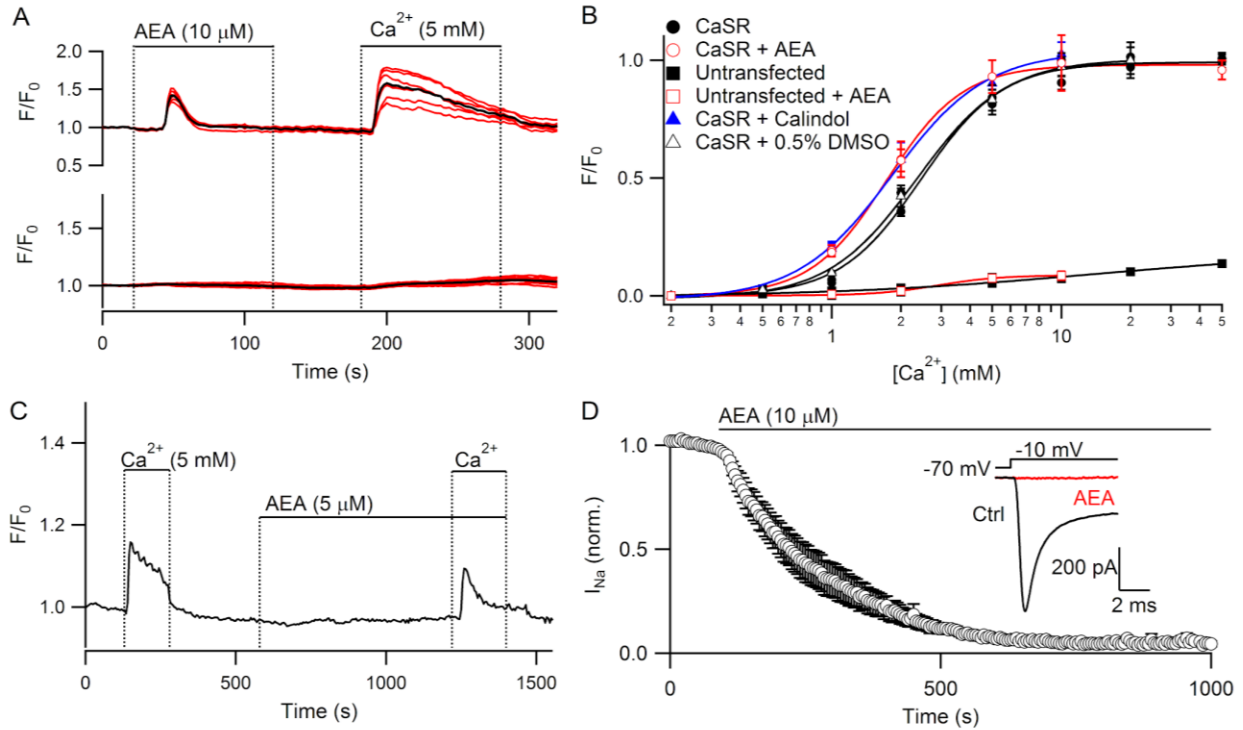


Figure 2.1. AEA activates the CaSR and inhibits VGSCs. (A) Upper trace, F/F_0 levels versus time in transfected HEK cells increased following AEA (10 μM) application and an increase in $[\text{Ca}^{2+}]_o$ (1 to 5 mM; $n = 6$). Red traces reflect individual cells on same coverslip. Black curve represents average response ($n = 6$). Application denoted by horizontal bars and broken vertical lines. Lower trace, reflects response of untransfected cells to AEA and increased bath Ca^{2+} ($n = 6$) (B) AEA (5 μM) left shifts the CaSR dose-response curve for $[\text{Ca}^{2+}]_o$ in *Casr*-EGFP transfected HEK cells (red open circles) to a similar degree as CaSR positive allosteric modulator calindol (5 μM , blue closed triangles). Untransfected cells were only modestly sensitive to changes in $[\text{Ca}^{2+}]_o$ (black closed squares) and were unaffected by AEA (red open squares). The dose response curves for CaSR response to $[\text{Ca}^{2+}]_o$ are shown in control conditions (black closed circles) and with 0.5% DMSO (black open triangles), the vehicle control for AEA.

(C) F/F_0 versus time in transfected, X-Rhod1-loaded HEK cells following AEA (5 μM) application and increased $[\text{Ca}^{2+}]_o$ (1 to 5 mM). Black curve represents average response of 13 cells transfected with CaSR-E837I. Application denoted by horizontal bars and broken vertical lines. (D) Plot of average normalized VGSC current elicited by a 30 ms test pulse to -10 mV from a holding potential of -70 mV every 5 s during bath perfusion of 10 μM AEA. *Inset*, Representative VGSC current in control conditions (ctrl, black) and at maximal AEA-induced block (red). Error bars show mean value \pm SEM.

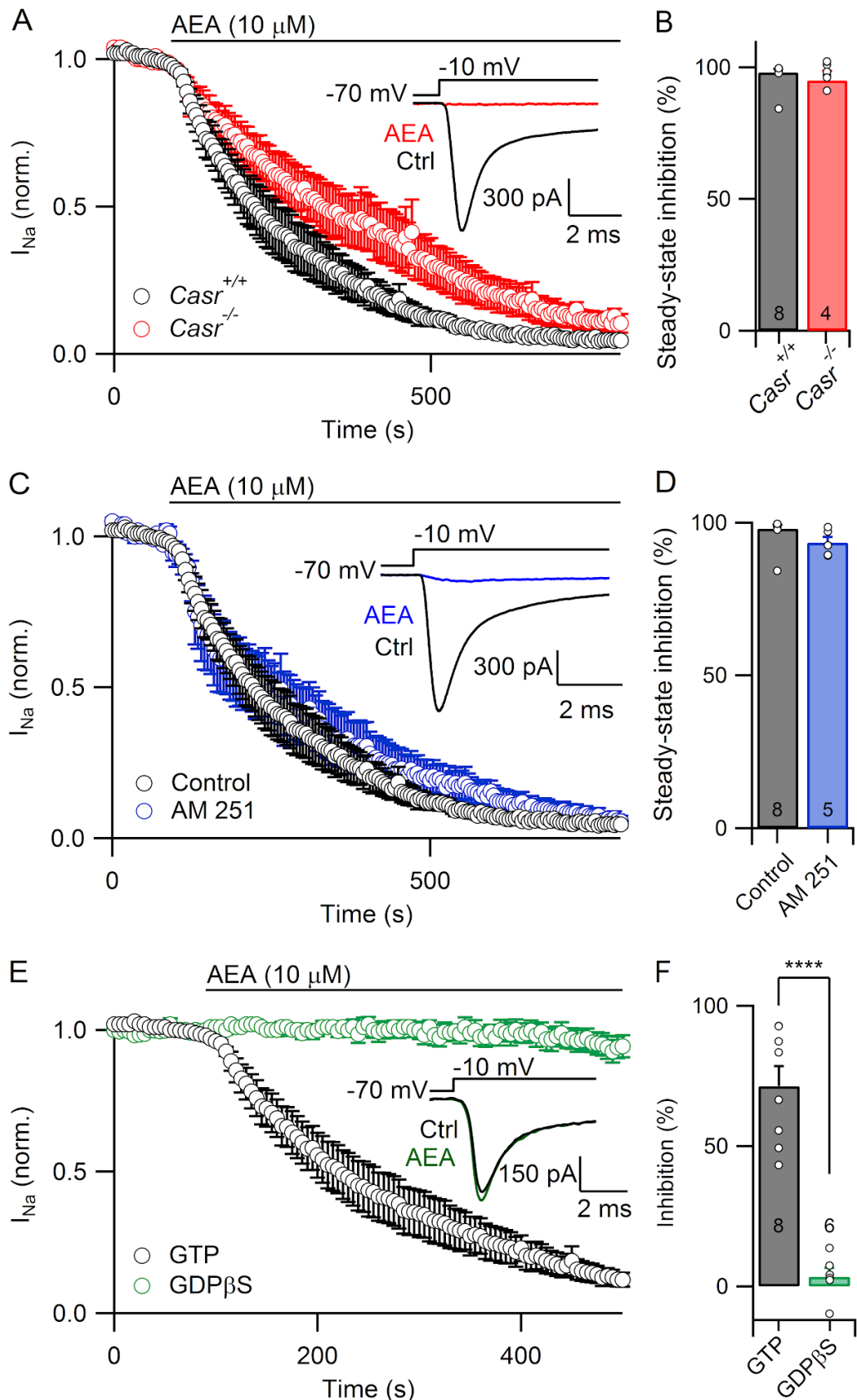


Figure 2.2. AEA inhibition of VGSCs is independent of CB₁ receptors and CaSRs but requires G-protein signaling. (A) Plot of average normalized VGSC current elicited by a 30 ms, 60 mV test pulse every 5 s during perfusion of 10 μM AEA in wildtype cultured neocortical neurons (black, n = 8) and in neocortical neurons prepared from *Casr*^{-/-} mutants (red, n = 4). *Inset*, Representative VGSC current in control conditions (ctrl, black) and at maximal AEA-induced block (red) in neocortical neurons prepared from *Casr*^{-/-} mutants. (B) Graph summarizing the effects of 10 μM AEA on VGSC current in *Casr*^{+/+} (black) and *Casr*^{-/-} (red) neocortical neurons. (C) Plot of average normalized VGSC current elicited as in 2.2A during perfusion of 10 μM AEA in control (black, n = 8) and in the presence of CB₁ receptor antagonist AM 251 (10 μM) (blue, n = 5). *Inset*, Representative VGSC current in control conditions (ctrl, black) and at maximal AEA-induced block (blue) in the presence of AM 251. (D) Graph summarizing the effects of 10 μM AEA on VGSC current in control conditions (black) and in the presence of AM 251 (blue). (E) Plot of average normalized VGSC current elicited as in 2.2A during perfusion of 10 μM AEA in control (black, n = 8) and in recordings with 2 mM GDPβS in pipette solution (green, n = 6). *Inset*, Representative traces show VGSC current baseline in the presence of 2 mM GDPβS prior to the application of AEA (ctrl, black) and at the timepoint 250 s after the application of AEA (green). (F) Graph summarizing the effects of 10 μM AEA on VGSC current in control conditions (black) and in recordings with 2 mM GDPβS (green) 250 s following drug exposure. Number in middle of bar indicates *n* for the given data set. Error bars show mean value ± SEM.

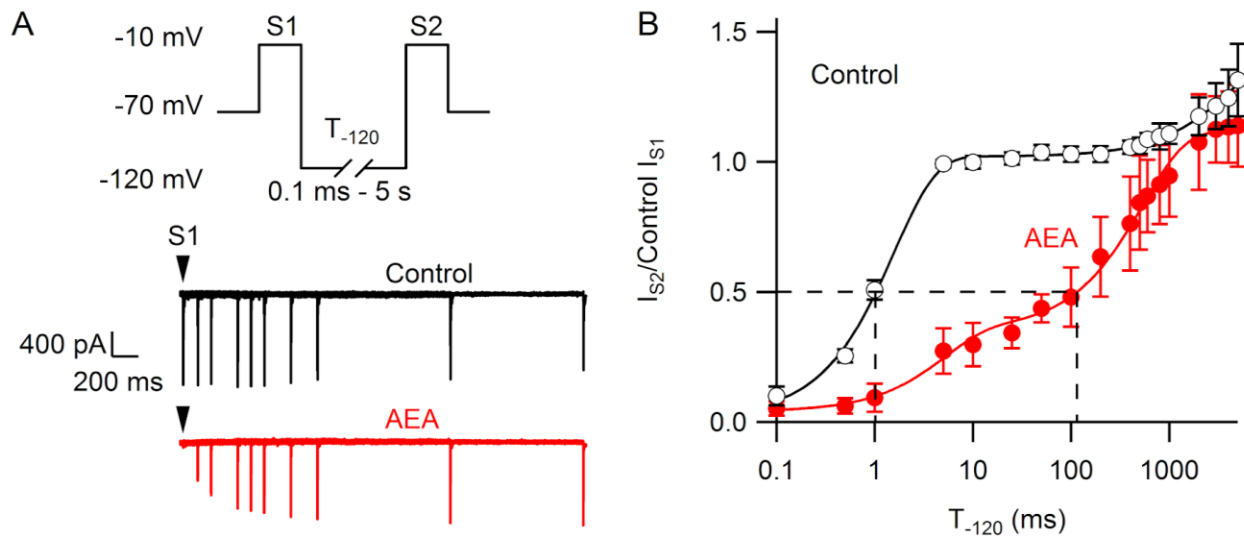


Figure 2.3. AEA inhibition of VGSCs is reversed by strong hyperpolarization. (A) Representative traces from a double pulse protocol (S1 and S2) used to elicit VGSC currents in control (top, black) or after complete block by 10 μ M AEA (bottom, red). Test pulses S1 and S2 are 10 ms in length and separated by a variable-length recovery period at -120 mV. (B) Graph showing double-exponential increase in VGSC current amplitude with increased time at -120 mV in control conditions (black) ($T_1 = 1.65 \pm 0.231$ ms, $T_2 = 3880 \pm 2520$ ms, $n = 3$) and after full inhibition with 10 μ M AEA (red) with increased period at -120 mV ($T_1 = 2.60 \pm 0.721$ ms, $T_2 = 828 \pm 67.9$ ms; $n = 2$). Error bars show mean value \pm SEM.

Summary and Conclusions

Voltage-gated sodium channels are integral to a number of physiological processes in excitable cells, from action potential generation, conduction, and signal integration to determining action potential firing patterns by setting the refractory period (Catterall 2012; Hodgkin and Huxley 1952). The regulation of these channels can alter the transmission of cellular signals in response to local stimuli. Neurotransmitters such as acetylcholine (Cantrell et al. 1996) and dopamine (Cantrell et al. 1999) have been shown to inhibit VGSCs via G-protein pathways. The data presented in this dissertation examines new pathways for G-protein modulation of VGSCs by allosteric modulators of the CaSR, including the endogenous cannabinoid anandamide, which change the input-output relationships of cortical neurons.

All of the five allosteric modulators of the CaSR tested exhibited similar mechanisms and kinetics of VGSC inhibition. Cinacalcet, calhex, NPS 2143, calindol, and AEA reliably produced near-complete VGSC inhibition with slow kinetics (full inhibition occurring in 100s of seconds), dependence on G-proteins, and a shift in the steady-state inactivation of VGSCs (shown with cinacalcet and AEA). Inhibition in all cases was shown to be CaSR-independent and AEA-induced inhibition independent of CB₁ receptors, indicating unconventional off-target effects within the cortex. Of the CaSR allosteric modulators tested, AEA is the only endogenous ligand. The participation of this major cortical signaling molecule in the G-protein-dependent mechanism for VGSC inhibition points to a significant physiological role for this pathway in the process of intraneuronal signal integration and synaptic transmission.

G-Protein Modulation of Voltage-Gated Sodium Channels

While it was once believed that VGSCs were not subject to regulation by second messenger systems (Hille 2001), recent studies have upended prior claims and accrued evidence for G-protein modulation of VGSCs in the central nervous system. G-protein-dependent inhibition of VGSCs occurs downstream of dopamine D₁-like (Cantrell et al. 1999), mAChR M₁ (Cantrell et al. 1996), mGluR1 (Carlier et al. 2006), and serotonin 5HT_{2A/C} (Carr et al. 2002) receptors in the cortex (reviewed in Cantrell and Catterall 2001). Both the abundance of GPCRs in the cortex (Vassilatis et al. 2003) and the strategic positioning of VGSCs to serve roles in the modulation of excitability suggest additional opportunities for the G-protein modulation of VGSCs.

The CaSR allosteric modulator pathway for VGSC inhibition is distinct from known modes of GPCR VGSC inhibition. First and foremost, VGSCs in cultured neocortical neurons that respond to AEA and cinacalcet do not respond to agonists of mAChR M₁ or dopamine D₁-like receptors, indicating these are distinct pathways for VGSC modulation (Figures 1.9A, 1.9C, and 1.9E). Earlier studies showed that VGSC currents in the neocortex and hippocampus were reduced by ~20-40% at saturating concentrations of mAChR M₁, D₁-like dopamine receptor, mGluR1, and serotonin 5-HT_{2A/C} receptor agonists with 84-100% of neurons responding (Carr et al. 2002; Cantrell et al. 1996; Cantrell et al. 1999; Carlier et al. 2006; Maurice et al. 2001). In contrast, CaSR allosteric modulators produced near-complete VGSC inhibition with low micromolar concentrations of ligand in all neurons tested (Figure 1.1E). This indicates

that the CaSR allosteric modulator pathway has heightened potency on VGSCs and a different distribution to other G-protein dependent pathways that modulate VGSCs. Furthermore, the known pathways for VGSC modulation by GPCRs thus far (mAChR, mGluR1, D1-like, 5HT_{2A/C}) all rely on PKA or PKC (Cantrell et al. 1996; Cantrell et al. 1997; Carr et al. 2002; Carlier et al. 2006). These kinases phosphorylate serine residues in the intracellular loop connecting domains I and II of the VGSC α subunit to produce steric interactions that change VGSC availability (Cantrell and Catterall 2001). This common theme is one major divergence from the CaSR allosteric modulator pathway. Experiments with cinacalcet showed that the G-protein inhibition induced by this CaSR allosteric modulator was independent of PKA and PKC (Figure 1.4H). Interestingly, the phosphorylation of VGSCs by PKC downstream of mGluR1 (Carlier et al. 2006) and 5-HT_{2A/C} (Carr et al. 2002) shifts VGSC inactivation in the hyperpolarizing direction, similar to observations with cinacalcet and AEA (Figures 1.6E and 2.3B). In this study we targeted PKA and PKC with chelerythrine chloride, PKI₆₋₂₂, PKI₁₉₋₃₆, and staurosporine and concluded that neither kinase is involved in the CaSR allosteric modulator VGSC inhibition. However, we cannot rule out the involvement of staurosporine-resistant kinases. Phosphorylation of VGSCs downstream of AEA may still influence this pathway. Collectively, the differences between known GPCR pathways for VGSC modulation and the CaSR allosteric modulator pathway detailed in this dissertation suggest a novel G-protein-dependent mechanism for the regulation of neuronal excitability.

CaSR Allosteric Modulators Shift Voltage-Gated Sodium Channels into a Deeply Inactivated State

Upon depolarization, VGSCs move from several closed resting states through a current-producing open state to one or several inactivated states, where the channels are in a stable, non-conducting conformation (Armstrong 2006; Hodgkin and Huxley 1952). Recovery from inactivation does not pass through the open state (Kuo and Bean 1994a) except in the case of resurgent VGSC current (Lewis and Raman 2014; Afshari et al. 2004; Raman and Bean 2001). While models vary, some suggested that VGSCs can exhibit up to five closed states and at least three inactivation states (Armstrong 2006; Armstrong and Gilly 1979). Inactivation states vary in time scale, biophysical mechanism, and pharmacological sensitivity (reviewed in Goldin 2003).

VGSCs are capable of fast inactivation, taking place over the timescale of a single action potential, and multiple forms of non-fast inactivation with time constants ranging from 100 ms to several minutes (Ulbricht 2005). The mechanism of fast inactivation is well-studied and occurs when an intracellular linker between domains III and IV forms a gate that occludes the channel pore. The slower forms of inactivation have been termed “slow,” “intermediate,” and “ultraslow” (Hilber et al. 2001), distinguished by the length of depolarization necessary to develop the state. Since the structural basis for slow inactivation, unlike fast inactivation, has not been fully resolved and no gate identified, all forms of non-fast inactivation are often grouped under the general term “slow inactivation.” Slow inactivation is produced by prolonged depolarizations over tens of seconds or a series of brief, sequential depolarizations (reviewed in Goldfarb 2012).

Slow inactivation is thought to occur by a conformational rearrangement of the VGSC outer pore region (Goldin 2003). Mutational studies also implicate long distance interactions with other structural regions including involvement of residues in domain IV S4 (Mitrovic et al. 2000), IV S6 (Cervenka et al. 2018; Carboni et al. 2005), and II S6 (O'Reilly et al. 2001) although a comprehensive model is still being built. Regardless of mechanism, all forms of slow inactivation decrease VGSC availability and reduce repetitive action potential firing and back propagation (Ruff et al. 1988) in a way that is dependent on the previous history of neuronal activity (Toib et al. 1998; Mickus et al. 1999).

Here, we investigated the action of CaSR allosteric modulators on VGSCs gating using protocols to look at cinacalcet-mediated changes in activation and inactivation in addition to recovery from inactivation after AEA- and cinacalcet- induced inhibition. Data showed three important findings relevant to VGSC gating. First, cinacalcet shifted steady-state inactivation of VGSCs toward more hyperpolarized potentials (Figures 1.6E). This reduces VGSC current during depolarization and severely diminishes neuronal excitability. Second, prolonged hyperpolarizing pulses recovered VGSC current following inhibition by AEA and cinacalcet (Figures 1.7B and 2.3). Slowing of recovery from inactivation can result from high affinity binding and slow dissociation of a modifier to a preferred channel state or increased stability of an inactivated state (Karoly et al. 2010). Third, inhibition by cinacalcet was reduced when VGSCs were not activated following application of the drug (Figures 1.7C and 1.7E), indicating channels must pass through the open or fast inactivated state for block to occur.

Since the effect of cinacalcet is enhanced by VGSCs cycling through different states, use-dependence is indicated at low cycling frequencies (Courtney 1975). Use-dependence occurs in three scenarios: 1) when the ligand has increased affinity for a specific state (Hille 1977; Hondeghem and Katzung 1977), 2) when channel opening exposes an agonist binding site as is the case with MK-801 and N-methyl-D-aspartate (NMDA) receptors (Huettner and Bean 1988; Starmer et al. 1984) or 3) when channel activation enhances the shift into a specific state preferred by the modifier such as Brilliant blue G binding to the inactivated state of VGSCs (Jo and Bean 2011). In the case of allosteric CaSR modifiers, this use-dependence, as well as the delayed recovery from inactivation in the presence of both cinacalcet and AEA, suggests allosteric CaSR modulators promote a deep inactivated channel conformation occurring via either slow modifier dissociation rate or stabilization of a slow inactivation state. Slow dissociation and the stabilization of an inactivation state are two fundamentally different mechanisms that have qualitatively similar effects on excitability. Slow dissociation occurs when modifiers bind with high affinity to a specific state-dependent conformation of the channel (Hille, 1977; Hondeghem and Katzung, 1977). Since channel state varies during the course of an action potential and activity-induced state cycling, drugs that bind preferentially to channel inactivated states slow recovery of excitability. Stabilization occurs when a modifiers bind to native slow inactivation states and accelerate the time course of development of this state during cycling (Khodorov et al., 1976; Zilberter Yu et al., 1991; Balser et al., 1996b; Kambouris et al., 1998; Chen et

al., 2000). Notably, the mechanisms of slow drug dissociation and stabilization of inactivated states can operate in concert (Nuss et al. 2000).

Since modifier interactions with VGSCs alter channel gating rates such that the rate of recovery from fast inactivation can overlap with the rate of recovery from slow inactivation and the rate of state-dependent association and dissociation of a modifier will also obscure results (Karoly et al. 2010), fast- and slow- state preferring and thereby fast- and slow-inactivated state-stabilizing drugs cannot be differentiated. Thus, it is difficult to discern if CaSR allosteric modulators push VGSCs into a deeply inactivated state via slow modifier dissociation rate or stabilization of a slow inactivation state.

Regardless of mechanism, both cinacalcet and AEA altered VGSC gating to reduce overall neuronal excitability. The use-dependent action of cinacalcet implies that the CaSR allosteric modulator pathway is most influential when neuronal excitability is increased and may be activated during periods of high synaptic activity to reduce action potential firing in much the same way as slow inactivation develops during repeated depolarizations. This would serve to increase spike threshold, reduce firing bursts, and limit back propagation into dendritic regions (Jung et al. 1997; Maurice et al. 2004). Importantly, slow-inactivated state preferring drugs, such as the antiepileptic lacosimide (Sheets et al. 2008), have been proposed as having distinct therapeutic advantage as anticonvulsants (Errington et al. 2008; Lenkowski et al. 2007) and antiarrhythmics (Remy et al. 2004). Should CaSR allosteric modulators provide specific modulation of

VGSC slow inactivation would be a powerful tool for approaching diseases of excitability.

Anandamide Inhibits VGSCs through Direct and Indirect Mechanisms

Due to its analgesic effect (Clapper et al. 2010; Walker et al. 1999), the action of AEA on VGSCs has already come under preliminary investigation. AEA has been shown to inhibit VGSCs in the low- to mid- micromolar range (Nicholson et al. 2003) with a concomitant hyperpolarizing shift in the voltage-dependence of channel inactivation (Al Kury, Voitychuk, Yang, et al. 2014; Kim et al. 2005; Okura et al. 2014). Data show that this inhibition was not blocked by CB₁ antagonist AM 251 (Al Kury, Voitychuk, Ali, et al. 2014; Nicholson et al. 2003; Kim et al. 2005), CB₂ antagonist AM 630 (Kim et al. 2005), CB₂ antagonist SR 144528 (Al Kury, Voitychuk, Ali, et al. 2014), or G_{i/o} signaling inhibitor pertussis toxin (PTx) (Al Kury, Voitychuk, Yang, et al. 2014). The absence of CB₁ or CB₂ involvement suggests action on an off-target receptor or direct effect on VGSCs. This data is in keeping with the characteristics of the CaSR allosteric modulators pathway for VGSC inhibition where we showed that AEA-induced VGSC inhibition is independent of CB₁ receptors and cinacalcet-induced inhibition is independent of the G_{i/o} subfamily of G-proteins (Figure 1.4F). Radioligand studies have also shown that AEA reduces [³H] batrachotoxinin A 20-alpha benzoate ([³H]BTX-B) binding to VGSCs (Al Kury, Voitychuk, Ali, et al. 2014; Nicholson et al. 2003). This indicates that AEA can act directly on VGSCs and provides a plausible mechanism for a proportion of AEA-induced VGSC inhibition. However, it does not exclude the possibility of off-target effects of AEA on GPCRs or G-proteins and indirect mechanisms of

inhibition. Interestingly, all data provided for AEA inhibition of VGSCs shows that steady-state inhibition takes place over 5-10 minutes (Al Kury, Voitychuk, Yang, et al. 2014; Kim et al. 2005; Okura et al. 2014). This rate of inhibition is more characteristic of second messenger inhibition than direct interaction with an ion channel (Lohse et al. 2008; Zerangue and Jan 1998; Linderman 2009).

Our data show that VGSC inhibition by AEA is relieved by the inclusion of G-protein signaling inhibitor GDP β S. Thus we concluded that AEA acts via second messengers on VGSCs and not via a direct mechanism. A similar indirect mechanism for endocannabinoid block of VGSCs has been described. Okada *et al.* showed that VGSCs in the frog parathyroid were inhibited by application of endocannabinoid 2-arachidonoylglycerol (2-AG) with a time course of 10 s of minutes (Okada et al. 2005) similar to previous studies of AEA-induced VGSC inhibition (Al Kury, Voitychuk, Yang, et al. 2014; Kim et al. 2005; Okura et al. 2014). 2-AG inhibition was enhanced by the G-protein activator GTP γ S, suggesting a G-protein-dependent mechanism for VGSC modulation. Intriguingly, frog parathyroid tissue lacks CB₁ and CB₂ receptors. Furthermore, VGSC currents were not affected by CaSR agonist spermine, indicating that this action was also CaSR-independent. As was observed in our study, AEA shifted VGSC inactivation and inhibition continued in the presence of PKC inhibitor chelerythrine chloride (Okada et al. 2005). These data support the conclusions of our study that a novel endocannabinoid pathway exists for indirect VGSC modulation independent of PKC with alterations in channel gating.

Cumulatively, evidence shows that AEA can produce substantial, physiologically-relevant modulation of VGSCs. This inhibition can prove important to AEA's role in signal processing and disease states. While AEA has been suggested to act directly on VGSCs, other systems demonstrate it can participate in VGSC inhibition via second messengers. Neither role, indirect or direct, is exclusive of the other and these actions may in fact prove synergistic to AEA function.

Anandamide's Roles in Synaptic Transmission

AEA is known to signal primarily through CB₁, CB₂, and transient receptor potential cation channel subfamily vanilloid receptor 1 (TRPV₁) receptors (Zygmunt et al. 1999). However, AEA has been demonstrated to bind to the GPCRs mAChR M1 and M4, adenosine A3, 5-HT₁ & 5-HT₂, S1P1, GPR18, GPR55, GPR119 with affinities in the nanomolar to micromolar range (Pertwee 2015). Furthermore, studies show that eCBs act on as-yet unidentified receptors in the cortex (Okada et al. 2005; Hájos et al. 2001) (reviewed in Begg et al. 2005). In a screen for modulators of the CaSR, we determined for the first time that AEA serves as a positive allosteric modulator of the CaSR with unexplored roles in the cortex. Additionally, the data presented in this dissertation indicate yet another unknown G-protein target for AEA in the cortex, as the inhibition of VGSCs by AEA was shown to be independent of both CB₁ and the CaSR. With the identification of AEA targets in the brain, we can then fully delineate the roles of this eCB in neuronal function.

Currently, the best characterized role for eCB signaling in the central nervous system is the inhibition of presynaptic release of L-glutamic acid (depolarization-induced suppression of excitation; DSE) (Lévénés et al. 1998; Maejima et al. 2001; Kreitzer and Regehr 2001b) and GABA (depolarization-induced suppression of inhibition; DSI) (Kreitzer and Regehr 2001a; Yoshida et al. 2002; Diana et al. 2002). While mechanisms of DSI and DSE are shown to primarily require CB₁ receptor activation (Ohno-Shosaku et al. 2001; Wilson and Nicoll 2001; Maejima et al. 2001; Kreitzer and Regehr 2001b), some studies have indicated a role of other cannabinoid targets in the suppression of neurotransmitter release (Hájos and Freund 2002; Rouach and Nicoll 2003; Breivogel et al. 2001). Hájos *et al.* reported that the synthetic cannabinoid agonist WIN 55,212-2 inhibited evoked excitatory postsynaptic currents (eEPSCs) in CA1 pyramidal cells in CB₁ receptor knockout mice (Hájos et al. 2001) and the effect was insensitive to AM 251 (Hájos and Freund 2002). The research concluded that a presynaptic receptor distinct from CB₁ or CB₂ is present on glutamatergic terminals in the mouse hippocampus. In support of this claim, mGluRs-triggered eCB release causes short-term depression of excitatory transmission in the CA1 region of the hippocampus of both wild-type and CB₁ knockout mice (Rouach and Nicoll 2003). Furthermore, AEA, but not other cannabinoid agonists, stimulates guanosine 5'-O-[gamma-thio]triphosphate (GTPγS) binding in brain plasma membranes from CB₁ receptor knockout mice (Breivogel et al. 2001). These data all demonstrate a G-protein-coupled cannabinoid receptor in the brain other than CB₁ that can participate in DSI and DSE.

Studies show that CB₁ receptor-mediated DSI and DSE can occur via inhibition of N- and P/Q-type VGCCs (Mackie et al. 1995; Twitchell et al. 1997; Nogueron et al. 2001; Kreitzer and Regehr 2001b; Mackie and Hille 1992) and via increased potassium conductance (Deadwyler et al. 1993; Schweitzer 2000) and the activation of GIRKs (Mackie et al. 1995; Henry and Chavkin 1995). DSI has been observed in the presence of VGSC blocker tetrodotoxin (TTX), indicating that it does not rely on VGSCs and subsequent axonal conduction block for expression (Wilson and Nicoll 2001). However, TTX-insensitive DSI of mini inhibitory postsynaptic currents (mIPSCs) has also been shown to be more variable and less robust than DSI of evoked inhibitory postsynaptic currents (eIPSCs) or of spontaneous inhibitory postsynaptic currents (sIPSCs) in the absence of TTX (Wilson and Nicoll 2001). Moreover, mIPSC DSI has not been shown to account quantitatively for eIPSC DSI. Hence, the data do not rule out other mechanisms for DSI expression. In our current understanding of AEA action in the cortex through the activation of CB₁ receptors, the inhibition of VGSCs would prove synergistic. Our data show that AEA inhibits VGSCs in low to mid micromolar concentrations. The concentration of AEA within synaptic clefts of the cortex during periods of high activity is unknown. However, the basal AEA level is quite high and may reach 0.8 μmoles/kg brain tissue (Cravatt et al. 2001). This makes it likely that high synaptic concentrations of AEA following postsynaptic depolarization can reduce VGSC current and enhance DSI. AEA inhibition of VGSCs at the terminal would both limit the ability of additional action potentials to invade the bouton and trigger further transmitter release of L-glutamic acid and GABA.

Clinical Significance of an Endocannabinoid Pathway for VGSC Inhibition

Of the CaSR allosteric modulators tested in this study, AEA is the only endogenous ligand. The participation of this major cortical signaling molecule in the G-protein-dependent mechanism for VGSC inhibition points to a significant physiological role for this pathway. eCBs contribute to a range of physiological processes, including synaptic plasticity and learning (Heifets and Castillo 2009), pain (Sagar et al. 2008; Karbarz et al. 2009; Guindon and Hohmann 2009; Calignano et al. 1998; Richardson et al. 1998; Guindon et al. 2006), metabolism and energy homeostasis (Viveros et al. 2008), and neural development (Fride 2008). Dysregulation of the eCB system has been implicated in neuropsychiatric conditions, such as depression (Huang et al. 2016), autism (Zamberletti et al. 2017), schizophrenia (Desfossés et al. 2012), addiction (Parsons and Hurd 2015; Volkow et al. 2017), and anxiety (Ruehle et al. 2012; Hillard 2014; Mechoulam and Parker 2013). Endocannabinoids have also shown therapeutic promise for Tourette's syndrome (Müller-Vahl 2013), Huntington's disease (Pazos et al. 2008), epilepsy (Alger 2004; Alger 2014), Alzheimer's disease (Maroof et al. 2013), depression (Huang et al. 2016), and stroke (Hillard 2008). The addition of an AEA pathway for VGSC regulation to these roles and our understanding of eCB systems as they relate to disease states.

Mechanisms for Voltage-Gated Sodium Channel Modulation

G-proteins mediate a number of cellular responses in neurons. Several second messenger pathways downstream of G-proteins are well-mapped while others remain to be elucidated. Our research shows that G-protein activation by CaSR allosteric

modulators inhibits VGSCs, though the participants in this pathway have not yet been identified. A number of protein effectors can be activated by G-proteins and these proteins can interact with or modify VGSCs to alter their gating and reduce VGSC current amplitude. Notably, VGSCs are substrates for phosphorylation (Sigel and Baur 1988) and other post-translational modifications, interact with calcium and calmodulin (Pitt and Lee 2016), and can be directly influenced by the G $\beta\gamma$ dimer (Mantegazza et al. 2005).

Voltage-Gated Sodium Channel Gating is Sensitive to Phosphorylation

Protein kinases can modulate VGSC function via electronic interference between negatively charged phosphate groups and the channel voltage-sensor (Zhou et al. 2002). Phosphorylation can also create or disrupt binding sites for interaction with other regulatory proteins that modulate VGSCs (Zhou et al. 2002; Shenoy and Lefkowitz 2011). The large intracellular linker between VGSC α subunit domains I and II contains at least five well-characterized phosphorylation sites for PKA (Rossie et al. 1987; Rossie and Catterall 1989) and the loop between domains III and IV contains two sites for phosphorylation by PKC (Numann et al. 1991; Cantrell et al. 2002). Phosphorylation at any of these sites reduces VGSC current (Berendt et al. 2010; Mantegazza et al. 2005). The known pathways for VGSC modulation by GPCRs thus far (mAChR, mGluR1, D1-like, 5HT_{2A/C}) all rely on the activity of either PKA or PKC (Schiffmann et al. 1995; Cantrell et al. 1997; Carlier et al. 2006; Cantrell et al. 1996; Carr et al. 2002). Experiments undertaken in this study show that cinacalcet-induced VGSC inhibition is independent of either PKA or PKC (Figure 1.4H) using PKA inhibitor PKI₆₋₂₂, PKC

inhibitors PKI₁₉₋₃₆ and chelerythrine chloride, and broad spectrum kinase inhibitor staurosporine. However, we cannot rule out the involvement of staurosporine-resistant kinases in this pathway. VGSCs also interact with the Src family of tyrosine kinases, including Fyn, which enhance sodium channel inactivation via a negative shift in steady-state inactivation (Hilborn et al. 1998; Ahn et al. 2007). In addition, studies show phosphorylation of VGSCs by p38 mitogen-activated kinase (MAPK) (Wittmack et al. 2005) and Ca²⁺/calmodulin-dependent protein kinase (CaMK) CaMKII with inhibitory action (Tan et al. 2002), indicating VGSCs can interact with a diverse plethora of kinases. Phosphorylation of VGSCs downstream of AEA may still be the mechanism of neuromodulation for this pathway.

Additionally, dephosphorylation of VGSCs changes channel output. Just as they receive phosphorylation, VGSCs are substrates for dephosphorylation by multiple phosphoprotein phosphatases (Gershon et al. 1992). The serine phosphatases calcineurin and phosphatase 2A have been shown to dephosphorylate VGSCs and reduce VGSC current (Gershon et al. 1992; Murphy et al. 1993). The tyrosine phosphatase receptor tyrosine phosphatase beta (RPTP β) shifts the voltage-dependence of channel inactivation toward hyperpolarized potentials to reduce overall VGSC current (Ratcliffe et al. 2000). Phosphorylation and dephosphorylation occur downstream of GPCR activation in several established G-protein signaling cascades and these processes are known to alter VGSC gating in a manner similar to that observed by CaSR allosteric modulators. Phosphorylation and dephosphorylation of

either α or β VGSC subunits, therefore, can provide the mechanism for VGSC inhibition by CaSR allosteric modulators.

Calcium and Calmodulin Regulate VGSCs

Through several different processes, many G-protein signaling pathways alter calcium concentrations within neurons. In turn, calcium has been proposed to modulate VGSC function as means of rapid and dynamic tuning. Yet cells dialyzed with either low or high Ca^{2+} have produced varied, unreproducible experimental results and failed to elucidate the mechanism of Ca^{2+} -sensing for VGSCs (reviewed in Ben-Johny et al. 2015). More robust, quantitative analysis with Ca^{2+} -photo-uncaging reveal that $\text{Na}_V1.5$ does not respond to changes in intracellular Ca^{2+} while $\text{Na}_V1.4$ currents are reduced by Ca^{2+} -photo-uncaging without changes to time course of channel inactivation (Ben-Johny et al. 2014), indicating that Ca^{2+} modulation of VGSCs occurs but is isoform-specific. The action of calcium on additional VGSC isoforms has yet to be thoroughly investigated and the complete picture of Ca^{2+} regulation of VGSCs unresolved but this ion-to-channel interaction may be regulated downstream of G-proteins.

Calmodulin (CaM) is a major Ca^{2+} target, which enables CaM to act as a part of many signaling pathways to activate kinases, such as CaMK, and phosphatases, as well as act directly on ion channels (reviewed in Ben-Johny et al. 2015). The interaction of CaM and Ca^{2+} drives cellular responses to changes in intracellular Ca^{2+} and is known to play a role in synaptic plasticity (Solà et al., 2001). Biochemical studies show that VGSCs directly bind both apo-CaM and Ca^{2+} -bound CaM with an IQ domain of the channel's C

terminus, providing opportunities for both Ca^{2+} -dependent and Ca^{2+} -independent binding effects (Gabelli et al. 2014; Herzog et al. 2003; Reddy Chichili et al. 2013; Gabelli et al. 2016; Mori et al. 2000; Wang et al. 2014). Coexpression of dominant negative CaM (CaM₁₂₃₄) with Na_v1.4 channels disrupted Ca^{2+} regulation and provided functional evidence that, along with the accrued structural evidence, established CaM as the Ca^{2+} sensor for VGSCs (Kim et al. 2004; Sarhan et al. 2012).

While it is widely accepted that VGSCs and CaM interact, studies of the functional outcomes of this relationship have produced heterogenous and conflicting results and no consensus model has been fully ascribed. Deschenes *et al.*, 2002, reported that Ca^{2+} -bound CaM produced an inhibitory hyperpolarizing shift in the voltage-dependence of steady-state inactivation of Na_v1.4 (Deschênes et al. 2002). However, Herzog *et al.*, 2003, independently reported that while the inactivation properties of Na_v1.6 were regulated by CaM in a Ca^{2+} -dependent manner, Na_v1.4 gating was not. Data further indicated CaM regulates the properties of VGSCs in an isoform-specific ways and via both Ca^{2+} -dependent and Ca^{2+} -independent mechanisms (Herzog et al. 2003). Conflicting conclusions across studies of VGSC-CaM regulation do not allow for predictions of VGSC gating behavior as a result of Ca^{2+} changes downstream of a G-protein signaling pathway. Nevertheless, the biological implications of CaM-VGSC interactions represent an exciting new avenue of research.

CaM involvement in the CaSR allosteric modulator pathway is unlikely as the inhibitory response of cinacalcet did not exhibit a dependence on Ca^{2+} . Neither increasing $[\text{Ca}^{2+}]_o$

to 10 mM or blocking VGCCs with Cd^+ altered the kinetics of cinacalcet-induced VGSC inhibition (Figure 1.8). However, G-protein signaling pathways can increase $[\text{Ca}^{2+}]_i$ via the manipulation of intracellular $[\text{Ca}^{2+}]$ stores, a Ca^{2+} change that would not be affected by an increase in $[\text{Ca}^{2+}]_o$ or extracellular Cd^+ . Therefore, CaM involvement cannot be ruled out altogether and Ca^{2+} /CaM modulation of VGSCs may still prove vital to this VGSC inhibition mechanism, adding another level of physiological depth (reviewed in Gabelli et al. 2016).

Further Post-translational Modifications of Voltage-Gated Sodium Channels

In addition to phosphorylation, post-translational modifications of VGSCs that alter channel gating include peptides, phosphoryl groups, ubiquitin moieties and/or carbohydrates (reviewed in Laedermann et al. 2015). The addition of any charged groups on intracellular or transmembrane domains of the channels modifies VGSC intrinsic properties to alter current amplitudes (Zhou et al. 2002). For example, glycosylation is known to influence VGSC gating properties (Recio-Pinto et al., 1990; Bennett et al., 1997; Zhang et al., 1999; Tyrrell et al., 2001) by interfering with the electric field near the gating sensors (Bennett et al., 1997; Cronin et al., 2004).

Post-translational modifications of VGSC β subunits can also alter overall channel kinetics. β -subunits regulate α -subunit gating properties by direct steric interactions that interfere with the voltage-sensor (Zimmer and Benndorf, 2002). Auxiliary β -subunits are themselves substrates for glycosylation (Isom et al., 1992) and phosphorylation (Malhotra et al., 2002), which ultimately modulates VGSC function (Johnson et al.,

2004; Johnson and Bennett, 2006). Whether these additional forms of VGSC modification play a role in the CaSR modulator pathway is not yet known and requires further experimentation (reviewed in Laedermann et al. 2015).

Gβγ Directly Binds VGSCs

One mechanism proposed for G-protein modulation of VGSCs is direct Gβγ binding and alteration of the channels. The first evidence of Gβγ modulation of ion channels showed the activation of cardiac VGPCs downstream of mAChRs by Gβγ (Logothetis et al. 1987). Since that discovery, it has been well-established that the Gβγ dimer interacts with ion channels, inhibiting VGCCs (Ikeda 1996) and activating GIRKs (Logothetis et al. 1987). The binding of Gβγ to VGSCs has been briefly addressed by Ma *et al.* (1997). The group showed that Gβγ increased persistent VGSC current from Na_v1.2 in tsA-201 cells by slowing channel gating. Gβγ subunits were shown to interact with that C-terminal site of Na_v1.2 (Ma et al. 1997) at a motif proposed to be a consensus Gβγ binding sequence (Chen et al. 1995). Consistent with this idea, G-protein β subunits immunoprecipitate with sodium channel α subunits from cortical neuron preparations (Marin et al. 2001). This is valuable evidence for G-protein modulation of VGSCs independent of post-translational modifications.

Determining if Gβγ interaction with VGSCs is responsible for modulation of VGSCs by CaSR allosteric modulators requires reliable, specific Gβγ signaling blockers. The small molecule Gβγ inhibitor gallein/M119 did not reduce cinacalcet-mediated VGSC inhibition in this study (Figure 1.5B). However, this drug shows selectivity for specific Gβγ

interactions, the extent of which is not known (Mathews et al. 2008; Bonacci et al. 2006; Casey et al. 2010). Therefore, the tools currently available to test this hypothesis are insufficient and we cannot verify whether or not G $\beta\gamma$ participates in this pathway. Because G $\beta\gamma$ signaling is membrane-delimited, modulation by G $\beta\gamma$ occurs in membrane microdomains (Galbiati et al. 2001) that are strategically positioned to affect action potential generation in the axon hillock and back-propagation at dendritic branches. Such tightly delimited modulation might be critically important for integrative properties of the neuron.

Potential G-protein-Coupled Receptors for CaSR Allosteric Modulator Binding

NPS 2143, calindol, calhex 231 and cinacalcet are structurally related phenylalkylamines, containing two aromatic rings connected by a flexible chain with a positively charged amino group (reviewed in Jensen and Bräuner-Osborne 2007). Studies have revealed calcimimetics and calcilytics target a similar interaction sites in a crevice formed by transmembrane domains (TMs) 3, 5, 6, and 7. The binding pocket for both calcimimetics and calcilytics of the CaSR involves residues Trp-818, Phe-821, Glu-837, and Ile-841 located in TM 6 and TM7, with differences observed between each compound (Petrel et al. 2004). Critically, all four compounds form ionic interactions between their amino groups and negatively charged amino acid Glu-837 located in TM7 (Magno et al. 2011). A glutamate to isoleucine mutation of this residue abolishes the modulatory effect of AEA on the CaSR, suggesting it also requires this interaction for binding to the GPCR (Figure 2.1C). Thus, the binding sites for all four compounds are largely overlapping but not identical. The shared binding pocket for all five CaSR

allosteric modulators points to, though does not prove, the existence of a structurally similar binding pocket on a separate GPCR mediating VGSC inhibition. The similar binding requirements for these compounds in addition to the similarities in VGSC inhibition characteristics of each present a high likelihood that they all exert their effects on VGSCs via the same GPCR with structural similarities to the CaSR in the region of drug binding.

GPRC6A

Orphan receptor GPRC6A is the most closely related homologue of the CaSR. It responds to L-amino acids and divalent cations (Christiansen et al. 2007; Kuang et al. 2005; Wellendorph et al. 2005). Negative CaSR allosteric modulator NPS 2143 and positive CaSR allosteric modulator calindol both inhibit L-ornithine activation of GPRC6A (Faure et al. 2009). While it is unknown if cinacalcet, calhex, or AEA bind to GPRC6A, this indicates a binding site on GPRC6A that can accommodate CaSR allosteric modulators. This positions GPRC6A as a potential candidate for CaSR allosteric modulator-induced inhibition of VGSCs, however, lack of specific inhibitors or knockouts makes this hypothesis difficult to test.

Orphan Receptors GPR55, GPR18, and GPR119

GPR18, GPR55, and GPR119 are three cannabinoid-like orphan GPCRS expressed in the central nervous system (Vassilatis et al. 2003; Sawzdargo et al. 1999; Mackie and Stella 2006; Pertwee et al. 2010). Little is yet known of the physiological functions of these receptors. AEA is identified as a partial agonist of GPR18 with an EC₅₀ of 3.38 μM

(Rajaraman et al. 2016), GPR55 with an EC_{50} of 18 nM (Pertwee 2015), and GPR119 (Overton et al. 2006). GPR18 serves roles in microglial migration in the central nervous system and is suggested to have a sympathoinhibitory role in neurons of the rostral ventrolateral medulla (Penumarti and Abdel-Rahman 2014). Research on GPR119 has focused on its role in the modulation of insulin release by pancreatic β -cells and of GLP-1 secretion by gut enteroendocrine cells (Overton et al. 2008). The action of either of these receptors in the cortex is not yet known. Lastly, GPR55 activation is known to stimulate RhoA, cdc42, rac1 (Sawzdargo et al. 1999), small GTPases associated with cytoskeleton regulation. These three GPCRs serve as putative targets for AEA to stimulate the pathway for VGSC inhibition. Exploring the role of these receptors in the pathway will require the development of knockout mice and/or highly specific receptor inhibitors. Without these tools, testing for VGSC inhibition via GPR18, GPR55, or GPR119 will be difficult to conclude.

Summary and Conclusions

In this work, I identify five ligands that inhibit VGSC current via a G-protein pathway. All of the ligands are known to act on the CaSR with either negative or positive allosteric effects. The action of synthetic modulators of the CaSR, cinacalcet, calhex, NPS 2143, and calindol, are characterized in Chapter 1. All produce complete inhibition of VGSC current in a dose-dependent fashion. Inhibition was alleviated in the presence of G-protein signaling inhibitor GDP β S, indicating a G-protein dependent mechanism for the modulation of VGSCs. Cinacalcet, calindol, NPS 2143, and calhex exert their effects independently of the CaSR, showing an off-target effect of these drugs in the

cortex. We investigated the identity of the target GPCR by first looking at candidates within the class C GPCR family, second, eliminating a class of G-protein with PTx, and third, determining the involvement of downstream effector proteins with PKA and PKC inhibitors. Using this methodology, data showed that cinacalcet does not act through mGluR1, mGluR5, or GABA_B receptors. Cinacalcet inhibition of VGSCs also does not require G_{i/o} G-proteins, eliminating a class of G-protein and narrowing the range of GPCR candidates. Lastly, cinacalcet inhibition of VGSCs does not require the activation of PKA or PKC. These findings leave a number of possibilities for the composition of this pathway: G_q, G₁₂, and G_s G-proteins, staurosporine-resistance kinases, phosphatases, phospholipases, Gβγ signaling, intracellular calcium-signaling, and a multitude of other factors, which were addressed in this discussion. The kinetics of cinacalcet-induced inhibition were quantified in-depth. It was shown that cinacalcet produces inhibition of VGSC current by shifting the steady-state inhibition of the channels toward more hyperpolarized potentials. This inhibition could be completely reversed by long hyperpolarizing steps. This finding suggests that cinacalcet pushes VGSCs into a deeply inactivated state and may stabilize a slow inactivation state.

In Chapter 2, I show that this type of inhibition is also enacted by endogenous cannabinoid anandamide. This is important as AEA is natively present in the cortex and establishes that the pathway may play a role in synaptic communication. AEA, as with the other CaSR modulators, produced complete inhibition of VGSC current over time. This inhibition was relieved with GDPβS and independent of the CaSR. Surprisingly, inhibition was also independent of AEA target CB₁. Like cinacalcet, AEA shifted

inactivation of VGSCs and this inactivation-produced inhibition was completely reversed with strong hyperpolarizing pulses. It is highly likely given their commonality as CaSR allosteric modulators and the similar manner in which they affect VGSC inactivation, that all CaSR allosteric modulators act via the same pathway to reduce VGSC current. While NPS 2143, cinacalcet, calhex, and calindol aided in the characterization of this pathway, AEA's participation in this pathway emphasizes the importance to synaptic physiology. Here, we establish a pathway from ligand to G-protein to changes in VGSC output. This may represent a novel homeostatic mechanism to reduce neuronal excitability and possesses therapeutic potential for diseases of excitability.

References

- Afshari, F.S., Ptak, K., Khaliq, Z.M., Grieco, T.M., Slater, N.T., McCrimmon, D.R. and Raman, I.M. 2004. Resurgent Na currents in four classes of neurons of the cerebellum. *Journal of Neurophysiology* 92(5), pp. 2831–2843.
- Ahern, C.A., Payandeh, J., Bosmans, F. and Chanda, B. 2016. The hitchhiker's guide to the voltage-gated sodium channel galaxy. *The Journal of General Physiology* 147(1), pp. 1–24.
- Ahn, M., Beacham, D., Westenbroek, R.E., Scheuer, T. and Catterall, W.A. 2007. Regulation of Na(v)1.2 channels by brain-derived neurotrophic factor, TrkB, and associated Fyn kinase. *The Journal of Neuroscience* 27(43), pp. 11533–11542.
- Al Kury, L.T., Voitychuk, O.I., Ali, R.M., Galadari, S., Yang, K.-H.S., Howarth, F.C., Shuba, Y.M. and Oz, M. 2014. Effects of endogenous cannabinoid anandamide on excitation-contraction coupling in rat ventricular myocytes. *Cell Calcium* 55(2), pp. 104–118.
- Al Kury, L.T., Voitychuk, O.I., Yang, K.-H.S., Thayyullathil, F.T., Doroshenko, P., Ramez, A.M., Shuba, Y.M., Galadari, S., Howarth, F.C. and Oz, M. 2014. Effects of the endogenous cannabinoid anandamide on voltage-dependent sodium and calcium channels in rat ventricular myocytes. *British Journal of Pharmacology* 171(14), pp. 3485–3498.
- Alger, B.E. 2004. Endocannabinoids and their implications for epilepsy. *Epilepsy Currents* 4(5), pp. 169–173.
- Alger, B.E. 2012. Endocannabinoids at the synapse a decade after the dies mirabilis (29 March 2001): what we still do not know. *The Journal of Physiology* 590(10), pp. 2203–2212.
- Alger, B.E. 2014. Seizing an opportunity for the endocannabinoid system. *Epilepsy Currents* 14(5), pp. 272–276.
- Aman, T.K., Grieco-Calub, T.M., Chen, C., Rusconi, R., Slat, E.A., Isom, L.L. and Raman, I.M. 2009. Regulation of persistent Na current by interactions between beta subunits of voltage-gated Na channels. *The Journal of Neuroscience* 29(7), pp. 2027–2042.
- Araya, R., Nikolenko, V., Eisenthal, K.B. and Yuste, R. 2007. Sodium channels amplify spine potentials. *Proceedings of the National Academy of Sciences of the United States of America* 104(30), pp. 12347–12352.
- Armstrong, C.M. 2006. Na channel inactivation from open and closed states. *Proceedings of the National Academy of Sciences of the United States of America* 103(47), pp. 17991–17996.
- Armstrong, C.M. and Gilly, W.F. 1979. Fast and slow steps in the activation of sodium channels. *The Journal of General Physiology* 74(6), pp. 691–711.
- Ashpole, N.M., Herren, A.W., Ginsburg, K.S., Brogan, J.D., Johnson, D.E., Cummins, T.R., Bers, D.M. and Hudmon, A. 2012. Ca²⁺/calmodulin-dependent protein kinase II (CaMKII) regulates cardiac sodium channel NaV1.5 gating by multiple phosphorylation sites. *The Journal of Biological Chemistry* 287(24), pp. 19856–19869.
- Auld, V.J., Goldin, A.L., Krafte, D.S., Marshall, J., Dunn, J.M., Catterall, W.A., Lester, H.A., Davidson, N. and Dunn, R.J. 1988. A rat brain Na⁺ channel alpha subunit with novel gating properties. *Neuron* 1(6), pp. 449–461.

- Bailey, T.W., Jin, Y.-H., Doyle, M.W., Smith, S.M. and Andresen, M.C. 2006. Vasopressin inhibits glutamate release via two distinct modes in the brainstem. *The Journal of Neuroscience* 26(23), pp. 6131–6142.
- Ballesteros, J.A., Jensen, A.D., Liapakis, G., Rasmussen, S.G., Shi, L., Gether, U. and Javitch, J.A. 2001. Activation of the beta 2-adrenergic receptor involves disruption of an ionic lock between the cytoplasmic ends of transmembrane segments 3 and 6. *The Journal of Biological Chemistry* 276(31), pp. 29171–29177.
- Balser, J.R. 1999. Structure and function of the cardiac sodium channels. *Cardiovascular Research* 42(2), pp. 327–338.
- Bean, B.P. 1989. Neurotransmitter inhibition of neuronal calcium currents by changes in channel voltage dependence. *Nature* 340(6229), pp. 153–156.
- Bean, B.P. 2007. The action potential in mammalian central neurons. *Nature Reviews. Neuroscience* 8(6), pp. 451–465.
- Beech, D.J., Bernheim, L., Mathie, A. and Hille, B. 1991. Intracellular Ca²⁺ buffers disrupt muscarinic suppression of Ca²⁺ current and M current in rat sympathetic neurons. *Proceedings of the National Academy of Sciences of the United States of America* 88(2), pp. 652–656.
- Begg, M., Pacher, P., Bátkai, S., Osei-Hyiaman, D., Offertáler, L., Mo, F.M., Liu, J. and Kunos, G. 2005. Evidence for novel cannabinoid receptors. *Pharmacology & Therapeutics* 106(2), pp. 133–145.
- Ben-Johny, M., Dick, I.E., Sang, L., Limpitikul, W.B., Kang, P.W., Niu, J., Banerjee, R., Yang, W., Babich, J.S., Issa, J.B., Lee, S.R., Namkung, H., Li, J., Zhang, M., Yang, P.S., Bazzazi, H., Adams, P.J., Joshi-Mukherjee, R., Yue, D.N. and Yue, D.T. 2015. Towards a Unified Theory of Calmodulin Regulation (Calmodulation) of Voltage-Gated Calcium and Sodium Channels. *Current molecular pharmacology* 8(2), pp. 188–205.
- Ben-Johny, M., Yang, P.S., Niu, J., Yang, W., Joshi-Mukherjee, R. and Yue, D.T. 2014. Conservation of Ca²⁺/calmodulin regulation across Na and Ca²⁺ channels. *Cell* 157(7), pp. 1657–1670.
- Berendt, F.J., Park, K.-S. and Trimmer, J.S. 2010. Multisite phosphorylation of voltage-gated sodium channel alpha subunits from rat brain. *Journal of Proteome Research* 9(4), pp. 1976–1984.
- Bernheim, L., Beech, D.J. and Hille, B. 1991. A diffusible second messenger mediates one of the pathways coupling receptors to calcium channels in rat sympathetic neurons. *Neuron* 6(6), pp. 859–867.
- Block, G.A. and Chertow, G.M. 2017. Dosing of Etelcalcetide vs Cinacalcet for Secondary Hyperparathyroidism-Reply. *The Journal of the American Medical Association* 317(20), pp. 2132–2133.
- Boiko, T., Van Wart, A., Caldwell, J.H., Levinson, S.R., Trimmer, J.S. and Matthews, G. 2003. Functional specialization of the axon initial segment by isoform-specific sodium channel targeting. *The Journal of Neuroscience* 23(6), pp. 2306–2313.

- Bonacci, T.M., Mathews, J.L., Yuan, C., Lehmann, D.M., Malik, S., Wu, D., Font, J.L., Bidlack, J.M. and Smrcka, A.V. 2006. Differential targeting of Gbetagamma-subunit signaling with small molecules. *Science* 312(5772), pp. 443–446.
- Borchhardt, K.A., Heinzl, H., Mayerwöger, E., Hörl, W.H., Haas, M. and Sunder-Plassmann, G. 2008. Cinacalcet increases calcium excretion in hypercalcemic hyperparathyroidism after kidney transplantation. *Transplantation* 86(7), pp. 919–924.
- Brackenbury, W.J. and Isom, L.L. 2011. Na Channel β Subunits: Overachievers of the Ion Channel Family. *Frontiers in pharmacology* 2, p. 53.
- Bräuner-Osborne, H., Wellendorph, P. and Jensen, A.A. 2007. Structure, pharmacology and therapeutic prospects of family C G-protein coupled receptors. *Current Drug Targets* 8(1), pp. 169–184.
- Breivogel, C.S., Griffin, G., Di Marzo, V. and Martin, B.R. 2001. Evidence for a new G protein-coupled cannabinoid receptor in mouse brain. *Molecular Pharmacology* 60(1), pp. 155–163.
- Brodie, M.J., Muir, S.E., Agnew, E., MacPhee, G.J., Volo, G., Teasdale, E. and MacPherson, P. 1985. Protein binding and CSF penetration of phenytoin following acute oral dosing in man. *British Journal of Clinical Pharmacology* 19(2), pp. 161–168.
- Brown, E.M. 2010. Clinical utility of calcimimetics targeting the extracellular calcium-sensing receptor (CaSR). *Biochemical Pharmacology* 80(3), pp. 297–307.
- Bünemann, M., Brandts, B., zu Heringdorf, D.M., van Koppen, C.J., Jakobs, K.H. and Pott, L. 1995. Activation of muscarinic K⁺ current in guinea-pig atrial myocytes by sphingosine-1-phosphate. *The Journal of Physiology* 489 (Pt 3), pp. 701–707.
- Butters, R.R., Chattopadhyay, N., Nielsen, P., Smith, C.P., Mithal, A., Kifor, O., Bai, M., Quinn, S., Goldsmith, P., Hurwitz, S., Krapcho, K., Busby, J. and Brown, E.M. 1997. Cloning and characterization of a calcium-sensing receptor from the hypercalcemic New Zealand white rabbit reveals unaltered responsiveness to extracellular calcium. *Journal of Bone and Mineral Research* 12(4), pp. 568–579.
- Caldwell, J.H., Schaller, K.L., Lasher, R.S., Peles, E. and Levinson, S.R. 2000. Sodium channel Na(v)1.6 is localized at nodes of ranvier, dendrites, and synapses. *Proceedings of the National Academy of Sciences of the United States of America* 97(10), pp. 5616–5620.
- Calhoun, J.D. and Isom, L.L. 2014. The role of non-pore-forming β subunits in physiology and pathophysiology of voltage-gated sodium channels. *Handbook of experimental pharmacology* 221, pp. 51–89.
- Calignano, A., La Rana, G., Giuffrida, A. and Piomelli, D. 1998. Control of pain initiation by endogenous cannabinoids. *Nature* 394(6690), pp. 277–281.
- Cantrell, A.R. and Catterall, W.A. 2001. Neuromodulation of Na⁺ channels: an unexpected form of cellular plasticity. *Nature Reviews. Neuroscience* 2(6), pp. 397–407.
- Cantrell, A.R., Ma, J.Y., Scheuer, T. and Catterall, W.A. 1996. Muscarinic modulation of sodium current by activation of protein kinase C in rat hippocampal neurons. *Neuron* 16(5), pp. 1019–1026.

- Cantrell, A.R., Scheuer, T. and Catterall, W.A. 1999. Voltage-dependent neuromodulation of Na⁺ channels by D1-like dopamine receptors in rat hippocampal neurons. *The Journal of Neuroscience* 19(13), pp. 5301–5310.
- Cantrell, A.R., Smith, R.D., Goldin, A.L., Scheuer, T. and Catterall, W.A. 1997. Dopaminergic modulation of sodium current in hippocampal neurons via cAMP-dependent phosphorylation of specific sites in the sodium channel alpha subunit. *The Journal of Neuroscience* 17(19), pp. 7330–7338.
- Cantrell, A.R., Tibbs, V.C., Yu, F.H., Murphy, B.J., Sharp, E.M., Qu, Y., Catterall, W.A. and Scheuer, T. 2002. Molecular mechanism of convergent regulation of brain Na⁽⁺⁾ channels by protein kinase C and protein kinase A anchored to AKAP-15. *Molecular and Cellular Neurosciences* 21(1), pp. 63–80.
- Carboni, M., Zhang, Z.S., Neplioueva, V., Starmer, C.F. and Grant, A.O. 2005. Slow sodium channel inactivation and use-dependent block modulated by the same domain IV S6 residue. *The Journal of Membrane Biology* 207(2), pp. 107–117.
- Carrier, E., Sourdet, V., Boudkkazi, S., Déglise, P., Ankri, N., Fronzaroli-Molinieres, L. and Debanne, D. 2006. Metabotropic glutamate receptor subtype 1 regulates sodium currents in rat neocortical pyramidal neurons. *The Journal of Physiology* 577(Pt 1), pp. 141–154.
- Carlson, G., Wang, Y. and Alger, B.E. 2002. Endocannabinoids facilitate the induction of LTP in the hippocampus. *Nature Neuroscience* 5(8), pp. 723–724.
- Carr, D.B., Cooper, D.C., Ulrich, S.L., Spruston, N. and Surmeier, D.J. 2002. Serotonin receptor activation inhibits sodium current and dendritic excitability in prefrontal cortex via a protein kinase C-dependent mechanism. *The Journal of Neuroscience* 22(16), pp. 6846–6855.
- Carr, D.B., Day, M., Cantrell, A.R., Held, J., Scheuer, T., Catterall, W.A. and Surmeier, D.J. 2003. Transmitter modulation of slow, activity-dependent alterations in sodium channel availability endows neurons with a novel form of cellular plasticity. *Neuron* 39(5), pp. 793–806.
- Casey, L.M., Pistner, A.R., Belmonte, S.L., Migdalovich, D., Stolpnik, O., Nwakanma, F.E., Vorobiof, G., Dunaevsky, O., Matavel, A., Lopes, C.M.B., Smrcka, A.V. and Blaxall, B.C. 2010. Small molecule disruption of G beta gamma signaling inhibits the progression of heart failure. *Circulation Research* 107(4), pp. 532–539.
- Castillo, P.E., Younts, T.J., Chávez, A.E. and Hashimoto, Y. 2012. Endocannabinoid signaling and synaptic function. *Neuron* 76(1), pp. 70–81.
- Catterall, W.A. 2000. From ionic currents to molecular mechanisms: the structure and function of voltage-gated sodium channels. *Neuron* 26(1), pp. 13–25.
- Catterall, W.A. 2012. Voltage-gated sodium channels at 60: structure, function and pathophysiology. *The Journal of Physiology* 590(11), pp. 2577–2589.
- Cervenka, R., Lukacs, P., Gawali, V.S., Ke, S., Koenig, X., Rubi, L., Zarrabi, T., Hilber, K., Sandtner, W., Stary-Weinzinger, A. and Todt, H. 2018. Distinct modulation of inactivation by a residue in the pore domain of voltage-gated Na⁺ channels: mechanistic insights from recent crystal structures. *Scientific reports* 8(1), p. 631.

- Chang, W., Tu, C., Chen, T.-H., Bikle, D. and Shoback, D. 2008. The extracellular calcium-sensing receptor (CaSR) is a critical modulator of skeletal development. *Science Signaling* 1(35), p. ra1.
- Chávez, A.E., Chiu, C.Q. and Castillo, P.E. 2010. TRPV1 activation by endogenous anandamide triggers postsynaptic long-term depression in dentate gyrus. *Nature Neuroscience* 13(12), pp. 1511–1518.
- Chen, C. and Cannon, S.C. 1995. Modulation of Na⁺ channel inactivation by the beta 1 subunit: a deletion analysis. *Pflügers Archiv: European Journal of Physiology* 431(2), pp. 186–195.
- Chen, J., DeVivo, M., Dingus, J., Harry, A., Li, J., Sui, J., Carty, D.J., Blank, J.L., Exton, J.H. and Stoffel, R.H. 1995. A region of adenylyl cyclase 2 critical for regulation by G protein beta gamma subunits. *Science* 268(5214), pp. 1166–1169.
- Chen, S., Sun, C., Wang, H. and Wang, J. 2015. The Role of Rho GTPases in Toxicity of *Clostridium difficile* Toxins. *Toxins* 7(12), pp. 5254–5267.
- Chen, W., Bergsman, J.B., Wang, X., Gilkey, G., Pierpoint, C.-R., Daniel, E.A., Awumey, E.M., Dauban, P., Dodd, R.H., Ruat, M. and Smith, S.M. 2010. Presynaptic external calcium signaling involves the calcium-sensing receptor in neocortical nerve terminals. *Plos One* 5(1), p. e8563.
- Chen, Y., Yu, F.H., Sharp, E.M., Beacham, D., Scheuer, T. and Catterall, W.A. 2008. Functional properties and differential neuromodulation of Na(v)1.6 channels. *Molecular and Cellular Neurosciences* 38(4), pp. 607–615.
- Chevalyere, V. and Castillo, P.E. 2004. Endocannabinoid-mediated metaplasticity in the hippocampus. *Neuron* 43(6), pp. 871–881.
- Chevalyere, V. and Castillo, P.E. 2003. Heterosynaptic LTD of hippocampal GABAergic synapses: a novel role of endocannabinoids in regulating excitability. *Neuron* 38(3), pp. 461–472.
- Christiansen, B., Hansen, K.B., Wellendorph, P. and Bräuner-Osborne, H. 2007. Pharmacological characterization of mouse GPRC6A, an L-alpha-amino-acid receptor modulated by divalent cations. *British Journal of Pharmacology* 150(6), pp. 798–807.
- Clapham, D.E. 1996. Intracellular signalling: more jobs for G beta gamma. *Current Biology* 6(7), pp. 814–816.
- Clapham, D.E. and Neer, E.J. 1997. G protein beta gamma subunits. *Annual Review of Pharmacology and Toxicology* 37, pp. 167–203.
- Clapper, J.R., Moreno-Sanz, G., Russo, R., Guijarro, A., Vacondio, F., Duranti, A., Tontini, A., Sanchini, S., Sciolino, N.R., Spradley, J.M., Hohmann, A.G., Calignano, A., Mor, M., Tarzia, G. and Piomelli, D. 2010. Anandamide suppresses pain initiation through a peripheral endocannabinoid mechanism. *Nature Neuroscience* 13(10), pp. 1265–1270.
- Conigrave, A.D. and Ward, D.T. 2013. Calcium-sensing receptor (CaSR): pharmacological properties and signaling pathways. *Best Practice & Research. Clinical Endocrinology & Metabolism* 27(3), pp. 315–331.
- Costa, M.R., Casnellie, J.E. and Catterall, W.A. 1982. Selective phosphorylation of the alpha

- subunit of the sodium channel by cAMP-dependent protein kinase. *The Journal of Biological Chemistry* 257(14), pp. 7918–7921.
- Costa, M.R. and Catterall, W.A. 1984. Cyclic AMP-dependent phosphorylation of the alpha subunit of the sodium channel in synaptic nerve ending particles. *The Journal of Biological Chemistry* 259(13), pp. 8210–8218.
- Courtney, K.R. 1975. Mechanism of frequency-dependent inhibition of sodium currents in frog myelinated nerve by the lidocaine derivative GEA. *The Journal of Pharmacology and Experimental Therapeutics* 195(2), pp. 225–236.
- Cravatt, B.F., Demarest, K., Patricelli, M.P., Bracey, M.H., Giang, D.K., Martin, B.R. and Lichtman, A.H. 2001. Supersensitivity to anandamide and enhanced endogenous cannabinoid signaling in mice lacking fatty acid amide hydrolase. *Proceedings of the National Academy of Sciences of the United States of America* 98(16), pp. 9371–9376.
- Cusack, N.J. and Hourani, S.M. 1981. Partial agonist behaviour of adenosine 5'-O-(2-thiodiphosphate) on human platelets. *British Journal of Pharmacology* 73(2), pp. 405–408.
- Cusdin, F.S., Clare, J.J. and Jackson, A.P. 2008. Trafficking and cellular distribution of voltage-gated sodium channels. *Traffic* 9(1), pp. 17–26.
- Davies, M.R. and Hruska, K.A. 2001. Pathophysiological mechanisms of vascular calcification in end-stage renal disease. *Kidney International* 60(2), pp. 472–479.
- Deadwyler, S.A., Hampson, R.E., Bennett, B.A., Edwards, T.A., Mu, J., Pacheco, M.A., Ward, S.J. and Childers, S.R. 1993. Cannabinoids modulate potassium current in cultured hippocampal neurons. *Receptors & channels* 1(2), pp. 121–134.
- Debanne, D. 2004. Information processing in the axon. *Nature Reviews. Neuroscience* 5(4), pp. 304–316.
- Deisz, R.A. and Lux, H.D. 1985. gamma-Aminobutyric acid-induced depression of calcium currents of chick sensory neurons. *Neuroscience Letters* 56(2), pp. 205–210.
- Deschênes, I., Neyroud, N., DiSilvestre, D., Marbán, E., Yue, D.T. and Tomaselli, G.F. 2002. Isoform-specific modulation of voltage-gated Na(+) channels by calmodulin. *Circulation Research* 90(4), pp. E49-57.
- Desfossés, J., Stip, E., Bentaleb, L.A., Lipp, O., Chiasson, J.-P., Furtos, A., Venne, K., Kouassi, E. and Potvin, S. 2012. Plasma Endocannabinoid Alterations in Individuals with Substance Use Disorder are Dependent on the “Mirror Effect” of Schizophrenia. *Frontiers in psychiatry* 3, p. 85.
- Devane, W.A., Hanus, L., Breuer, A., Pertwee, R.G., Stevenson, L.A., Griffin, G., Gibson, D., Mandelbaum, A., Etinger, A. and Mechoulam, R. 1992. Isolation and structure of a brain constituent that binds to the cannabinoid receptor. *Science* 258(5090), pp. 1946–1949.
- Diana, M.A., Levenes, C., Mackie, K. and Marty, A. 2002. Short-term retrograde inhibition of GABAergic synaptic currents in rat Purkinje cells is mediated by endogenous cannabinoids. *The Journal of Neuroscience* 22(1), pp. 200–208.
- Dolphin, A.C. and Scott, R.H. 1987. Calcium channel currents and their inhibition by (-)-baclofen in rat sensory neurones: modulation by guanine nucleotides. *The Journal of Physiology* 386, pp.

1–17.

- Drolet, P., Bilodeau, L., Chorvatova, A., Laflamme, L., Gallo-Payet, N. and Payet, M.D. 1997. Inhibition of the T-type Ca²⁺ current by the dopamine D1 receptor in rat adrenal glomerulosa cells: requirement of the combined action of the G betagamma protein subunit and cyclic adenosine 3',5'-monophosphate. *Molecular Endocrinology* 11(4), pp. 503–514.
- Eckstein, F., Cassel, D., Levkovitz, H., Lowe, M. and Selinger, Z. 1979. Guanosine 5'-O-(2-thiodiphosphate). An inhibitor of adenylate cyclase stimulation by guanine nucleotides and fluoride ions. *The Journal of Biological Chemistry* 254(19), pp. 9829–9834.
- Engel, D. and Jonas, P. 2005. Presynaptic action potential amplification by voltage-gated Na⁺ channels in hippocampal mossy fiber boutons. *Neuron* 45(3), pp. 405–417.
- Errington, A.C., Stöhr, T., Heers, C. and Lees, G. 2008. The investigational anticonvulsant lacosamide selectively enhances slow inactivation of voltage-gated sodium channels. *Molecular Pharmacology* 73(1), pp. 157–169.
- EVOLVE Trial Investigators, Chertow, G.M., Block, G.A., Correa-Rotter, R., Drüeke, T.B., Floege, J., Goodman, W.G., Herzog, C.A., Kubo, Y., London, G.M., Mahaffey, K.W., Mix, T.C.H., Moe, S.M., Trotman, M.-L., Wheeler, D.C. and Parfrey, P.S. 2012. Effect of cinacalcet on cardiovascular disease in patients undergoing dialysis. *The New England Journal of Medicine* 367(26), pp. 2482–2494.
- Faure, H., Gorojankina, T., Rice, N., Dauban, P., Dodd, R.H., Bräuner-Osborne, H., Rognan, D. and Ruat, M. 2009. Molecular determinants of non-competitive antagonist binding to the mouse GPRC6A receptor. *Cell Calcium* 46(5–6), pp. 323–332.
- Freeman, S.A., Desmazières, A., Fricker, D., Lubetzki, C. and Sol-Foulon, N. 2016. Mechanisms of sodium channel clustering and its influence on axonal impulse conduction. *Cellular and Molecular Life Sciences* 73(4), pp. 723–735.
- Fride, E. 2008. Multiple roles for the endocannabinoid system during the earliest stages of life: pre- and postnatal development. *Journal of Neuroendocrinology* 20 Suppl 1, pp. 75–81.
- Gabelli, S.B., Boto, A., Kuhns, V.H., Bianchet, M.A., Farinelli, F., Aripirala, S., Yoder, J., Jakoncic, J., Tomaselli, G.F. and Amzel, L.M. 2014. Regulation of the NaV1.5 cytoplasmic domain by calmodulin. *Nature Communications* 5, p. 5126.
- Gabelli, S.B., Yoder, J.B., Tomaselli, G.F. and Amzel, L.M. 2016. Calmodulin and Ca(2+) control of voltage gated Na(+) channels. *Channels* 10(1), pp. 45–54.
- Galbiati, F., Volonté, D., Liu, J., Capozza, F., Frank, P.G., Zhu, L., Pestell, R.G. and Lisanti, M.P. 2001. Caveolin-1 expression negatively regulates cell cycle progression by inducing G(0)/G(1) arrest via a p53/p21(WAF1/Cip1)-dependent mechanism. *Molecular Biology of the Cell* 12(8), pp. 2229–2244.
- Gasparini, S. and Magee, J.C. 2006. State-dependent dendritic computation in hippocampal CA1 pyramidal neurons. *The Journal of Neuroscience* 26(7), pp. 2088–2100.
- Gasparini, S., Migliore, M. and Magee, J.C. 2004. On the initiation and propagation of dendritic spikes in CA1 pyramidal neurons. *The Journal of Neuroscience* 24(49), pp. 11046–11056.

- Gershon, E., Weigl, L., Lotan, I., Schreibmayer, W. and Dascal, N. 1992. Protein kinase A reduces voltage-dependent Na⁺ current in *Xenopus* oocytes. *The Journal of Neuroscience* 12(10), pp. 3743–3752.
- Goldfarb, M. 2012. Voltage-gated sodium channel-associated proteins and alternative mechanisms of inactivation and block. *Cellular and Molecular Life Sciences* 69(7), pp. 1067–1076.
- Goldin, A.L. 2003. Mechanisms of sodium channel inactivation. *Current Opinion in Neurobiology* 13(3), pp. 284–290.
- Goldin, A.L. 2001. Resurgence of sodium channel research. *Annual Review of Physiology* 63, pp. 871–894.
- Grassi, F. and Lux, H.D. 1989. Voltage-dependent GABA-induced modulation of calcium currents in chick sensory neurons. *Neuroscience Letters* 105(1–2), pp. 113–119.
- Grudt, T.J. and Williams, J.T. 1993. kappa-Opioid receptors also increase potassium conductance. *Proceedings of the National Academy of Sciences of the United States of America* 90(23), pp. 11429–11432.
- Grueter, B.A., Brasnjo, G. and Malenka, R.C. 2010. Postsynaptic TRPV1 triggers cell type-specific long-term depression in the nucleus accumbens. *Nature Neuroscience* 13(12), pp. 1519–1525.
- Guindon, J., De Léan, A. and Beaulieu, P. 2006. Local interactions between anandamide, an endocannabinoid, and ibuprofen, a nonsteroidal anti-inflammatory drug, in acute and inflammatory pain. *Pain* 121(1–2), pp. 85–93.
- Guindon, J. and Hohmann, A.G. 2009. The endocannabinoid system and pain. *CNS & Neurological Disorders Drug Targets* 8(6), pp. 403–421.
- Hájos, N. and Freund, T.F. 2002. Pharmacological separation of cannabinoid sensitive receptors on hippocampal excitatory and inhibitory fibers. *Neuropharmacology* 43(4), pp. 503–510.
- Hájos, N., Ledent, C. and Freund, T.F. 2001. Novel cannabinoid-sensitive receptor mediates inhibition of glutamatergic synaptic transmission in the hippocampus. *Neuroscience* 106(1), pp. 1–4.
- Hamm, H.E. 1998. The many faces of G protein signaling. *The Journal of Biological Chemistry* 273(2), pp. 669–672.
- Hartshorne, R.P. and Catterall, W.A. 1981. Purification of the saxitoxin receptor of the sodium channel from rat brain. *Proceedings of the National Academy of Sciences of the United States of America* 78(7), pp. 4620–4624.
- Heidelberger, R., Heinemann, C., Neher, E. and Matthews, G. 1994. Calcium dependence of the rate of exocytosis in a synaptic terminal. *Nature* 371(6497), pp. 513–515.
- Heifets, B.D. and Castillo, P.E. 2009. Endocannabinoid signaling and long-term synaptic plasticity. *Annual Review of Physiology* 71, pp. 283–306.
- Henry, D.J. and Chavkin, C. 1995. Activation of inwardly rectifying potassium channels (GIRK1)

- by co-expressed rat brain cannabinoid receptors in *Xenopus oocytes*. *Neuroscience Letters* 186(2–3), pp. 91–94.
- Herkenham, M., Lynn, A.B., Little, M.D., Johnson, M.R., Melvin, L.S., de Costa, B.R. and Rice, K.C. 1990. Cannabinoid receptor localization in brain. *Proceedings of the National Academy of Sciences of the United States of America* 87(5), pp. 1932–1936.
- Herlitz, S., Garcia, D.E., Mackie, K., Hille, B., Scheuer, T. and Catterall, W.A. 1996. Modulation of Ca²⁺ channels by G-protein beta gamma subunits. *Nature* 380(6571), pp. 258–262.
- Hermans, E. 2003. Biochemical and pharmacological control of the multiplicity of coupling at G-protein-coupled receptors. *Pharmacology & Therapeutics* 99(1), pp. 25–44.
- Herzog, R.I., Liu, C., Waxman, S.G. and Cummins, T.R. 2003. Calmodulin binds to the C terminus of sodium channels Nav1.4 and Nav1.6 and differentially modulates their functional properties. *The Journal of Neuroscience* 23(23), pp. 8261–8270.
- Hilber, K., Sandtner, W., Kudlacek, O., Glaaser, I.W., Weisz, E., Kyle, J.W., French, R.J., Fozzard, H.A., Dudley, S.C. and Todt, H. 2001. The selectivity filter of the voltage-gated sodium channel is involved in channel activation. *The Journal of Biological Chemistry* 276(30), pp. 27831–27839.
- Hilborn, M.D., Vaillancourt, R.R. and Rane, S.G. 1998. Growth factor receptor tyrosine kinases acutely regulate neuronal sodium channels through the src signaling pathway. *The Journal of Neuroscience* 18(2), pp. 590–600.
- Hillard, C.J. 2008. Role of cannabinoids and endocannabinoids in cerebral ischemia. *Current Pharmaceutical Design* 14(23), pp. 2347–2361.
- Hillard, C.J. 2014. Stress regulates endocannabinoid-CB1 receptor signaling. *Seminars in Immunology* 26(5), pp. 380–388.
- Hille, B. 1992. G protein-coupled mechanisms and nervous signaling. *Neuron* 9(2), pp. 187–195.
- Hille, B. 1977. Local anesthetics: hydrophilic and hydrophobic pathways for the drug-receptor reaction. *The Journal of General Physiology* 69(4), pp. 497–515.
- Hille, B. 2001. Modulation, Slow Synaptic Action, and Second Messengers. In: *Ion Channels of Excitable Membranes*. 3rd ed. Sunderland, Massachusetts USA: Sinauer Associates, Inc, pp. 201–236.
- Hille, B., Dickson, E., Kruse, M. and Falkenburger, B. 2014. Dynamic metabolic control of an ion channel. *Progress in molecular biology and translational science* 123, pp. 219–247.
- Hodgkin, A.L. and Huxley, A.F. 1952. A quantitative description of membrane current and its application to conduction and excitation in nerve. *The Journal of Physiology* 117(4), pp. 500–544.
- Hoffmann, C., Zürn, A., Bünemann, M. and Lohse, M.J. 2008. Conformational changes in G-protein-coupled receptors-the quest for functionally selective conformations is open. *British Journal of Pharmacology* 153 Suppl 1, pp. S358-66.
- Holz, G.G., Rane, S.G. and Dunlap, K. 1986. GTP-binding proteins mediate transmitter

- inhibition of voltage-dependent calcium channels. *Nature* 319(6055), pp. 670–672.
- Hondeghem, L.M. and Katzung, B.G. 1977. Time- and voltage-dependent interactions of antiarrhythmic drugs with cardiac sodium channels. *Biochimica et Biophysica Acta* 472(3–4), pp. 373–398.
- Hotson, J.R., Prince, D.A. and Schwartzkroin, P.A. 1979. Anomalous inward rectification in hippocampal neurons. *Journal of Neurophysiology* 42(3), pp. 889–895.
- Huang, H. and Trussell, L.O. 2008. Control of presynaptic function by a persistent Na(+) current. *Neuron* 60(6), pp. 975–979.
- Huang, W.-J., Chen, W.-W. and Zhang, X. 2016. Endocannabinoid system: Role in depression, reward and pain control (Review). *Molecular medicine reports* 14(4), pp. 2899–2903.
- Huettnner, J.E. and Bean, B.P. 1988. Block of N-methyl-D-aspartate-activated current by the anticonvulsant MK-801: selective binding to open channels. *Proceedings of the National Academy of Sciences of the United States of America* 85(4), pp. 1307–1311.
- Ikeda, S.R. 1996. Voltage-dependent modulation of N-type calcium channels by G-protein beta gamma subunits. *Nature* 380(6571), pp. 255–258.
- Inanobe, A. and Kurachi, Y. 2014. Membrane channels as integrators of G-protein-mediated signaling. *Biochimica et Biophysica Acta* 1838(2), pp. 521–531.
- Jensen, A.A. and Bräuner-Osborne, H. 2007. Allosteric modulation of the calcium-sensing receptor. *Current neuropharmacology* 5(3), pp. 180–186.
- Jo, S. and Bean, B.P. 2011. Inhibition of neuronal voltage-gated sodium channels by brilliant blue G. *Molecular Pharmacology* 80(2), pp. 247–257.
- Johnson, D., Montpetit, M.L., Stocker, P.J. and Bennett, E.S. 2004. The sialic acid component of the beta1 subunit modulates voltage-gated sodium channel function. *The Journal of Biological Chemistry* 279(43), pp. 44303–44310.
- Jones, B.L. and Smith, S.M. 2016. Calcium-Sensing Receptor: A Key Target for Extracellular Calcium Signaling in Neurons. *Frontiers in physiology* 7, p. 116.
- Jung, H.Y., Mickus, T. and Spruston, N. 1997. Prolonged sodium channel inactivation contributes to dendritic action potential attenuation in hippocampal pyramidal neurons. *The Journal of Neuroscience* 17(17), pp. 6639–6646.
- Just, I., Selzer, J., Wilm, M., von Eichel-Streiber, C., Mann, M. and Aktories, K. 1995. Glucosylation of Rho proteins by Clostridium difficile toxin B. *Nature* 375(6531), pp. 500–503.
- Kane, S.P., Bress, A.P. and Tesoro, E.P. 2013. Characterization of unbound phenytoin concentrations in neurointensive care unit patients using a revised Winter-Tozer equation. *The Annals of Pharmacotherapy* 47(5), pp. 628–636.
- Kano, M., Ohno-Shosaku, T., Hashimotodani, Y., Uchigashima, M. and Watanabe, M. 2009. Endocannabinoid-mediated control of synaptic transmission. *Physiological Reviews* 89(1), pp. 309–380.
- Kaplan, D.I., Isom, L.L. and Petrou, S. 2016. Role of sodium channels in epilepsy. *Cold Spring*

Harbor perspectives in medicine 6(6).

Karbarz, M.J., Luo, L., Chang, L., Tham, C.-S., Palmer, J.A., Wilson, S.J., Wennerholm, M.L., Brown, S.M., Scott, B.P., Apodaca, R.L., Keith, J.M., Wu, J., Breitenbucher, J.G., Chaplan, S.R. and Webb, M. 2009. Biochemical and biological properties of 4-(3-phenyl-[1,2,4] thiadiazol-5-yl)-piperazine-1-carboxylic acid phenylamide, a mechanism-based inhibitor of fatty acid amide hydrolase. *Anesthesia and Analgesia* 108(1), pp. 316–329.

Karoly, R., Lenkey, N., Juhasz, A.O., Vizi, E.S. and Mike, A. 2010. Fast- or slow-inactivated state preference of Na⁺ channel inhibitors: a simulation and experimental study. *PLoS Computational Biology* 6(6), p. e1000818.

Katona, I. and Freund, T.F. 2012. Multiple functions of endocannabinoid signaling in the brain. *Annual Review of Neuroscience* 35, pp. 529–558.

Kazen-Gillespie, K.A., Ragsdale, D.S., D'Andrea, M.R., Mattei, L.N., Rogers, K.E. and Isom, L.L. 2000. Cloning, localization, and functional expression of sodium channel beta1A subunits. *The Journal of Biological Chemistry* 275(2), pp. 1079–1088.

Kim, H.I., Kim, T.H., Shin, Y.K., Lee, C.S., Park, M. and Song, J.-H. 2005. Anandamide suppression of Na⁺ currents in rat dorsal root ganglion neurons. *Brain Research* 1062(1–2), pp. 39–47.

Kim, J., Ghosh, S., Liu, H., Tateyama, M., Kass, R.S. and Pitt, G.S. 2004. Calmodulin mediates Ca²⁺ sensitivity of sodium channels. *The Journal of Biological Chemistry* 279(43), pp. 45004–45012.

Kleuss, C., Raw, A.S., Lee, E., Sprang, S.R. and Gilman, A.G. 1994. Mechanism of GTP hydrolysis by G-protein alpha subunits. *Proceedings of the National Academy of Sciences of the United States of America* 91(21), pp. 9828–9831.

Krapivinsky, G., Gordon, E.A., Wickman, K., Velimirović, B., Krapivinsky, L. and Clapham, D.E. 1995. The G-protein-gated atrial K⁺ channel IKACH is a heteromultimer of two inwardly rectifying K(+) channel proteins. *Nature* 374(6518), pp. 135–141.

Kreitzer, A.C. and Regehr, W.G. 2001a. Cerebellar depolarization-induced suppression of inhibition is mediated by endogenous cannabinoids. *The Journal of Neuroscience* 21(20), p. RC174.

Kreitzer, A.C. and Regehr, W.G. 2001b. Retrograde inhibition of presynaptic calcium influx by endogenous cannabinoids at excitatory synapses onto Purkinje cells. *Neuron* 29(3), pp. 717–727.

Kuang, D., Yao, Y., Lam, J., Tsushima, R.G. and Hampson, D.R. 2005. Cloning and characterization of a family C orphan G-protein coupled receptor. *Journal of Neurochemistry* 93(2), pp. 383–391.

Kuo, C.C. and Bean, B.P. 1994a. Na⁺ channels must deactivate to recover from inactivation. *Neuron* 12(4), pp. 819–829.

Kuo, C.C. and Bean, B.P. 1994b. Slow binding of phenytoin to inactivated sodium channels in rat hippocampal neurons. *Molecular Pharmacology* 46(4), pp. 716–725.

- Lacey, M.G., Mercuri, N.B. and North, R.A. 1988. On the potassium conductance increase activated by GABAB and dopamine D2 receptors in rat substantia nigra neurones. *The Journal of Physiology* 401, pp. 437–453.
- Laedermann, C.J., Abriel, H. and Decosterd, I. 2015. Post-translational modifications of voltage-gated sodium channels in chronic pain syndromes. *Frontiers in pharmacology* 6, p. 263.
- Lai, H.C. and Jan, L.Y. 2006. The distribution and targeting of neuronal voltage-gated ion channels. *Nature Reviews. Neuroscience* 7(7), pp. 548–562.
- Lambright, D.G., Noel, J.P., Hamm, H.E. and Sigler, P.B. 1994. Structural determinants for activation of the alpha-subunit of a heterotrimeric G protein. *Nature* 369(6482), pp. 621–628.
- Lambright, D.G., Sondek, J., Bohm, A., Skiba, N.P., Hamm, H.E. and Sigler, P.B. 1996. The 2.0 Å crystal structure of a heterotrimeric G protein. *Nature* 379(6563), pp. 311–319.
- Larkum, M.E., Waters, J., Sakmann, B. and Helmchen, F. 2007. Dendritic spikes in apical dendrites of neocortical layer 2/3 pyramidal neurons. *The Journal of Neuroscience* 27(34), pp. 8999–9008.
- Leach, K., Conigrave, A.D., Sexton, P.M. and Christopoulos, A. 2015. Towards tissue-specific pharmacology: insights from the calcium-sensing receptor as a paradigm for GPCR (patho)physiological bias. *Trends in Pharmacological Sciences* 36(4), pp. 215–225.
- Leão, R.M., Kushmerick, C., Pinaud, R., Renden, R., Li, G.-L., Taschenberger, H., Spirou, G., Levinson, S.R. and von Gersdorff, H. 2005. Presynaptic Na⁺ channels: locus, development, and recovery from inactivation at a high-fidelity synapse. *The Journal of Neuroscience* 25(14), pp. 3724–3738.
- Lefkowitz, R.J. 2013. A brief history of G-protein coupled receptors (Nobel Lecture). *Angewandte Chemie* 52(25), pp. 6366–6378.
- Lehmann, D.M., Seneviratne, A.M.P.B. and Smrcka, A.V. 2008. Small molecule disruption of G protein beta gamma subunit signaling inhibits neutrophil chemotaxis and inflammation. *Molecular Pharmacology* 73(2), pp. 410–418.
- Lenkowski, P.W., Batts, T.W., Smith, M.D., Ko, S.-H., Jones, P.J., Taylor, C.H., McCusker, A.K., Davis, G.C., Hartmann, H.A., White, H.S., Brown, M.L. and Patel, M.K. 2007. A pharmacophore derived phenytoin analogue with increased affinity for slow inactivated sodium channels exhibits a desired anticonvulsant profile. *Neuropharmacology* 52(3), pp. 1044–1054.
- Lerner, T.N. and Kreitzer, A.C. 2012. RGS4 is required for dopaminergic control of striatal LTD and susceptibility to parkinsonian motor deficits. *Neuron* 73(2), pp. 347–359.
- Lévénés, C., Daniel, H., Soubrié, P. and Crépel, F. 1998. Cannabinoids decrease excitatory synaptic transmission and impair long-term depression in rat cerebellar Purkinje cells. *The Journal of Physiology* 510 (Pt 3), pp. 867–879.
- Lewis, A.H. and Raman, I.M. 2014. Resurgent current of voltage-gated Na(+) channels. *The Journal of Physiology* 592(22), pp. 4825–4838.
- Liao, Y.J., Jan, Y.N. and Jan, L.Y. 1996. Heteromultimerization of G-protein-gated inwardly rectifying K⁺ channel proteins GIRK1 and GIRK2 and their altered expression in weaver brain.

The Journal of Neuroscience 16(22), pp. 7137–7150.

Lin, Y. and Smrcka, A.V. 2011. Understanding molecular recognition by G protein $\beta\gamma$ subunits on the path to pharmacological targeting. *Molecular Pharmacology* 80(4), pp. 551–557.

Linderman, J.J. 2009. Modeling of G-protein-coupled receptor signaling pathways. *The Journal of Biological Chemistry* 284(9), pp. 5427–5431.

Lipscombe, D., Kongsamut, S. and Tsien, R.W. 1989. Alpha-adrenergic inhibition of sympathetic neurotransmitter release mediated by modulation of N-type calcium-channel gating. *Nature* 340(6235), pp. 639–642.

Llinás, R. and Sugimori, M. 2012. Probing the functional properties of mammalian dendrites. 1980. *Cerebellum* 11(3), pp. 612–628.

Logothetis, D.E., Kurachi, Y., Galper, J., Neer, E.J. and Clapham, D.E. 1987. The beta gamma subunits of GTP-binding proteins activate the muscarinic K⁺ channel in heart. *Nature* 325(6102), pp. 321–326.

Lohse, M.J., Hein, P., Hoffmann, C., Nikolaev, V.O., Vilardaga, J.P. and Bünemann, M. 2008. Kinetics of G-protein-coupled receptor signals in intact cells. *British Journal of Pharmacology* 153 Suppl 1, pp. S125-32.

Losonczy, A., Makara, J.K. and Magee, J.C. 2008. Compartmentalized dendritic plasticity and input feature storage in neurons. *Nature* 452(7186), pp. 436–441.

Lu, V.B. and Ikeda, S.R. 2016. Strategies for Investigating G-Protein Modulation of Voltage-Gated Ca²⁺ Channels. *Cold Spring Harbor Protocols* 2016(5), p. pdb.top087072.

Lüscher, C., Jan, L.Y., Stoffel, M., Malenka, R.C. and Nicoll, R.A. 1997. G protein-coupled inwardly rectifying K⁺ channels (GIRKs) mediate postsynaptic but not presynaptic transmitter actions in hippocampal neurons. *Neuron* 19(3), pp. 687–695.

Ma, J.Y., Catterall, W.A. and Scheuer, T. 1997. Persistent sodium currents through brain sodium channels induced by G protein betagamma subunits. *Neuron* 19(2), pp. 443–452.

Mackie, K. and Hille, B. 1992. Cannabinoids inhibit N-type calcium channels in neuroblastoma-glioma cells. *Proceedings of the National Academy of Sciences of the United States of America* 89(9), pp. 3825–3829.

Mackie, K., Lai, Y., Westenbroek, R. and Mitchell, R. 1995. Cannabinoids activate an inwardly rectifying potassium conductance and inhibit Q-type calcium currents in AtT20 cells transfected with rat brain cannabinoid receptor. *The Journal of Neuroscience* 15(10), pp. 6552–6561.

Mackie, K. and Stella, N. 2006. Cannabinoid receptors and endocannabinoids: evidence for new players. *The AAPS Journal* 8(2), pp. E298-306.

Maejima, T., Hashimoto, K., Yoshida, T., Aiba, A. and Kano, M. 2001. Presynaptic inhibition caused by retrograde signal from metabotropic glutamate to cannabinoid receptors. *Neuron* 31(3), pp. 463–475.

Magno, A.L., Ward, B.K. and Ratajczak, T. 2011. The calcium-sensing receptor: a molecular perspective. *Endocrine Reviews* 32(1), pp. 3–30.

- Mantegazza, M., Yu, F.H., Powell, A.J., Clare, J.J., Catterall, W.A. and Scheuer, T. 2005. Molecular determinants for modulation of persistent sodium current by G-protein betagamma subunits. *The Journal of Neuroscience* 25(13), pp. 3341–3349.
- Marcocci, C., Chanson, P., Shoback, D., Bilezikian, J., Fernandez-Cruz, L., Orgiazzi, J., Henzen, C., Cheng, S., Sterling, L.R., Lu, J. and Peacock, M. 2009. Cinacalcet reduces serum calcium concentrations in patients with intractable primary hyperparathyroidism. *The Journal of Clinical Endocrinology and Metabolism* 94(8), pp. 2766–2772.
- Marin, P., Fagni, L., Torrens, Y., Alcaraz, G., Couraud, F., Bockaert, J., Glowinski, J. and Prémont, J. 2001. AMPA receptor activation induces association of G-beta protein with the alpha subunit of the sodium channel in neurons. *The European Journal of Neuroscience* 14(12), pp. 1953–1960.
- Maroof, N., Pardon, M.C. and Kendall, D.A. 2013. Endocannabinoid signalling in Alzheimer's disease. *Biochemical Society Transactions* 41(6), pp. 1583–1587.
- Martin, K.J., Bell, G., Pickthorn, K., Huang, S., Vick, A., Hodsmann, P. and Peacock, M. 2014. Velcalcetide (AMG 416), a novel peptide agonist of the calcium-sensing receptor, reduces serum parathyroid hormone and FGF23 levels in healthy male subjects. *Nephrology, Dialysis, Transplantation* 29(2), pp. 385–392.
- Maruyama, K. 1991. The Discovery of Adenosine Triphosphate and the Establishment of Its Structure. *Journal of the History of Biology* 24(1), p. 145.
- Mathews, J.L., Smrcka, A.V. and Bidlack, J.M. 2008. A novel Gbetagamma-subunit inhibitor selectively modulates mu-opioid-dependent antinociception and attenuates acute morphine-induced antinociceptive tolerance and dependence. *The Journal of Neuroscience* 28(47), pp. 12183–12189.
- Mattheisen, G.B., Tsintsadze, T. and Smith, S.M. 2018. Strong G-Protein-Mediated Inhibition of Sodium Channels. *Cell reports* 23(9), pp. 2770–2781.
- Maurice, N., Mercer, J., Chan, C.S., Hernandez-Lopez, S., Held, J., Tkatch, T. and Surmeier, D.J. 2004. D2 dopamine receptor-mediated modulation of voltage-dependent Na⁺ channels reduces autonomous activity in striatal cholinergic interneurons. *The Journal of Neuroscience* 24(46), pp. 10289–10301.
- Maurice, N., Tkatch, T., Meisler, M., Sprunger, L.K. and Surmeier, D.J. 2001. D1/D5 dopamine receptor activation differentially modulates rapidly inactivating and persistent sodium currents in prefrontal cortex pyramidal neurons. *The Journal of Neuroscience* 21(7), pp. 2268–2277.
- McFadzean, I. and Docherty, R.J. 1989. Noradrenaline- and Enkephalin-Induced Inhibition of Voltage-Sensitive Calcium Currents in NG108-15 Hybrid Cells. *The European Journal of Neuroscience* 1(2), pp. 141–147.
- Mechoulam, R. and Parker, L.A. 2013. The endocannabinoid system and the brain. *Annual review of psychology* 64, pp. 21–47.
- Messner, D.J. and Catterall, W.A. 1985. The sodium channel from rat brain. Separation and characterization of subunits. *The Journal of Biological Chemistry* 260(19), pp. 10597–10604.

- Metna-Laurent, M. and Marsicano, G. 2015. Rising stars: modulation of brain functions by astroglial type-1 cannabinoid receptors. *Glia* 63(3), pp. 353–364.
- Mickus, T., Jung, H. y and Spruston, N. 1999. Properties of slow, cumulative sodium channel inactivation in rat hippocampal CA1 pyramidal neurons. *Biophysical Journal* 76(2), pp. 846–860.
- Mitrovic, N., George, A.L. and Horn, R. 2000. Role of domain 4 in sodium channel slow inactivation. *The Journal of General Physiology* 115(6), pp. 707–718.
- Miyazaki, H., Oyama, F., Inoue, R., Aosaki, T., Abe, T., Kiyonari, H., Kino, Y., Kurosawa, M., Shimizu, J., Ogiwara, I., Yamakawa, K., Koshimizu, Y., Fujiyama, F., Kaneko, T., Shimizu, H., Nagatomo, K., Yamada, K., Shimogori, T., Hattori, N., Miura, M. and Nukina, N. 2014. Singular localization of sodium channel β 4 subunit in unmyelinated fibres and its role in the striatum. *Nature Communications* 5, p. 5525.
- Moe, S.M. and Thadhani, R. 2013. What have we learned about chronic kidney disease-mineral bone disorder from the EVOLVE and PRIMO trials? *Current Opinion in Nephrology and Hypertension* 22(6), pp. 651–655.
- Mori, M., Konno, T., Ozawa, T., Murata, M., Imoto, K. and Nagayama, K. 2000. Novel interaction of the voltage-dependent sodium channel (VDSC) with calmodulin: does VDSC acquire calmodulin-mediated Ca^{2+} -sensitivity? *Biochemistry* 39(6), pp. 1316–1323.
- Morinville, A., Fundin, B., Meury, L., Juréus, A., Sandberg, K., Krupp, J., Ahmad, S. and O'Donnell, D. 2007. Distribution of the voltage-gated sodium channel $\text{Na}(v)1.7$ in the rat: expression in the autonomic and endocrine systems. *The Journal of Comparative Neurology* 504(6), pp. 680–689.
- Morishige, K.I., Inanobe, A., Takahashi, N., Yoshimoto, Y., Kurachi, H., Miyake, A., Tokunaga, Y., Maeda, T. and Kurachi, Y. 1996. G protein-gated K^+ channel (GIRK1) protein is expressed presynaptically in the paraventricular nucleus of the hypothalamus. *Biochemical and Biophysical Research Communications* 220(2), pp. 300–305.
- Müller-Vahl, K.R. 2013. Treatment of Tourette syndrome with cannabinoids. *Behavioural neurology* 27(1), pp. 119–124.
- Murphy, B.J., Rossie, S., De Jongh, K.S. and Catterall, W.A. 1993. Identification of the sites of selective phosphorylation and dephosphorylation of the rat brain Na^+ channel alpha subunit by cAMP-dependent protein kinase and phosphoprotein phosphatases. *The Journal of Biological Chemistry* 268(36), pp. 27355–27362.
- Navarrete, M. and Araque, A. 2008. Endocannabinoids mediate neuron-astrocyte communication. *Neuron* 57(6), pp. 883–893.
- Navarrete, M., Díez, A. and Araque, A. 2014. Astrocytes in endocannabinoid signalling. *Philosophical Transactions of the Royal Society of London. Series B, Biological Sciences* 369(1654), p. 20130599.
- Navarro, B., Kennedy, M.E., Velimirović, B., Bhat, D., Peterson, A.S. and Clapham, D.E. 1996. Nonselective and G betagamma-insensitive weaver K^+ channels. *Science* 272(5270), pp. 1950–1953.

- Nemeth, E.F. and Goodman, W.G. 2016. Calcimimetic and calcilytic drugs: feats, flops, and futures. *Calcified Tissue International* 98(4), pp. 341–358.
- Nemeth, E.F., Heaton, W.H., Miller, M., Fox, J., Balandrin, M.F., Van Wagenen, B.C., Colloton, M., Karbon, W., Scherrer, J., Shatzen, E., Rishton, G., Scully, S., Qi, M., Harris, R., Lacey, D. and Martin, D. 2004. Pharmacodynamics of the type II calcimimetic compound cinacalcet HCl. *The Journal of Pharmacology and Experimental Therapeutics* 308(2), pp. 627–635.
- Neves, S.R., Ram, P.T. and Iyengar, R. 2002. G protein pathways. *Science* 296(5573), pp. 1636–1639.
- Nicholson, R.A., Liao, C., Zheng, J., David, L.S., Coyne, L., Errington, A.C., Singh, G. and Lees, G. 2003. Sodium channel inhibition by anandamide and synthetic cannabimimetics in brain. *Brain Research* 978(1–2), pp. 194–204.
- Noble, D. and Stein, R.B. 1966. The threshold conditions for initiation of action potentials by excitable cells. *The Journal of Physiology* 187(1), pp. 129–162.
- Nogueron, M.I., Porgilsson, B., Schneider, W.E., Stucky, C.L. and Hillard, C.J. 2001. Cannabinoid receptor agonists inhibit depolarization-induced calcium influx in cerebellar granule neurons. *Journal of Neurochemistry* 79(2), pp. 371–381.
- North, R.A., Williams, J.T., Surprenant, A. and Christie, M.J. 1987. Mu and delta receptors belong to a family of receptors that are coupled to potassium channels. *Proceedings of the National Academy of Sciences of the United States of America* 84(15), pp. 5487–5491.
- Numann, R., Catterall, W.A. and Scheuer, T. 1991. Functional modulation of brain sodium channels by protein kinase C phosphorylation. *Science* 254(5028), pp. 115–118.
- Nuss, H.B., Kambouris, N.G., Marbán, E., Tomaselli, G.F. and Balsler, J.R. 2000. Isoform-specific lidocaine block of sodium channels explained by differences in gating. *Biophysical Journal* 78(1), pp. 200–210.
- Oh, U., Ho, Y.K. and Kim, D. 1995. Modulation of the serotonin-activated K⁺ channel by G protein subunits and nucleotides in rat hippocampal neurons. *The Journal of Membrane Biology* 147(3), pp. 241–253.
- Ohno-Shosaku, T., Maejima, T. and Kano, M. 2001. Endogenous cannabinoids mediate retrograde signals from depolarized postsynaptic neurons to presynaptic terminals. *Neuron* 29(3), pp. 729–738.
- Okada, Y., Imendra, K.G., Miyazaki, T., Hotokezaka, H., Fujiyama, R., Zeredo, J.L., Miyamoto, T. and Toda, K. 2005. Biophysical properties of voltage-gated Na⁺ channels in frog parathyroid cells and their modulation by cannabinoids. *The Journal of Experimental Biology* 208(Pt 24), pp. 4747–4756.
- Okura, D., Horishita, T., Ueno, S., Yanagihara, N., Sudo, Y., Uezono, Y. and Sata, T. 2014. The endocannabinoid anandamide inhibits voltage-gated sodium channels Nav1.2, Nav1.6, Nav1.7, and Nav1.8 in *Xenopus* oocytes. *Anesthesia and Analgesia* 118(3), pp. 554–562.
- Oldham, W.M. and Hamm, H.E. 2008. Heterotrimeric G protein activation by G-protein-coupled receptors. *Nature Reviews. Molecular Cell Biology* 9(1), pp. 60–71.

- Oldham, W.M. and Hamm, H.E. 2007. How do receptors activate G proteins? *Advances in protein chemistry* 74, pp. 67–93.
- Overton, H.A., Babbs, A.J., Doel, S.M., Fyfe, M.C.T., Gardner, L.S., Griffin, G., Jackson, H.C., Procter, M.J., Rasamison, C.M., Tang-Christensen, M., Widdowson, P.S., Williams, G.M. and Reynet, C. 2006. Deorphanization of a G protein-coupled receptor for oleoylethanolamide and its use in the discovery of small-molecule hypophagic agents. *Cell Metabolism* 3(3), pp. 167–175.
- Overton, H.A., Fyfe, M.C.T. and Reynet, C. 2008. GPR119, a novel G protein-coupled receptor target for the treatment of type 2 diabetes and obesity. *British Journal of Pharmacology* 153 Suppl 1, pp. S76-81.
- O'Malley, H.A. and Isom, L.L. 2015. Sodium channel β subunits: emerging targets in channelopathies. *Annual Review of Physiology* 77(1), pp. 481–504.
- O'Reilly, J.P., Wang, S.Y. and Wang, G.K. 2001. Residue-specific effects on slow inactivation at V787 in D2-S6 of Na(v)1.4 sodium channels. *Biophysical Journal* 81(4), pp. 2100–2111.
- Padhi, D. and Harris, R. 2009. Clinical pharmacokinetic and pharmacodynamic profile of cinacalcet hydrochloride. *Clinical Pharmacokinetics* 48(5), pp. 303–311.
- Parfrey, P.S., Block, G.A., Correa-Rotter, R., Drüeke, T.B., Floege, J., Herzog, C.A., London, G.M., Mahaffey, K.W., Moe, S.M., Wheeler, D.C. and Chertow, G.M. 2016. Lessons Learned from EVOLVE for Planning of Future Randomized Trials in Patients on Dialysis. *Clinical Journal of the American Society of Nephrology* 11(3), pp. 539–546.
- Parsons, L.H. and Hurd, Y.L. 2015. Endocannabinoid signalling in reward and addiction. *Nature Reviews. Neuroscience* 16(10), pp. 579–594.
- Pasch, A., Block, G.A., Bachtler, M., Smith, E.R., Jahnen-Dechent, W., Arampatzis, S., Chertow, G.M., Parfrey, P., Ma, X. and Floege, J. 2017. Blood calcification propensity, cardiovascular events, and survival in patients receiving hemodialysis in the EVOLVE trial. *Clinical Journal of the American Society of Nephrology* 12(2), pp. 315–322.
- Patino, G.A. and Isom, L.L. 2010. Electrophysiology and beyond: multiple roles of Na⁺ channel β subunits in development and disease. *Neuroscience Letters* 486(2), pp. 53–59.
- Patlak, J.B. and Ortiz, M. 1985. Slow currents through single sodium channels of the adult rat heart. *The Journal of General Physiology* 86(1), pp. 89–104.
- Patlak, J.B. and Ortiz, M. 1986. Two modes of gating during late Na⁺ channel currents in frog sartorius muscle. *The Journal of General Physiology* 87(2), pp. 305–326.
- Pazos, M.R., Sagredo, O. and Fernández-Ruiz, J. 2008. The endocannabinoid system in Huntington's disease. *Current Pharmaceutical Design* 14(23), pp. 2317–2325.
- Penumarti, A. and Abdel-Rahman, A.A. 2014. The novel endocannabinoid receptor GPR18 is expressed in the rostral ventrolateral medulla and exerts tonic restraining influence on blood pressure. *The Journal of Pharmacology and Experimental Therapeutics* 349(1), pp. 29–38.
- Pertwee, R.G. 2015. Endocannabinoids and their pharmacological actions. *Handbook of experimental pharmacology* 231, pp. 1–37.

- Pertwee, R.G., Howlett, A.C., Abood, M.E., Alexander, S.P.H., Di Marzo, V., Elphick, M.R., Greasley, P.J., Hansen, H.S., Kunos, G., Mackie, K., Mechoulam, R. and Ross, R.A. 2010. International Union of Basic and Clinical Pharmacology. LXXIX. Cannabinoid receptors and their ligands: beyond CB₁ and CB₂. *Pharmacological Reviews* 62(4), pp. 588–631.
- Petrel, C., Kessler, A., Dauban, P., Dodd, R.H., Rognan, D. and Ruat, M. 2004. Positive and negative allosteric modulators of the Ca²⁺-sensing receptor interact within overlapping but not identical binding sites in the transmembrane domain. *The Journal of Biological Chemistry* 279(18), pp. 18990–18997.
- Pfaffinger, P.J., Martin, J.M., Hunter, D.D., Nathanson, N.M. and Hille, B. 1985. GTP-binding proteins couple cardiac muscarinic receptors to a K channel. *Nature* 317(6037), pp. 536–538.
- Phillips, C.G., Harnett, M.T., Chen, W. and Smith, S.M. 2008. Calcium-sensing receptor activation depresses synaptic transmission. *The Journal of Neuroscience* 28(46), pp. 12062–12070.
- Pitt, G.S. and Lee, S.-Y. 2016. Current view on regulation of voltage-gated sodium channels by calcium and auxiliary proteins. *Protein Science* 25(9), pp. 1573–1584.
- Platkiewicz, J. and Brette, R. 2010. A threshold equation for action potential initiation. *PLoS Computational Biology* 6(7), p. e1000850.
- Ponce, A., Bueno, E., Kentros, C., Vega-Saenz de Miera, E., Chow, A., Hillman, D., Chen, S., Zhu, L., Wu, M.B., Wu, X., Rudy, B. and Thornhill, W.B. 1996. G-protein-gated inward rectifier K⁺ channel proteins (GIRK1) are present in the soma and dendrites as well as in nerve terminals of specific neurons in the brain. *The Journal of Neuroscience* 16(6), pp. 1990–2001.
- Proft, J. and Weiss, N. 2015. G protein regulation of neuronal calcium channels: back to the future. *Molecular Pharmacology* 87(6), pp. 890–906.
- Puente, N., Cui, Y., Lassalle, O., Lafourcade, M., Georges, F., Venance, L., Grandes, P. and Manzoni, O.J. 2011. Polymodal activation of the endocannabinoid system in the extended amygdala. *Nature Neuroscience* 14(12), pp. 1542–1547.
- Qiao, X., Sun, G., Clare, J.J., Werkman, T.R. and Wadman, W.J. 2014. Properties of human brain sodium channel α -subunits expressed in HEK293 cells and their modulation by carbamazepine, phenytoin and lamotrigine. *British Journal of Pharmacology* 171(4), pp. 1054–1067.
- Qin, N., D'Andrea, M.R., Lubin, M.-L., Shafaei, N., Codd, E.E. and Correa, A.M. 2003. Molecular cloning and functional expression of the human sodium channel beta1B subunit, a novel splicing variant of the beta1 subunit. *European Journal of Biochemistry / FEBS* 270(23), pp. 4762–4770.
- Rajaraman, G., Simcocks, A., Hryciw, D.H., Hutchinson, D.S. and McAinch, A.J. 2016. G protein coupled receptor 18: A potential role for endocannabinoid signaling in metabolic dysfunction. *Molecular Nutrition & Food Research* 60(1), pp. 92–102.
- Raman, I.M. and Bean, B.P. 2001. Inactivation and recovery of sodium currents in cerebellar Purkinje neurons: evidence for two mechanisms. *Biophysical Journal* 80(2), pp. 729–737.

- Raman, I.M. and Bean, B.P. 1997. Resurgent sodium current and action potential formation in dissociated cerebellar Purkinje neurons. *The Journal of Neuroscience* 17(12), pp. 4517–4526.
- Raman, I.M., Sprunger, L.K., Meisler, M.H. and Bean, B.P. 1997. Altered subthreshold sodium currents and disrupted firing patterns in Purkinje neurons of Scn8a mutant mice. *Neuron* 19(4), pp. 881–891.
- Ratcliffe, C.F., Qu, Y., McCormick, K.A., Tibbs, V.C., Dixon, J.E., Scheuer, T. and Catterall, W.A. 2000. A sodium channel signaling complex: modulation by associated receptor protein tyrosine phosphatase beta. *Nature Neuroscience* 3(5), pp. 437–444.
- Reddy Chichili, V.P., Xiao, Y., Seetharaman, J., Cummins, T.R. and Sivaraman, J. 2013. Structural basis for the modulation of the neuronal voltage-gated sodium channel NaV1.6 by calmodulin. *Scientific reports* 3, p. 2435.
- Remy, C., Remy, S., Beck, H., Swandulla, D. and Hans, M. 2004. Modulation of voltage-dependent sodium channels by the delta-agonist SNC80 in acutely isolated rat hippocampal neurons. *Neuropharmacology* 47(7), pp. 1102–1112.
- Richardson, J.D., Kilo, S. and Hargreaves, K.M. 1998. Cannabinoids reduce hyperalgesia and inflammation via interaction with peripheral CB1 receptors. *Pain* 75(1), pp. 111–119.
- Robillard, L., Ethier, N., Lachance, M. and Hébert, T.E. 2000. Gbetagamma subunit combinations differentially modulate receptor and effector coupling in vivo. *Cellular Signalling* 12(9–10), pp. 673–682.
- Rogers, K.V., Dunn, C.K., Hebert, S.C. and Brown, E.M. 1997. Localization of calcium receptor mRNA in the adult rat central nervous system by in situ hybridization. *Brain Research* 744(1), pp. 47–56.
- Rosenbaum, D.M., Rasmussen, S.G.F. and Kobilka, B.K. 2009. The structure and function of G-protein-coupled receptors. *Nature* 459(7245), pp. 356–363.
- Rossie, S. and Catterall, W.A. 1989. Phosphorylation of the alpha subunit of rat brain sodium channels by cAMP-dependent protein kinase at a new site containing Ser686 and Ser687. *The Journal of Biological Chemistry* 264(24), pp. 14220–14224.
- Rossie, S., Gordon, D. and Catterall, W.A. 1987. Identification of an intracellular domain of the sodium channel having multiple cAMP-dependent phosphorylation sites. *The Journal of Biological Chemistry* 262(36), pp. 17530–17535.
- Rothe, H.M., Liangos, O., Biggar, P., Petermann, A. and Ketteler, M. 2011. Cinacalcet treatment of primary hyperparathyroidism. *International journal of endocrinology* 2011, p. 415719.
- Rouach, N. and Nicoll, R.A. 2003. Endocannabinoids contribute to short-term but not long-term mGluR-induced depression in the hippocampus. *The European Journal of Neuroscience* 18(4), pp. 1017–1020.
- Ruat, M., Molliver, M.E., Snowman, A.M. and Snyder, S.H. 1995. Calcium sensing receptor: molecular cloning in rat and localization to nerve terminals. *Proceedings of the National Academy of Sciences of the United States of America* 92(8), pp. 3161–3165.
- Ruehle, S., Rey, A.A., Remmers, F. and Lutz, B. 2012. The endocannabinoid system in anxiety,

- fear memory and habituation. *Journal of Psychopharmacology* 26(1), pp. 23–39.
- Ruff, R.L., Simoncini, L. and Stühmer, W. 1988. Slow sodium channel inactivation in mammalian muscle: a possible role in regulating excitability. *Muscle & Nerve* 11(5), pp. 502–510.
- Rush, A.M., Dib-Hajj, S.D. and Waxman, S.G. 2005. Electrophysiological properties of two axonal sodium channels, Nav1.2 and Nav1.6, expressed in mouse spinal sensory neurones. *The Journal of Physiology* 564(Pt 3), pp. 803–815.
- Sagar, D.R., Kendall, D.A. and Chapman, V. 2008. Inhibition of fatty acid amide hydrolase produces PPAR-alpha-mediated analgesia in a rat model of inflammatory pain. *British Journal of Pharmacology* 155(8), pp. 1297–1306.
- Sarhan, M.F., Tung, C.-C., Van Petegem, F. and Ahern, C.A. 2012. Crystallographic basis for calcium regulation of sodium channels. *Proceedings of the National Academy of Sciences of the United States of America* 109(9), pp. 3558–3563.
- Saugstad, J.A., Segerson, T.P. and Westbrook, G.L. 1996. Metabotropic glutamate receptors activate G-protein-coupled inwardly rectifying potassium channels in *Xenopus* oocytes. *The Journal of Neuroscience* 16(19), pp. 5979–5985.
- Savio-Galimberti, E., Gollob, M.H. and Darbar, D. 2012. Voltage-gated sodium channels: biophysics, pharmacology, and related channelopathies. *Frontiers in pharmacology* 3, p. 124.
- Sawzdargo, M., Nguyen, T., Lee, D.K., Lynch, K.R., Cheng, R., Heng, H.H., George, S.R. and O’Dowd, B.F. 1999. Identification and cloning of three novel human G protein-coupled receptor genes GPR52, PsiGPR53 and GPR55: GPR55 is extensively expressed in human brain. *Brain research. Molecular brain research* 64(2), pp. 193–198.
- Scheuer, T. 2011. Regulation of sodium channel activity by phosphorylation. *Seminars in Cell & Developmental Biology* 22(2), pp. 160–165.
- Schiffmann, S.N., Lledo, P.M. and Vincent, J.D. 1995. Dopamine D1 receptor modulates the voltage-gated sodium current in rat striatal neurones through a protein kinase A. *The Journal of Physiology* 483 (Pt 1), pp. 95–107.
- Schneggenburger, R. and Neher, E. 2000. Intracellular calcium dependence of transmitter release rates at a fast central synapse. *Nature* 406(6798), pp. 889–893.
- Schweitzer, P. 2000. Cannabinoids decrease the K(+) M-current in hippocampal CA1 neurons. *The Journal of Neuroscience* 20(1), pp. 51–58.
- Schwiebert, E.M. and Zsembery, A. 2003. Extracellular ATP as a signaling molecule for epithelial cells. *Biochimica et Biophysica Acta* 1615(1–2), pp. 7–32.
- Seifert, R. and Wenzel-Seifert, K. 2002. Constitutive activity of G-protein-coupled receptors: cause of disease and common property of wild-type receptors. *Naunyn-Schmiedeberg’s Archives of Pharmacology* 366(5), pp. 381–416.
- Seneviratne, A.M.P.B., Burroughs, M., Giralt, E. and Smrcka, A.V. 2011. Direct-reversible binding of small molecules to G protein $\beta\gamma$ subunits. *Biochimica et Biophysica Acta* 1814(9), pp. 1210–1218.

- Shapiro, D.A., Kristiansen, K., Weiner, D.M., Kroeze, W.K. and Roth, B.L. 2002. Evidence for a model of agonist-induced activation of 5-hydroxytryptamine 2A serotonin receptors that involves the disruption of a strong ionic interaction between helices 3 and 6. *The Journal of Biological Chemistry* 277(13), pp. 11441–11449.
- Shapiro, M.S., Loose, M.D., Hamilton, S.E., Nathanson, N.M., Gomeza, J., Wess, J. and Hille, B. 1999. Assignment of muscarinic receptor subtypes mediating G-protein modulation of Ca(2+) channels by using knockout mice. *Proceedings of the National Academy of Sciences of the United States of America* 96(19), pp. 10899–10904.
- Sheets, P.L., Heers, C., Stoehr, T. and Cummins, T.R. 2008. Differential block of sensory neuronal voltage-gated sodium channels by lacosamide [(2R)-2-(acetylamino)-N-benzyl-3-methoxypropanamide], lidocaine, and carbamazepine. *The Journal of Pharmacology and Experimental Therapeutics* 326(1), pp. 89–99.
- Shenoy, S.K. and Lefkowitz, R.J. 2011. β -Arrestin-mediated receptor trafficking and signal transduction. *Trends in Pharmacological Sciences* 32(9), pp. 521–533.
- Sigel, E. and Baur, R. 1988. Activation of protein kinase C differentially modulates neuronal Na⁺, Ca²⁺, and gamma-aminobutyrate type A channels. *Proceedings of the National Academy of Sciences of the United States of America* 85(16), pp. 6192–6196.
- Skiba, N.P., Bae, H. and Hamm, H.E. 1996. Mapping of effector binding sites of transducin alpha-subunit using G alpha t/G alpha i1 chimeras. *The Journal of Biological Chemistry* 271(1), pp. 413–424.
- Smith, R.D. and Goldin, A.L. 1996. Phosphorylation of brain sodium channels in the I-II linker modulates channel function in *Xenopus* oocytes. *The Journal of Neuroscience* 16(6), pp. 1965–1974.
- Smith, S.M., Bergsman, J.B., Harata, N.C., Scheller, R.H. and Tsien, R.W. 2004. Recordings from single neocortical nerve terminals reveal a nonselective cation channel activated by decreases in extracellular calcium. *Neuron* 41(2), pp. 243–256.
- Smith, S.M., Chen, W., Vyleta, N.P., Williams, C., Lee, C.-H., Phillips, C. and Andresen, M.C. 2012. Calcium regulation of spontaneous and asynchronous neurotransmitter release. *Cell Calcium* 52(3–4), pp. 226–233.
- Soejima, M. and Noma, A. 1984. Mode of regulation of the ACh-sensitive K-channel by the muscarinic receptor in rabbit atrial cells. *Pflugers Archiv: European Journal of Physiology* 400(4), pp. 424–431.
- Sondek, J., Bohm, A., Lambright, D.G., Hamm, H.E. and Sigler, P.B. 1996. Crystal structure of a G-protein beta gamma dimer at 2.1A resolution. *Nature* 379(6563), pp. 369–374.
- Stafstrom, C.E., Schwandt, P.C., Chubb, M.C. and Crill, W.E. 1985. Properties of persistent sodium conductance and calcium conductance of layer V neurons from cat sensorimotor cortex in vitro. *Journal of Neurophysiology* 53(1), pp. 153–170.
- Starmer, C.F., Grant, A.O. and Strauss, H.C. 1984. Mechanisms of use-dependent block of sodium channels in excitable membranes by local anesthetics. *Biophysical Journal* 46(1), pp. 15–27.

- Stella, N. 2010. Cannabinoid and cannabinoid-like receptors in microglia, astrocytes, and astrocytomas. *Glia* 58(9), pp. 1017–1030.
- Stühmer, W., Conti, F., Suzuki, H., Wang, X.D., Noda, M., Yahagi, N., Kubo, H. and Numa, S. 1989. Structural parts involved in activation and inactivation of the sodium channel. *Nature* 339(6226), pp. 597–603.
- Suh, B.-C., Horowitz, L.F., Hirdes, W., Mackie, K. and Hille, B. 2004. Regulation of KCNQ2/KCNQ3 current by G protein cycling: the kinetics of receptor-mediated signaling by Gq. *The Journal of General Physiology* 123(6), pp. 663–683.
- Tan, H.L., Kupersmidt, S., Zhang, R., Stepanovic, S., Roden, D.M., Wilde, A.A.M., Anderson, M.E. and Balser, J.R. 2002. A calcium sensor in the sodium channel modulates cardiac excitability. *Nature* 415(6870), pp. 442–447.
- Tfelt-Hansen, J. and Brown, E.M. 2005. The calcium-sensing receptor in normal physiology and pathophysiology: a review. *Critical reviews in clinical laboratory sciences* 42(1), pp. 35–70.
- Thompson, C.H., Hawkins, N.A., Kearney, J.A. and George, A.L. 2017. CaMKII modulates sodium current in neurons from epileptic Scn2a mutant mice. *Proceedings of the National Academy of Sciences of the United States of America* 114(7), pp. 1696–1701.
- Tikhonov, D.B. and Zhorov, B.S. 2005. Modeling P-loops domain of sodium channel: homology with potassium channels and interaction with ligands. *Biophysical Journal* 88(1), pp. 184–197.
- Toib, A., Lyakhov, V. and Marom, S. 1998. Interaction between duration of activity and time course of recovery from slow inactivation in mammalian brain Na⁺ channels. *The Journal of Neuroscience* 18(5), pp. 1893–1903.
- Trimmer, J.S., Cooperman, S.S., Tomiko, S.A., Zhou, J.Y., Crean, S.M., Boyle, M.B., Kallen, R.G., Sheng, Z.H., Barchi, R.L. and Sigworth, F.J. 1989. Primary structure and functional expression of a mammalian skeletal muscle sodium channel. *Neuron* 3(1), pp. 33–49.
- Truett, G.E., Heeger, P., Mynatt, R.L., Truett, A.A., Walker, J.A. and Warman, M.L. 2000. Preparation of PCR-quality mouse genomic DNA with hot sodium hydroxide and tris (HotSHOT). *Biotechniques* 29(1), pp. 52, 54.
- Twitchell, W., Brown, S. and Mackie, K. 1997. Cannabinoids inhibit N- and P/Q-type calcium channels in cultured rat hippocampal neurons. *Journal of Neurophysiology* 78(1), pp. 43–50.
- Ui, M., Katada, T., Nogimori, K., Tamura, M. and Yajima, M. 1986. [Pertussis toxin--islet-activating protein (IAP)]. *Tanpakushitsu Kakusan Koso. Protein, Nucleic Acid, Enzyme* 31(4 Suppl), pp. 300–323.
- Ulbricht, W. 2005. Sodium channel inactivation: molecular determinants and modulation. *Physiological Reviews* 85(4), pp. 1271–1301.
- Urwyler, S. 2011. Allosteric modulation of family C G-protein-coupled receptors: from molecular insights to therapeutic perspectives. *Pharmacological Reviews* 63(1), pp. 59–126.
- Valle, C., Rodriguez, M., Santamaría, R., Almaden, Y., Rodriguez, M.E., Cañadillas, S., Martín-Malo, A. and Aljama, P. 2008. Cinacalcet reduces the set point of the PTH-calcium curve. *Journal of the American Society of Nephrology* 19(12), pp. 2430–2436.

- Vassilatis, D.K., Hohmann, J.G., Zeng, H., Li, F., Ranchalis, J.E., Mortrud, M.T., Brown, A., Rodriguez, S.S., Weller, J.R., Wright, A.C., Bergmann, J.E. and Gaitanaris, G.A. 2003. The G protein-coupled receptor repertoires of human and mouse. *Proceedings of the National Academy of Sciences of the United States of America* 100(8), pp. 4903–4908.
- Viveros, M.P., de Fonseca, F.R., Bermudez-Silva, F.J. and McPartland, J.M. 2008. Critical role of the endocannabinoid system in the regulation of food intake and energy metabolism, with phylogenetic, developmental, and pathophysiological implications. *Endocrine, metabolic & immune disorders drug targets* 8(3), pp. 220–230.
- Volkow, N.D., Wise, R.A. and Baler, R. 2017. The dopamine motive system: implications for drug and food addiction. *Nature Reviews. Neuroscience* 18(12), pp. 741–752.
- Walker, J.M., Huang, S.M., Strangman, N.M., Tsou, K. and Sañudo-Peña, M.C. 1999. Pain modulation by release of the endogenous cannabinoid anandamide. *Proceedings of the National Academy of Sciences of the United States of America* 96(21), pp. 12198–12203.
- Wang, C., Chung, B.C., Yan, H., Wang, H.-G., Lee, S.-Y. and Pitt, G.S. 2014. Structural analyses of Ca²⁺/CaM interaction with NaV channel C-termini reveal mechanisms of calcium-dependent regulation. *Nature Communications* 5, p. 4896.
- Ward, D.T. and Riccardi, D. 2012. New concepts in calcium-sensing receptor pharmacology and signalling. *British Journal of Pharmacology* 165(1), pp. 35–48.
- Weiss, N. and Zamponi, G.W. 2015. All roads lead to presynaptic calcium channel inhibition by the ghrelin receptor: Separate agonist-dependent and -independent signaling pathways. *The Journal of General Physiology* 146(3), pp. 201–204.
- Wellendorph, P., Hansen, K.B., Balsgaard, A., Greenwood, J.R., Egebjerg, J. and Bräuner-Osborne, H. 2005. Deorphanization of GPRC6A: a promiscuous L-alpha-amino acid receptor with preference for basic amino acids. *Molecular Pharmacology* 67(3), pp. 589–597.
- West, J.W., Numann, R., Murphy, B.J., Scheuer, T. and Catterall, W.A. 1991. A phosphorylation site in the Na⁺ channel required for modulation by protein kinase C. *Science* 254(5033), pp. 866–868.
- Westenbroek, R.E., Merrick, D.K. and Catterall, W.A. 1989. Differential subcellular localization of the RI and RII Na⁺ channel subtypes in central neurons. *Neuron* 3(6), pp. 695–704.
- Westenbroek, R.E., Noebels, J.L. and Catterall, W.A. 1992. Elevated expression of type II Na⁺ channels in hypomyelinated axons of shiverer mouse brain. *The Journal of Neuroscience* 12(6), pp. 2259–2267.
- Wettschureck, N. and Offermanns, S. 2005. Mammalian G proteins and their cell type specific functions. *Physiological Reviews* 85(4), pp. 1159–1204.
- Wilson, R.I. and Nicoll, R.A. 2001. Endogenous cannabinoids mediate retrograde signalling at hippocampal synapses. *Nature* 410(6828), pp. 588–592.
- Winters, J.J. and Isom, L.L. 2016. Developmental and Regulatory Functions of Na(+) Channel Non-pore-forming β Subunits. *Current topics in membranes* 78, pp. 315–351.
- Wittmack, E.K., Rush, A.M., Hudmon, A., Waxman, S.G. and Dib-Hajj, S.D. 2005. Voltage-gated

- sodium channel Nav1.6 is modulated by p38 mitogen-activated protein kinase. *The Journal of Neuroscience* 25(28), pp. 6621–6630.
- Yakubovich, D., Rishal, I. and Dascal, N. 2005. Kinetic modeling of Na(+)-induced, Gbetagamma-dependent activation of G protein-gated K(+) channels. *Journal of Molecular Neuroscience* 25(1), pp. 7–19.
- Yamada, M., Inanobe, A. and Kurachi, Y. 1998. G protein regulation of potassium ion channels. *Pharmacological Reviews* 50(4), pp. 723–760.
- Yan, H., Wang, C., Marx, S.O. and Pitt, G.S. 2017. Calmodulin limits pathogenic Na⁺ channel persistent current. *The Journal of General Physiology* 149(2), pp. 277–293.
- Yoshida, T., Hashimoto, K., Zimmer, A., Maejima, T., Araishi, K. and Kano, M. 2002. The cannabinoid CB1 receptor mediates retrograde signals for depolarization-induced suppression of inhibition in cerebellar Purkinje cells. *The Journal of Neuroscience* 22(5), pp. 1690–1697.
- Yu, E.J., Ko, S.-H., Lenkowski, P.W., Pance, A., Patel, M.K. and Jackson, A.P. 2005. Distinct domains of the sodium channel beta3-subunit modulate channel-gating kinetics and subcellular location. *The Biochemical Journal* 392(Pt 3), pp. 519–526.
- Yu, F.H. and Catterall, W.A. 2003. Overview of the voltage-gated sodium channel family. *Genome Biology* 4(3), p. 207.
- Yu, F.H., Westenbroek, R.E., Silos-Santiago, I., McCormick, K.A., Lawson, D., Ge, P., Ferriera, H., Lilly, J., DiStefano, P.S., Catterall, W.A., Scheuer, T. and Curtis, R. 2003. Sodium channel beta4, a new disulfide-linked auxiliary subunit with similarity to beta2. *The Journal of Neuroscience* 23(20), pp. 7577–7585.
- Zamberletti, E., Gabaglio, M. and Parolaro, D. 2017. The Endocannabinoid System and Autism Spectrum Disorders: Insights from Animal Models. *International Journal of Molecular Sciences* 18(9).
- Zamponi, G.W. and Currie, K.P.M. 2013. Regulation of Ca(V)₂ calcium channels by G protein coupled receptors. *Biochimica et Biophysica Acta* 1828(7), pp. 1629–1643.
- Zeng, Z., Hill-Yardin, E.L., Williams, D., O'Brien, T., Serelis, A. and French, C.R. 2016. Effect of phenytoin on sodium conductances in rat hippocampal CA1 pyramidal neurons. *Journal of Neurophysiology* 116(4), pp. 1924–1936.
- Zerangue, N. and Jan, L.Y. 1998. G-protein signaling: fine-tuning signaling kinetics. *Current Biology* 8(9), pp. R313-6.
- Zhou, J., Shin, H.-G., Yi, J., Shen, W., Williams, C.P. and Murray, K.T. 2002. Phosphorylation and putative ER retention signals are required for protein kinase A-mediated potentiation of cardiac sodium current. *Circulation Research* 91(6), pp. 540–546.
- Zhou, W. and Goldin, A.L. 2004. Use-dependent potentiation of the Nav1.6 sodium channel. *Biophysical Journal* 87(6), pp. 3862–3872.
- Zygmunt, P.M., Petersson, J., Andersson, D.A., Chuang, H., Sørsgård, M., Di Marzo, V., Julius, D. and Högestätt, E.D. 1999. Vanilloid receptors on sensory nerves mediate the vasodilator action of anandamide. *Nature* 400(6743), pp. 452–457.